[redacted]

TRANSONIC AERODYNAMIC CHARACTERISTICS OF A HORIZONTAL TAKE-OFF AND LANDING REUSABLE BOOSTER HAVING VARIATIONS IN WING PLANFORM

By Bernard Spencer, Jr., Beverly Z. Henry, Jr., and W. Pelham Phillips

Langley Research Center
Langley Station, Hampton, Va.

[redacted]

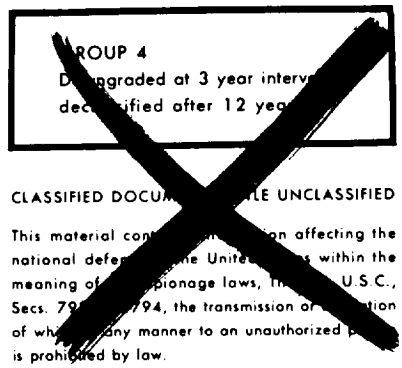

NATIONAL AERONAUTICS AND SPACE ADMINISTRATION

[redacted]

TRANSONIC AERODYNAMIC CHARACTERISTICS OF A HORIZONTAL TAKE-OFF AND LANDING REUSABLE BOOSTER HAVING VARIATIONS IN WING PLANFORM*

By Bernard Spencer, Jr., Beverly Z. Henry, Jr.,
and W. Pelham Phillips
Langley Research Center

SUMMARY

An investigation has been made in the Langley high-speed 7- by 10-foot tunnel at Mach numbers from 0.40 to 1.13 to determine the aerodynamic characteristics of a preliminary design manned, horizontal take-off, horizontal landing, reusable booster configuration having advanced turboramjet engines for propulsion. Three wing planforms were tested with the basic fuselage-engine arrangement, and included a 75° delta wing, a 75° modified arrow wing, and a 70°-80° cranked wing. Horizontal stabilizers were located at the base of the engine package. The effects of vertical-tail size and location were also investigated.

A comparison of the transonic longitudinal aerodynamic characteristics of the 75° delta, 75° modified arrow, and 70°-80° cranked wing configurations, having approximately equal planform areas and maximum thickness ratios, indicates that the 75° modified arrow wing exhibited lower minimum drag and drag due to lift, and higher values of untrimmed maximum lift-drag ratio, than either the 75° delta or the 70°-80° cranked wing configuration, throughout the Mach number range of the investigation. The low-lift aerodynamic-center shift due to increasing Mach number was approximately equal for the three wing planforms.

Low values of control effectiveness at low angles of attack resulted from deflection of the horizontal stabilizers at -30° dihedral. Large increases in effectiveness accompanied increases in angle of attack. The horizontal stabilizer was sufficient, however, to trim the configuration at moderate lift coefficients and angles of attack at all test Mach numbers. The 75° modified arrow wing configuration having the horizontal stabilizer on at -30° dihedral, and the small center vertical tail, exhibited directional stability to approximately 10° angle of attack. Increasing the center-vertical-tail area and the addition of outboard vertical tails increased the directional stability of the configuration up to angles of attack of approximately 16°, with slight reductions in lift coefficient above 12° angle of attack resulting from addition of the outboard vertical tails. The modifications to the vertical-tail geometry had little or no effect on the low-lift longitudinal aerodynamic characteristics of the configuration. Only slight effects of increasing Mach number on the lateral-directional characteristics of the configurations were noted. The largest directional destabilizing effect at the higher angles of attack was caused by the fuselage at all test Mach numbers. All configurations exhibited positive effective dihedral through the test angle-of-attack range and at all test Mach numbers.

*Title, Unclassified.

INTRODUCTION

The National Aeronautics and Space Administration is currently conducting general research programs to determine the aerodynamic characteristics of configurations having application as manned recoverable boosters. Basic mission requirements for vehicles of this nature encompass either horizontal or vertical take-off, with release of upper stages in the hypersonic speed range, and glide return with conventional horizontal landings. The desirability of such configurations, from both economic considerations and the capability of widening choices of landing or launch sites becomes greater as the frequency of inserting payloads into orbit increases. The anticipated aerodynamic problem areas for a vehicle encountering such a large range of Mach numbers include the provision for compatible levels of longitudinal and lateral stability at all flight Mach numbers while maintaining low transonic and hypersonic drag characteristics. Sufficiently high lifts and lift-drag ratios are necessary for take-off and landing on existing runways.

The aerodynamic characteristics of several multistage rocket-powered vehicle concepts having recoverable first-stage boosters have been reported in references 1 and 2. These vehicles include vertical and horizontal take-off configurations, with the various stages arranged in tandem. Although tandem staging possibly reduces problems of stage separation (as compared with internally carried upper stages, for example), the extreme center-of-gravity and center-of-pressure shifts resulting from stage separation could present major problem areas in stability considerations. Internal carriage of the upper stages, while minimizing center-of-gravity travel, could also reduce total configuration wetted area and the overall drag of the configuration.

The purpose of the present investigation was to determine the transonic aerodynamic characteristics of a preliminary design first-stage horizontal take-off and landing recoverable booster configuration having advanced, hydrogen-fueled, turboramjet engines for propulsion. The inlets for these engines were shoulder-mounted and designed to operate in the wing pressure field at reduced Mach numbers, for a free-stream Mach number of 8.0. The unmanned upper stage was considered as carried internally, with stage separation to occur at a velocity of approximately 8,000 to 10,000 feet per second at altitudes between 95,000 and 125,000 feet. The payload-in-orbit weight was assumed to be 2,000 pounds for a 300-nautical-mile orbit and is considered suitable as a supply package for an orbiting space station. Take-off gross weight of such an assumed system was estimated to be about 100,000 pounds. The aerodynamic characteristics were determined for the basic fuselage-engine arrangement with each of three wings differing in planform but having approximately equal wing area and maximum thickness ratio. These planforms included a 75° delta wing, a 75° modified arrow wing, and a 70°-80° cranked wing.

Tests were made in the Langley high-speed 7- by 10-foot tunnel at Mach numbers from 0.40 to 1.13 with a maximum angle-of-attack range, from approximately -5° to 22° at sideslip angles of 0° and -5°. The range of average test Reynolds numbers per foot varied from approximately 2.5×10^6 to 3.7×10^6.

SYMBOLS

Longitudinal data of the investigation are referred to the stability axes and the lateral data to the body axes with all forces and moments nondimensionalized with respect to the planform area, root chord, and span of the corresponding wing. The center of gravity was located longitudinally at approximately 66 percent of the theoretical body length (including the engines) behind the body apex and vertically 1.44 percent body length below the engine thrust line for all tests unless otherwise noted.

A	aspect ratio, b^2/S
b	wing span, ft
C_D	drag coefficient, $\frac{\text{Drag}}{qS}$
$C_{D,i}$	induced drag coefficient, $C_D - C_{D,o}$
$C_{D,i}/C_L^2$	drag-due-to-lift parameter
$C_{D,o}$	drag at $C_L = 0$
C_L	lift coefficient, $\frac{\text{Lift}}{qS}$
C_{L_α}	lift-curve slope at $\alpha = 0^\circ$, per deg
C_l	rolling-moment coefficient, $\frac{\text{Rolling moment}}{qSb}$
C_{l_β}	effective-dihedral parameter, $\Delta C_l/\Delta\beta$, per deg
C_m	pitching-moment coefficient, $\frac{\text{Pitching moment}}{qSc_r}$
$C_{m_{i_t}}$	horizontal-stabilizer control effectiveness parameter, per deg
$\partial C_m/\partial C_L$	longitudinal-stability parameter
C_n	yawing-moment coefficient, $\frac{\text{Yawing moment}}{qSb}$
C_{n_β}	directional-stability parameter, $\Delta C_n/\Delta\beta$, per deg

C_Y	side-force coefficient, $\frac{\text{Side force}}{qS}$
C_{Y_β}	side-force parameter, $\Delta C_Y/\Delta\beta$, per deg
c	local chord, ft
c_r	wing root chord, ft
i_t	horizontal-stabilizer incidence angle (positive with trailing edge down, measured in vertical plane), deg
L/D	lift-drag ratio
l	fuselage length, ft
M	Mach number
q	dynamic pressure, lb/sq ft
S	wing planform area, sq ft
t	thickness, ft
x	fuselage longitudinal ordinate, ft
y	fuselage lateral ordinate, ft
Γ_t	horizontal-stabilizer dihedral angle (positive with tip chord up), deg

Subscripts:

max	maximum
trim	trimmed condition
$\alpha\approx0$	near-zero angle-of-attack condition

Model components:

W_1	75° delta wing, S = 0.758 sq ft, A = 1.075
W_2	75° modified arrow wing, S = 0.758 sq ft, A = 0.894
W_3	70°-80° cranked wing, S = 0.709 sq ft, A = 0.836
B	fuselage
H	horizontal stabilizer, (0.053) $S_{(\text{wing 1})}$ (total exposed area)
V_1	small center vertical tail, (0.100) $S_{(\text{wing 1})}$ (total exposed area)

V_2 large center vertical tail, (0.225) $S_{(\text{wing 1})}$ (total exposed area)

V_o outboard vertical tails, (0.136) $S_{(\text{wing 1})}$

MODEL

The model of the present investigation represents approximately a 1/60-scale version of a preliminary design horizontal take-off and landing recoverable booster configuration using advanced, hydrogen-fueled, turboramjet engines. Gross weight at take-off was estimated to be about 100,000 pounds. All fuel was assumed to be contained within the fuselage which was sized to provide sufficient fuel for acceleration of the system to about 10,000 feet per second with a 5-minute cruise capability at this velocity. The fuselage utilized a modified 2/3-power forebody shape $\left(y = \frac{y_{max}}{l^{2/3}} x^{2/3}\right)$ and had a height-width ratio of approximately 2 with flat sides. This cross section was selected to provide large volumes for fuel storage ahead, behind, and above the payload bay to reduce center-of-gravity shift between take-off (fully loaded) and landing (empty) configurations. Boattailing of the afterbody was used to reduce transonic-subsonic drag.

Relative placement of wing leading edges and inlet lips was determined by assuming that the inlets operated at a reduced Mach number in the wing pressure field. The ratio of the inlet capture area to the reference area of wing 1 was approximately 0.0176. Design conditions were for a free-stream Mach number of 8.0 and an angle of attack of 8°, as referenced to the configuration thrust line. The wings were designed to have a flat lower surface to serve as a ramp for the engine inlets. Inlet external compression surfaces were not included in the preliminary studies of the present configurations. Drawings and dimensions of the various models and components tested are presented in figure 1, with pertinent geometry of the various wings listed in the table of figure 1. Photographs of the 75° delta wing configuration (W_1BV_2H) are presented as figure 2.

Three wing planforms, consisting of a 75° delta, a 75° modified arrow, and a 70°-80° cranked wing, were tested with the wing sections having modified wedge airfoils. Leading-edge radii based on sweep and maximum temperature considerations were determined for each wing. (See fig. 1.) The wing maximum thickness was located at the 75-percent wing-chord stations.

Longitudinal control was provided by all-movable horizontal stabilizers located near the engine exits with maximum incidence of -20° and maximum dihedral of -60° obtainable for each horizontal stabilizer. The airfoil sections of these stabilizers were designed similar to the wings, in that the leading-edge radii were determined from sweep and temperature considerations and maximum thickness occurred at the 75-percent stabilizer-chord station presented in figure 1.

Location for the vertical tails tested included a center-line location for wings 1, 2, and 3, and an additional outboard vertical tail for wing 2. A large and a small center vertical tail having ratios of exposed area to reference area (wing 1) of 0.225 and 0.100, respectively, were tested. Wedge airfoil sections were used for the small center vertical tail (fig. 1(b)), and flat-plate sections with round leading edge and beveled trailing edge were used for the large center vertical tail (V_2). Half-wedge airfoil sections were used for the outboard vertical tails (V_o). (See fig. 1(b).) The ratio of the total outboard-tail area to reference area (wing 1) was 0.136.

TESTS AND CORRECTIONS

The present investigation was made in the Langley high-speed 7- by 10-foot tunnel in the range of Mach numbers from 0.40 to 1.13, corresponding to average test Reynolds numbers per foot varying from approximately 2.5×10^6 to 3.7×10^6. The model was sting supported with forces and moments measured by use of a six-component internally mounted strain-gage balance. The maximum angle-of-attack range of the investigation was from approximately -5° to 22° at 0° and -5° of sideslip.

For all tests, transition was fixed on the wings, horizontal stabilizers, and vertical tails at the 10-percent-chord station by using No. 180 (0.0035-inch nominal diameter) carborundum grains, as determined by the method described in reference 3.

Corrections to the angle of attack and angle of sideslip due to deflection of the sting and balance under load have been applied to the data herein. The drag has been adjusted to correspond to a condition of free-stream static pressure in the base regions with corrections for momentum and internal skin-friction losses due to restricted airflow in the inlets.

PRESENTATION OF RESULTS

The basic data and summary lateral and longitudinal aerodynamic characteristics of the configurations tested are presented in the following figures:

DISCUSSION

Basic longitudinal aerodynamic characteristics of the various configurations and model components in combination are presented in figures 3 to 7. Summary plots of the lateral aerodynamic parameters C_{n_β}, C_{Y_β}, and C_{l_β} are presented in figures 8 and 9, with summary plots of the longitudinal aerodynamic parameters C_{L_α}, $(L/D)_{max}$, $\partial C_m/\partial C_L$, $C_{D,i}/C_L^2$, and $C_{D,o}$ being presented in figure 10. The longitudinal trimmed characteristics associated with the three wing planform configurations are presented in figures 11 and 12. Most of the discussion is confined to the summary figures except for pertinent observations to be noted from the basic data.

A comparison of the lift, drag, and pitching-moment variations with angle of attack for the three wing planform and fuselage configurations at a Mach number of 0.40 is presented in figure 3(a). Although the lift-curve slopes (near $\alpha = 0^\circ$) for the configurations with wings 1 and 2 are approximately the same, higher values of lift coefficient are indicated for the W_2BV_1 configuration throughout the angle-of-attack range investigated. Slightly lower values of $C_{D,o}$ are also indicated for the W_2BV_1 configuration, as compared with the W_1BV_1 and W_3BV_1 configurations, with the result that higher untrimmed values of $(L/D)_{max}$ occur for the 75° modified arrow wing (W_2). Similar results are noted throughout the range of test Mach numbers (see figs. 3(b) to 3(g)) and are summarized in figure 10(a), which indicates that the 75° modified arrow wing (W_2) has lower minimum drag and drag due to lift $\left(C_{D,i}/C_L^2\right)$, and higher values of maximum untrimmed lift-drag ratio, than either the 75° delta wing (W_1) or 70°-80° cranked wing (W_3) throughout the Mach number range of the investigation. At transonic speeds, the highest values of lift-curve slope occur for the 75° delta wing (W_1).

A comparison of the longitudinal stability characteristics of the three wing planforms with horizontal stabilizers off indicate that the low-lift stability $(\partial C_m/\partial C_L)$ is approximately the same for each of the wings throughout the test Mach number range (fig. 10(a)). The variations in pitching-moment coefficient associated with the three wing planforms indicate slight stabilizing effects above $C_L = 0.20$ at low subsonic speeds (fig. 3(a)) with the largest increases in stability noted for wing 3. These increases in stability were greatly reduced at the higher Mach numbers (fig. 3(g)).

The effects of the addition of the horizontal stabilizers on the longitudinal aerodynamic characteristics of each wing configuration are presented in figure 4 at various Mach numbers. An increase in the low-lift static margin of approximately 5 percent results from addition of the stabilizers to the 75° delta (W_1) and 75° modified arrow wing (W_2) throughout the Mach number range of the investigation, and an increase of 6 percent in static margin results for the 70°-80° cranked wing (W_3). (See fig. 10(b).) It is interesting to note that changing the horizontal-stabilizer dihedral angle from -30° to -60° caused no loss in static margin and even increased the static margin at transonic speeds. This result is apparently associated with a strong mutual interference between the body and tail. Rather low values of horizontal-stabilizer effectiveness are prevalent throughout the Mach number range for the horizontal stabilizer at $\Gamma_t = -30^\circ$, with slight increases in effectiveness accompanying increases in Mach number (fig. 10(b)).

Figure 11 presents a summary of the trimmed lift, lift-drag ratio, angle of attack, and corresponding values of $\partial C_m/\partial C_L$ at $C_m = 0$ from $M = 0.40$ to 1.13 associated with deflection of the horizontal stabilizers to -10° incidence. The values of $(L/D)_{trim}$ are not maximum trimmed values, since trimmed $(L/D)_{max}$ would occur at tail incidences less than -10°. The figure is presented, however, to show that moderate deflection of the horizontal stabilizer is sufficient to trim the configuration having either wing 1, 2, or 3 at moderate lift coefficients

and angles of attack at all test Mach numbers. Static longitudinal stability exists at $C_{L,trim}$ for each configuration tested at all Mach numbers. Sufficient longitudinal control is provided by deflection of the horizontal stabilizer to $i_t = -10^\circ$ to trim the configuration having either wing 1, wing 2, or wing 3 to approximately 7° to 10° angle of attack at all test Mach numbers. (See figs. 5 and 12.)

Because of the necessity of producing moderate to high values of lift and lift-drag ratio for the configuration during take-off or landing, at angles of attack restricted by both pilot vision and ground clearance considerations, summary plots of the low-speed trimmed lift and lift-drag ratio at the corresponding angle of attack and at a Mach number of 0.40 are presented in figure 12, along with the horizontal-stabilizer control-effectiveness variation with angle of attack. Low values of $C_{L,trim}$ are shown in figure 11 for all configurations. Values of $C_{L,trim}$ of 0.70 or less were obtained for angles of attack less than 16°, which may be considered reasonable as take-off or landing attitudes. The resultant take-off velocities may be expected, therefore, to be high, dependent upon configuration wing loading. For the present configurations, where design take-off wing loadings are approximately 37 pounds per square foot, lift-off velocities may approach 200 feet per second.

The addition of outboard vertical tails to the W_2BH configuration at a Mach number of 0.40 (fig. 7(a)) produced an increase in lift-curve slope near $\alpha = 0^\circ$ but indicated losses in lift coefficient above 4° with corresponding reduction in the stabilizing effects of the horizontal stabilizer at high angles of attack noted for the outboard vertical tails off. Figure 7(a) also indicated that addition of the outboard tails increased the minimum drag of the configuration, but reduced drag due to lift. These effects, when combined with the reduced stability at high lift, result in improved $(L/D)_{trim}$ at $C_L > 0.10$ and the ability to trim to higher C_L with a given tail incidence. The 75° modified arrow wing configuration having the horizontal stabilizer located below and behind the wing appears to offer the most efficient subsonic to transonic aerodynamic characteristics, compared with the 75° delta and 70°-80° cranked wing configurations tested.

Lateral-Directional Characteristics

A summary of the lateral-directional characteristics of the 75° modified arrow wing and various model components in combination is presented in figures 8 and 9. The effects of the addition of the small center vertical tail (V_1) indicate an increment in positive C_{n_β} of approximately 0.004 realized from addition of the tail, with an additional incremental increase in positive C_{n_β} of 0.002 produced by increasing Γ_t of the horizontal stabilizer from -30° to -60°. (See fig. 8.) Directional instability occurs, however, above 10° angle of attack as a result of the large destabilizing effect of the fuselage. This effect is a result of the increasing instability of the body with angle of attack. Similar results were found for a fineness-ratio-10 body, having elliptic cross section,

and a vertical- to horizontal-axis ratio of 2.5. (See ref. 4.) There are little or no effects of increasing Mach number on the directional stability characteristics of the configuration.

The effects of the addition of the large center vertical tail (V_2) and outboard vertical surfaces (V_o) to the 75° modified arrow wing configuration with the horizontal stabilizers on are presented in figure 9. Positive values of C_{n_β} are indicated for the configuration having the large center vertical tail and outboard tails in combination up to angles of attack of approximately 16° at M = 0.40. Similar results are noted at the higher Mach numbers. All configurations tested indicated positive effective dihedral at all positive angles of attack and Mach numbers.

SUMMARY OF RESULTS

Results of an investigation to determine the effects of wing planform on the transonic aerodynamic characteristics of a preliminary design horizontal take-off and landing recoverable booster configuration may be summarized in the following observations:

1. A comparison of the transonic longitudinal aerodynamic characteristics of the 75° delta, 75° modified arrow, and 70°-80° cranked wing configurations, having approximately equal planform areas and maximum thickness ratios, indicates that the 75° modified arrow wing exhibited lower minimum drag and drag due to lift, and higher values of untrimmed maximum lift-drag ratio, than either the 75° delta or the 70°-80° cranked wing configuration, throughout the Mach number range of the investigation. The low-lift aerodynamic-center shift due to increasing Mach number was approximately equal for the three wing planforms.

2. The horizontal stabilizer which was located below and behind the wings at -30° dihedral, indicated rather low values of control effectiveness at low angles of attack. However, large increases in effectiveness accompanied increases in angle of attack. The horizontal stabilizer was sufficient, however, to trim the configurations at moderate lift coefficients and angles of attack at all test Mach numbers.

3. The 75° modified arrow wing configuration having the horizontal stabilizer on at -30° dihedral, and the small center vertical tail, exhibited directional stability to approximately 10° angle of attack. Increasing the area of the center vertical tail and addition of outboard vertical tails, located at the wing tips, increased the directional stability of the configuration up to an angle of attack of approximately 16°, with slight reductions in lift coefficient above 12° angle of attack resulting from addition of the outboard vertical tails. The modifications to the vertical-tail geometry had little or no effect on the low-lift longitudinal aerodynamic characteristics of the configuration. Only slight effects of increasing Mach number on the lateral-directional characteristics of the configurations were noted.

4. The largest directional destabilizing effect at the higher angles of attack was caused by the fuselage at all test Mach numbers. All configurations exhibited positive effective dihedral through the test angle-of-attack range and at all test Mach numbers.

Langley Research Center,
National Aeronautics and Space Administration,
Langley Station, Hampton, Va., February 29, 1964.

REFERENCES

1. Pierpont, P. Kenneth: Transonic Stability of a Preliminary Vertical-Take-Off Launch Configuration With a Horizontal-Landing Recoverable Booster. NASA TM X-689, 1962.

2. Pierpont, P. Kenneth: Transonic Longitudinal and Lateral Aerodynamic Characteristics of a Preliminary Concept of a First-Stage Horizontal-Take-Off-and-Horizontal-Landing Recoverable Booster With a 70° Delta Wing. NASA TM X-691, 1962.

3. Braslow, Albert L., and Knox, Eugene C.: Simplified Method for Determination of Critical Height of Distributed Roughness Particles for Boundary-Layer Transition at Mach Numbers From 0 to 5. NACA TN 4363, 1958.

4. Spencer, Bernard, Jr., and Phillips, W. Pelham: Effects of Cross-Section Shape on the Low-Speed Aerodynamic Characteristics of a Low-Wave-Drag Hypersonic Body. NASA TN D-1963, 1963.

Wing Geometry

Wing	A	b, in.	S, ft^2	c_r, in.
1	1.080	10.80	0.758	20.20
2	.894	9.88	.758	18.44
3	.836	9.24	.709	18.92

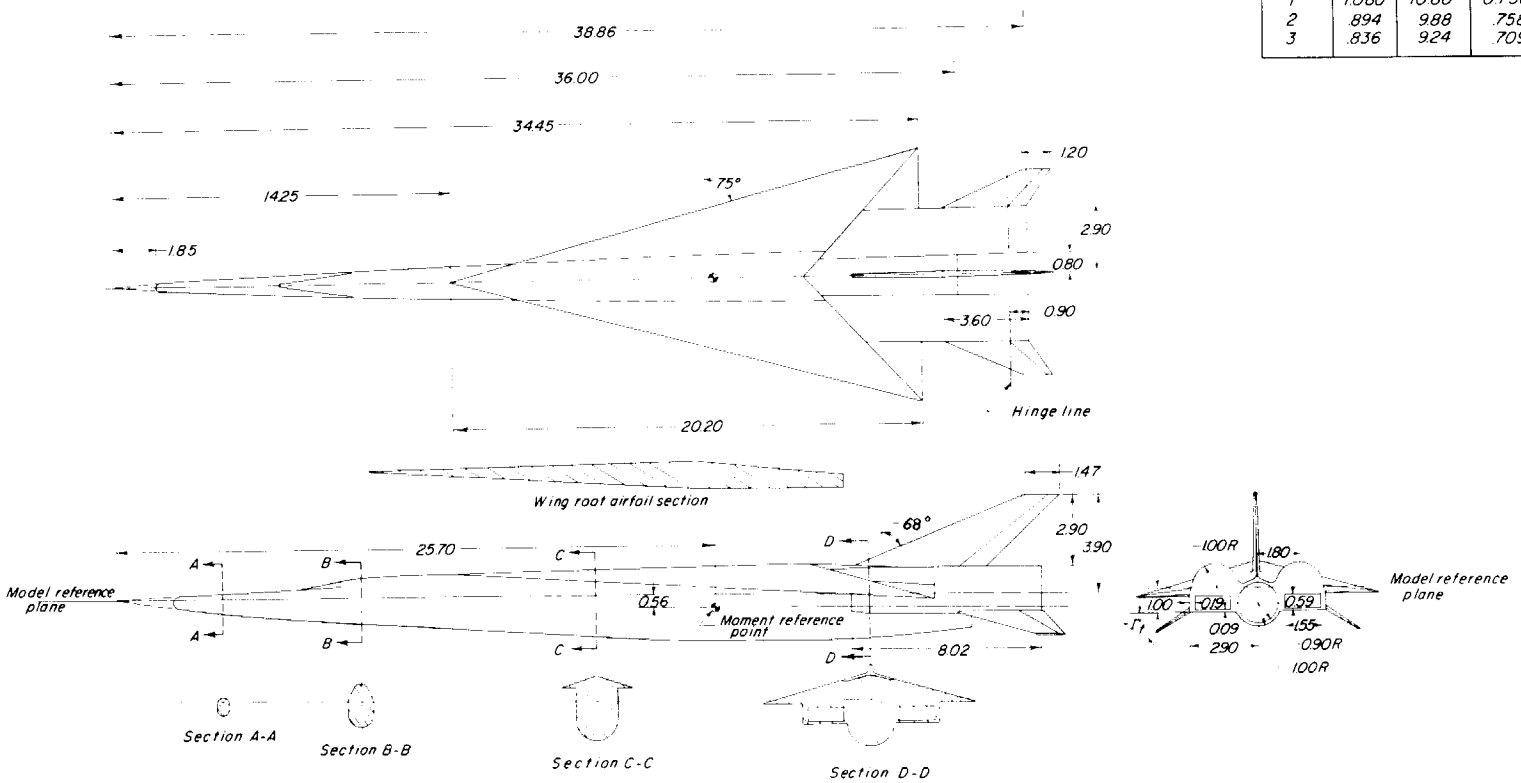

(a) Body with wing 1.

Figure 1.- Details of model.

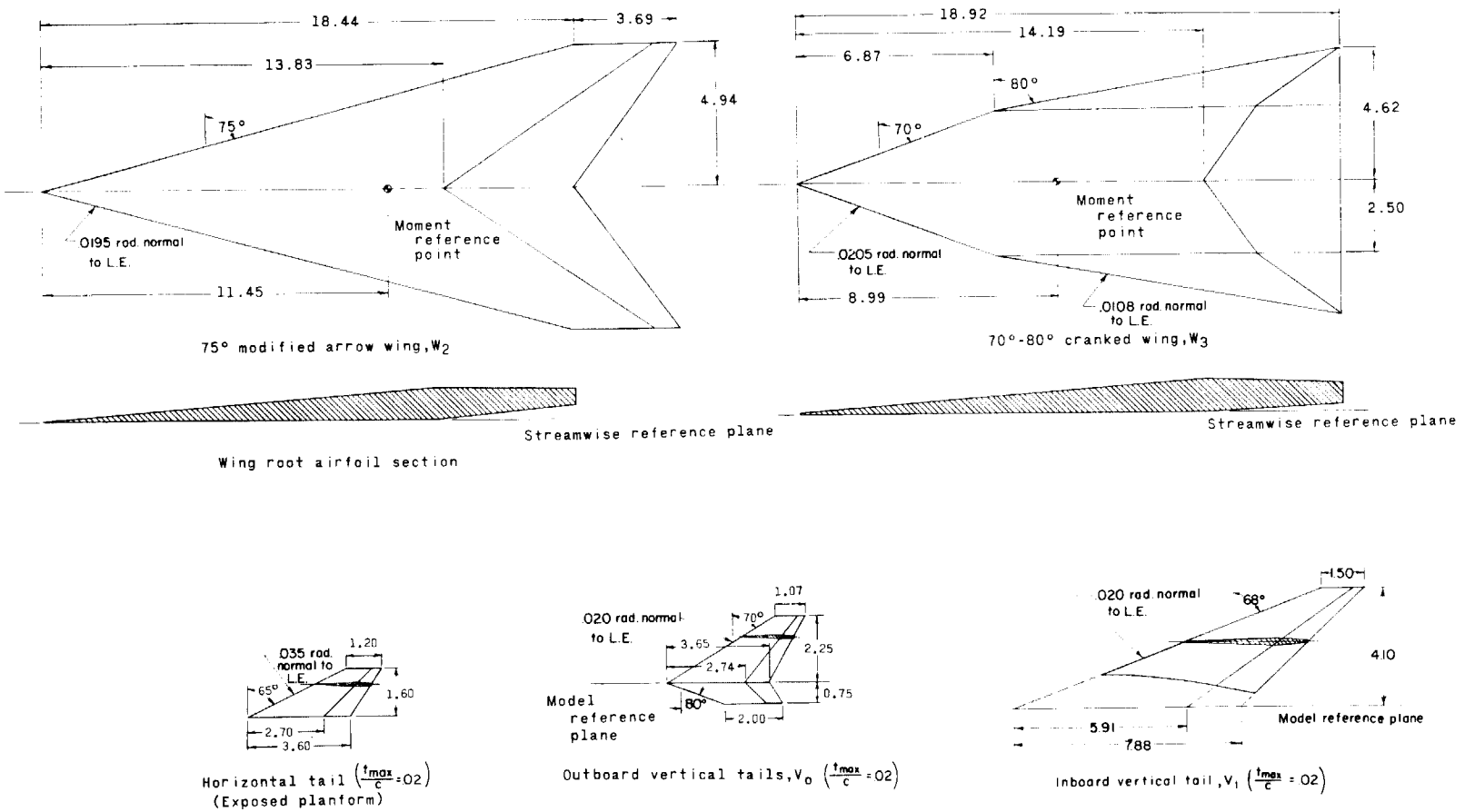

(b) Body with wings 2 and 3 and control surfaces.

Figure 1.- Concluded.

(a) Side view. L-63-5407

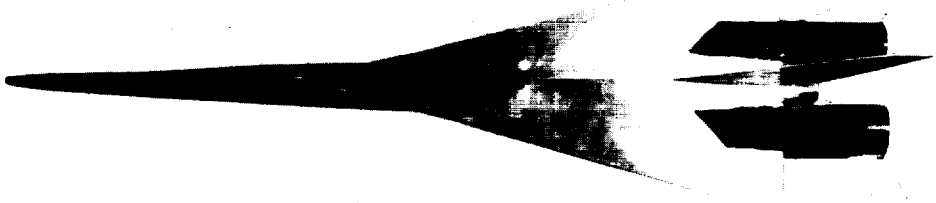

(b) Plan view. L-63-5408

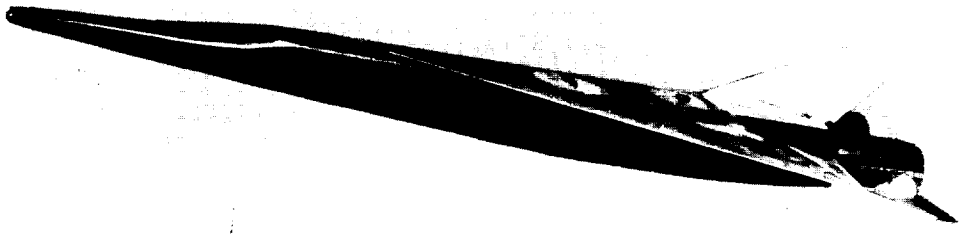

(c) Three-quarter side view. L-63-5406

Figure 2.- Photographs of configuration W_1BV_2H. $\Gamma_t = -30^\circ$; $i_t = 0^\circ$.

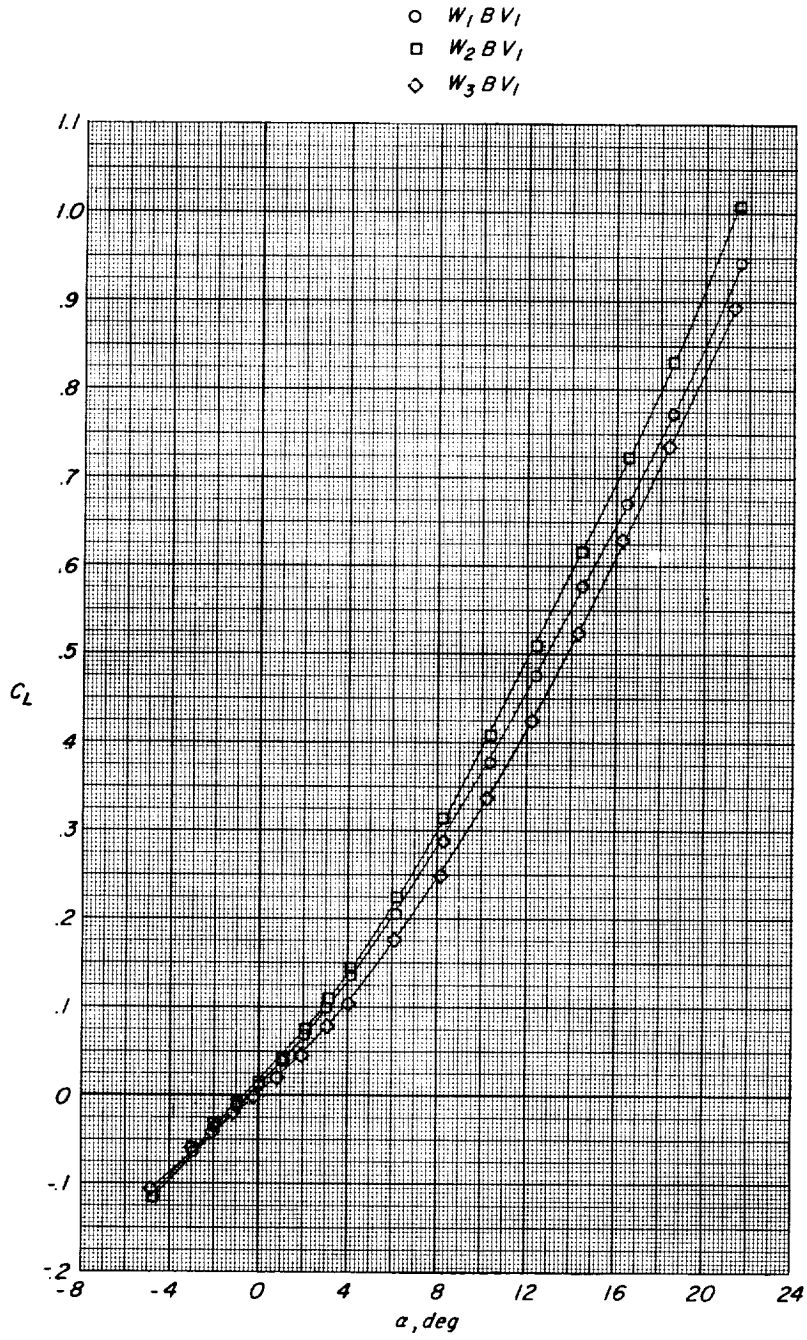

(a) M = 0.40.

Figure 3.- Effects of wing planform on the longitudinal aerodynamic characteristics of the configuration having horizontal stabilizers off at various Mach numbers. Small center vertical tail (V_1) on.

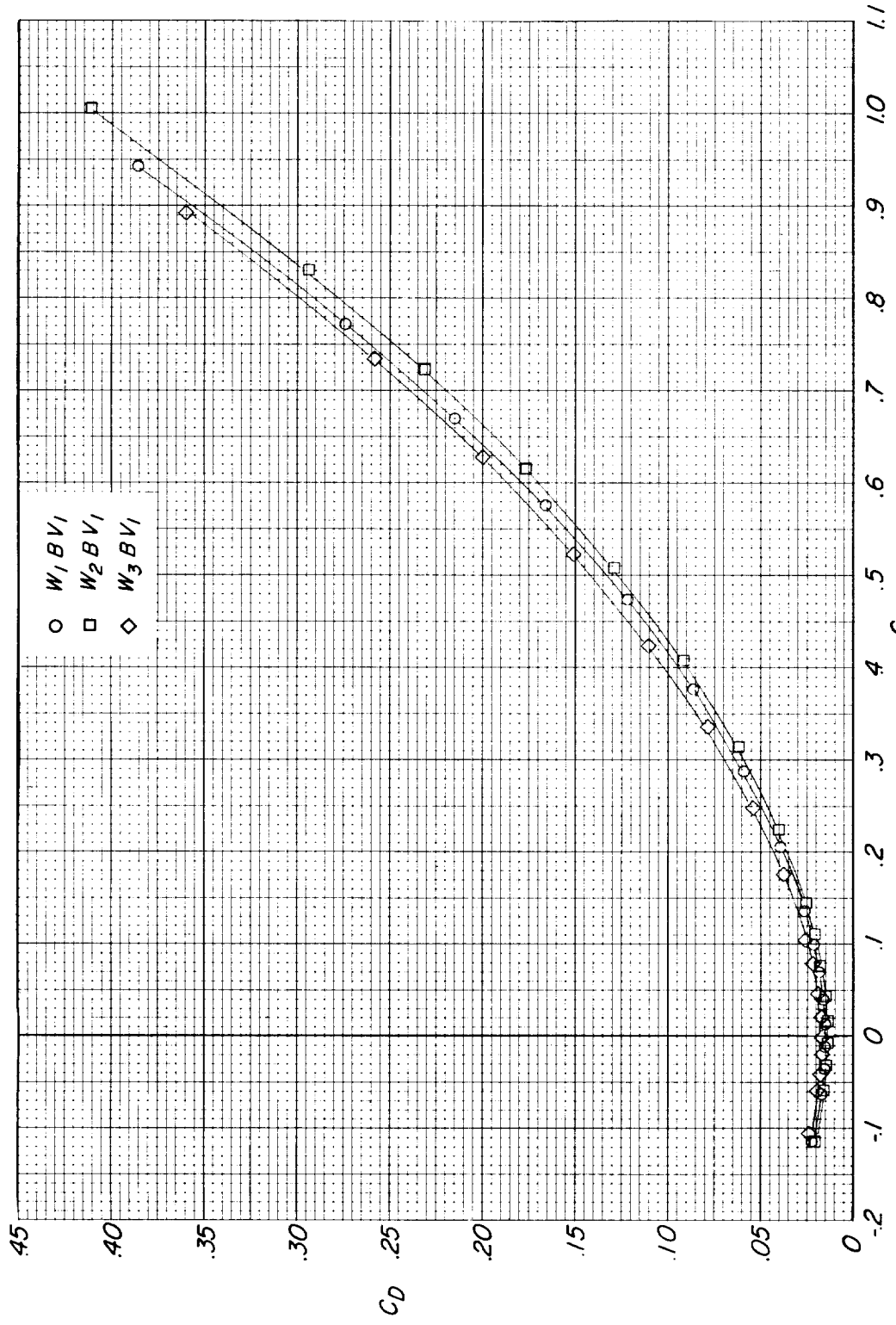

(a) Continued.

Figure 3.- Continued.

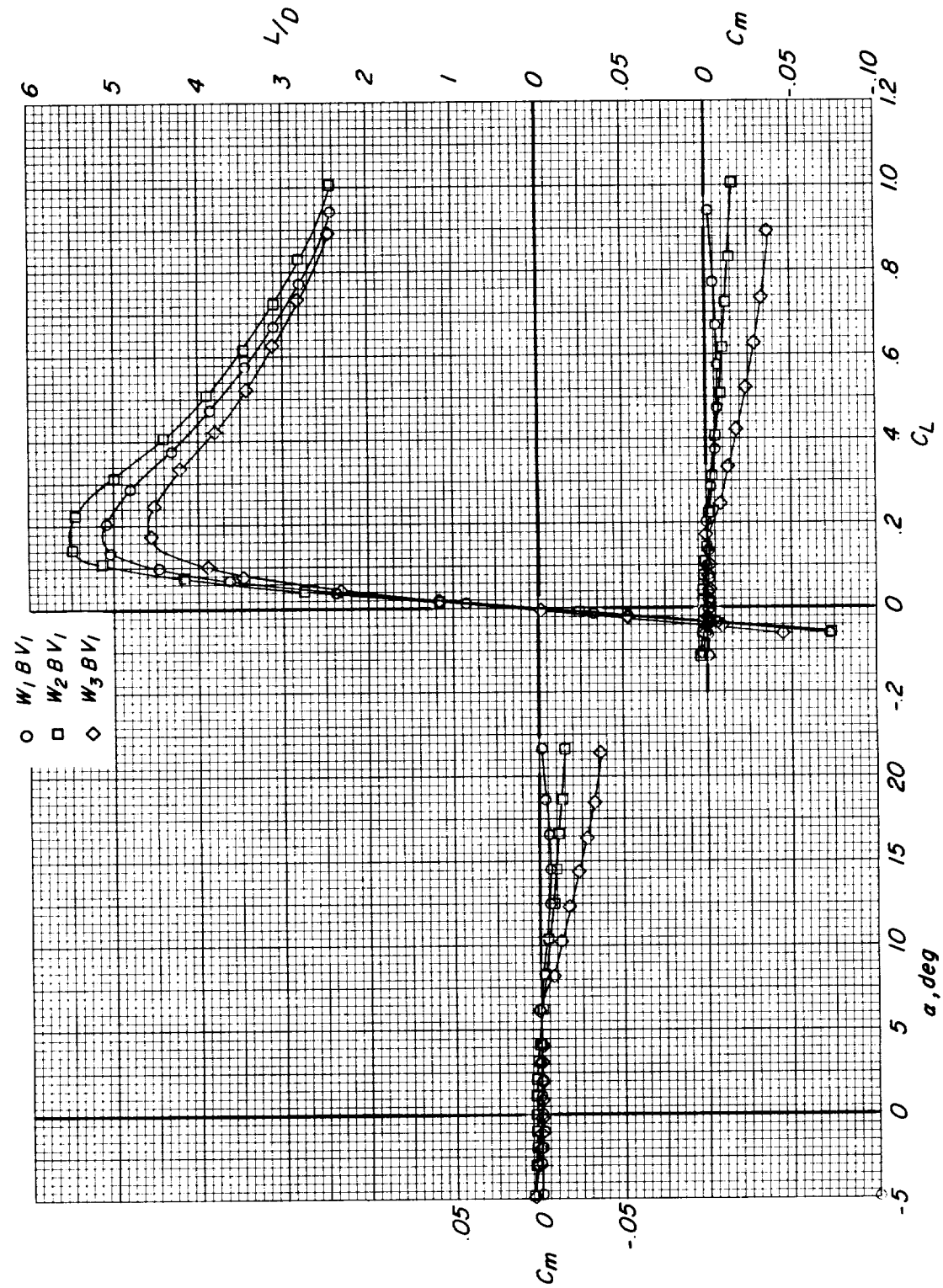

(a) Concluded.

Figure 3.- Continued.

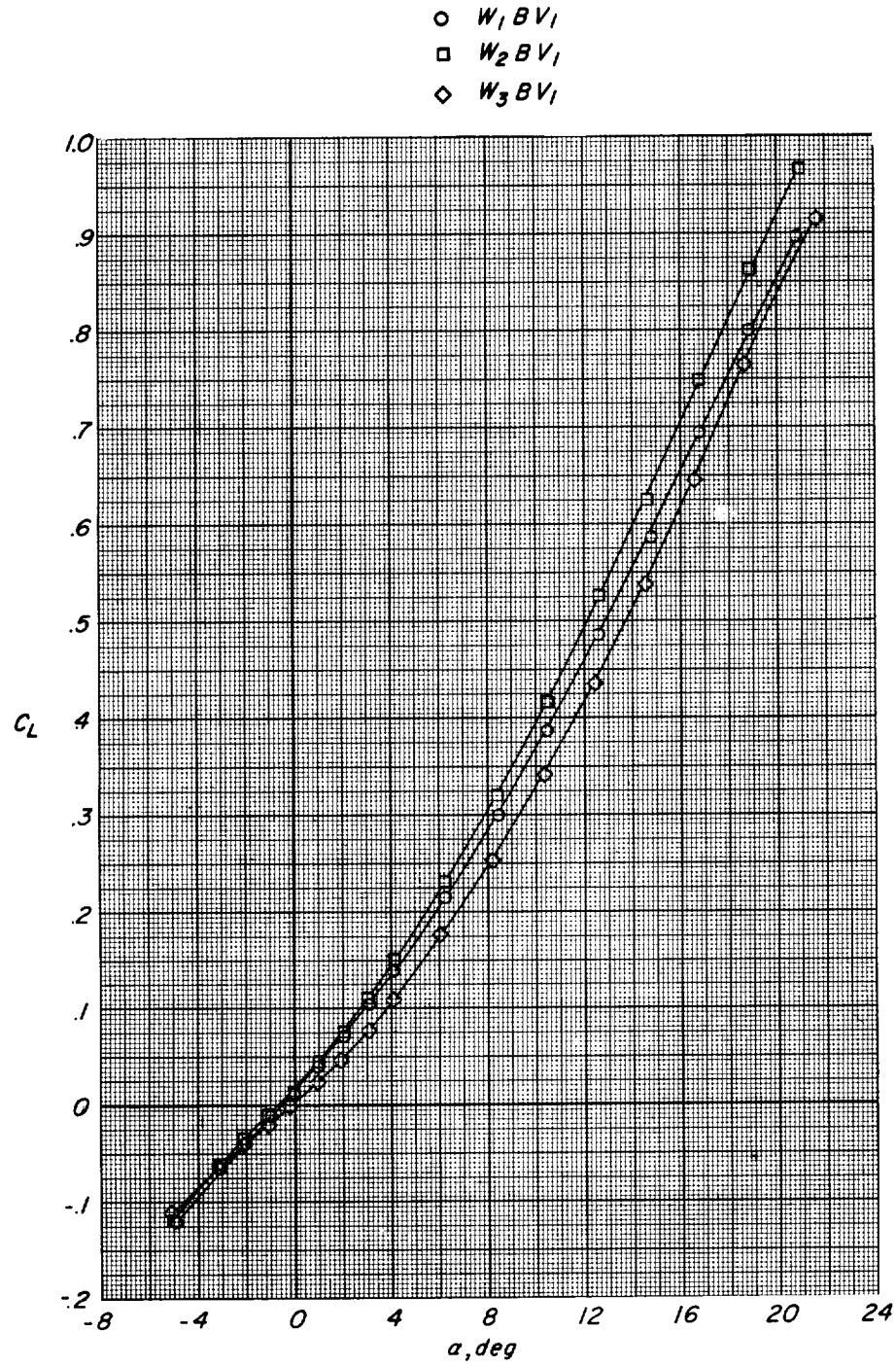

(b) M = 0.60.

Figure 3.- Continued.

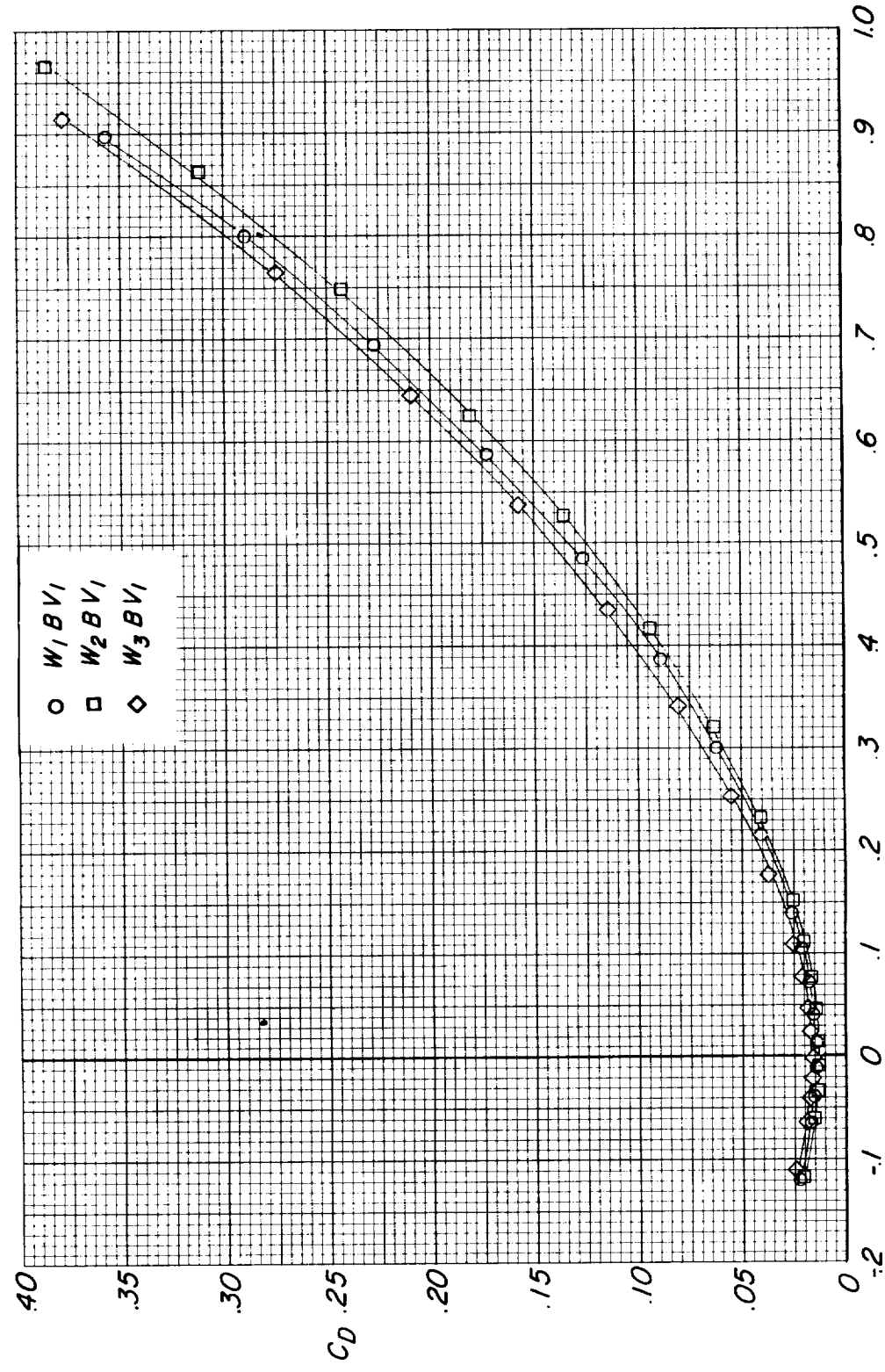

(b) Continued.

Figure 3.- Continued.

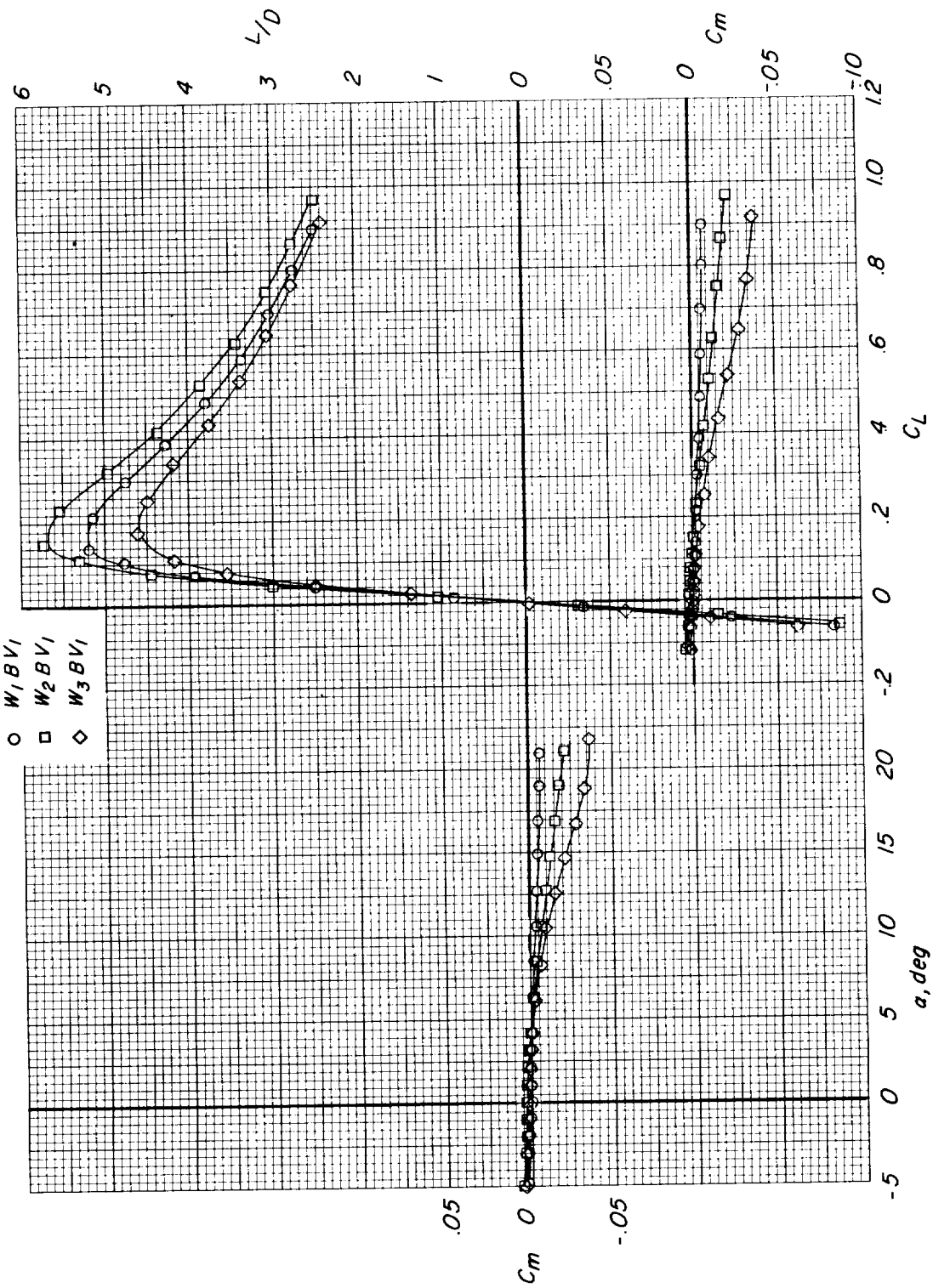

(b) Concluded.

Figure 3.- Continued.

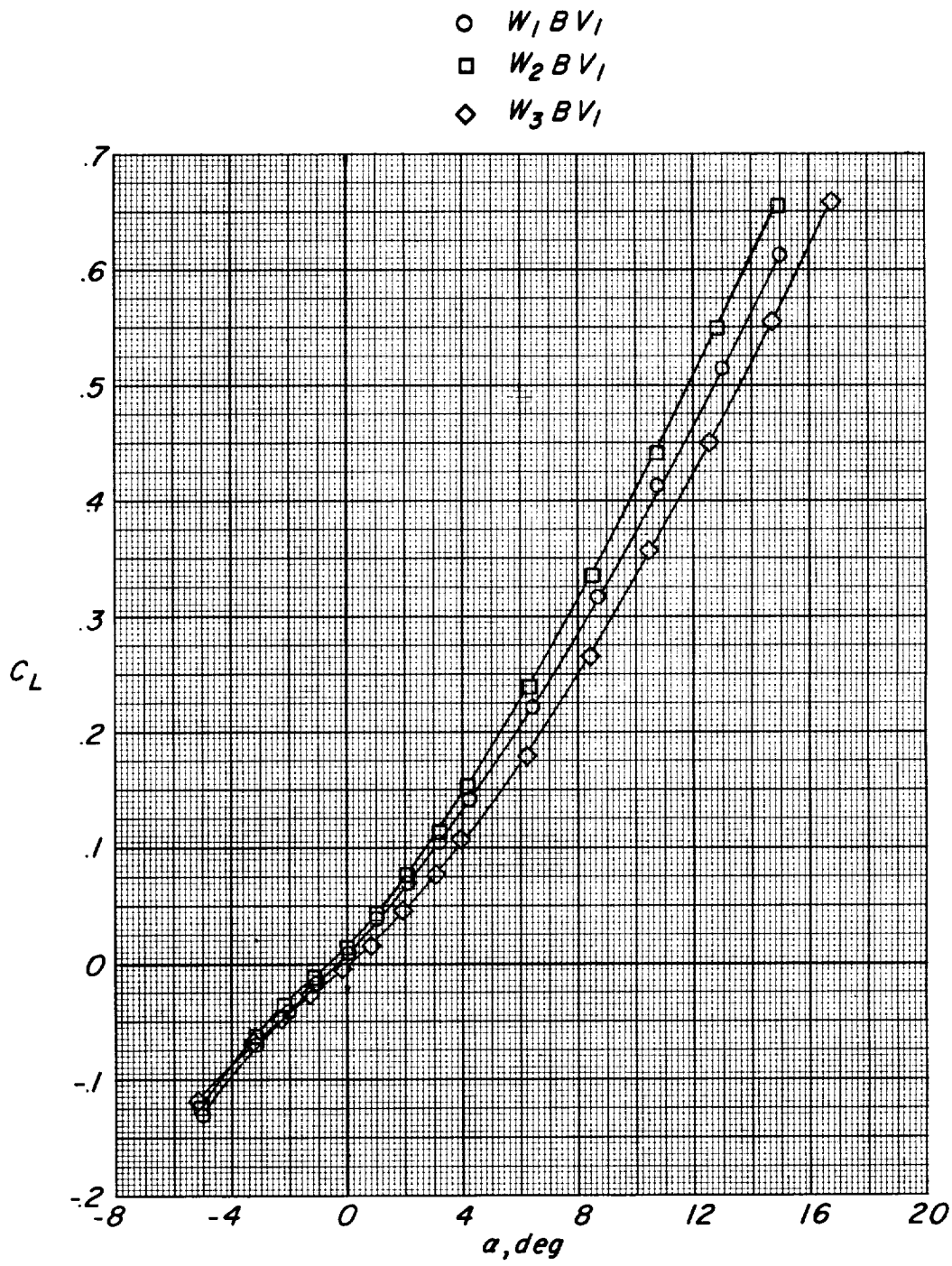

(c) M = 0.80.

Figure 3.- Continued.

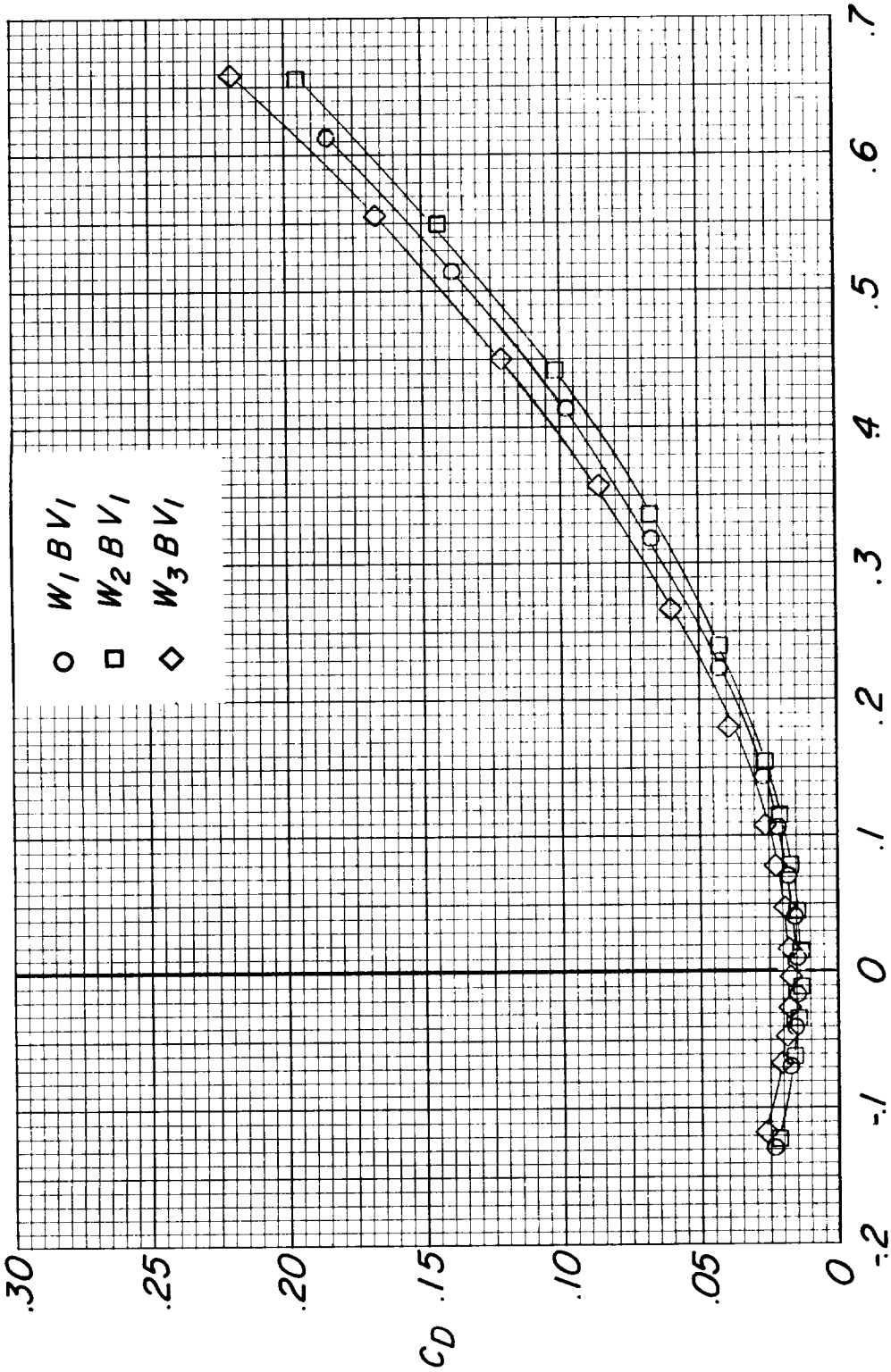

(c) Continued.

Figure 3.- Continued.

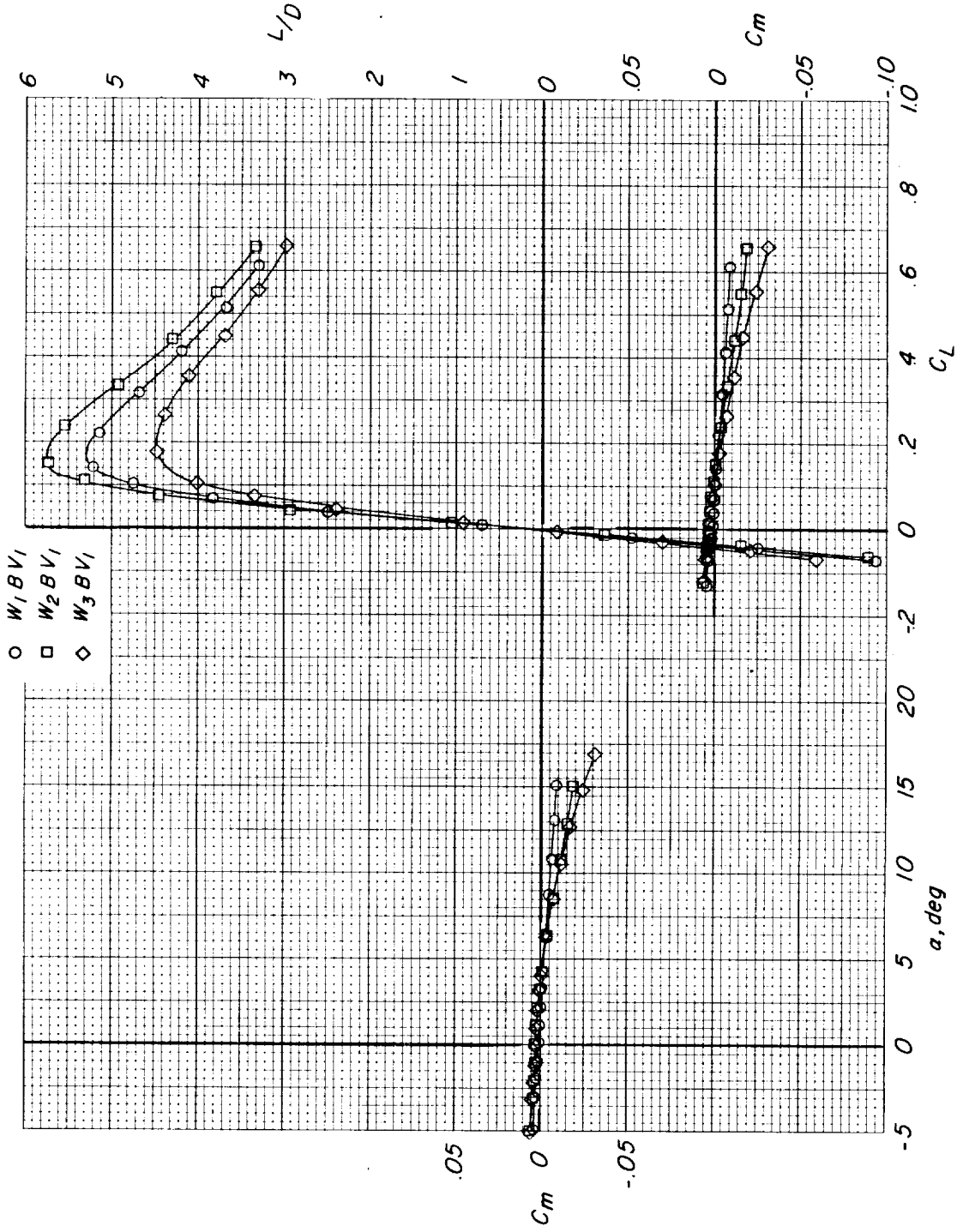

(c) Concluded.

Figure 3.- Continued.

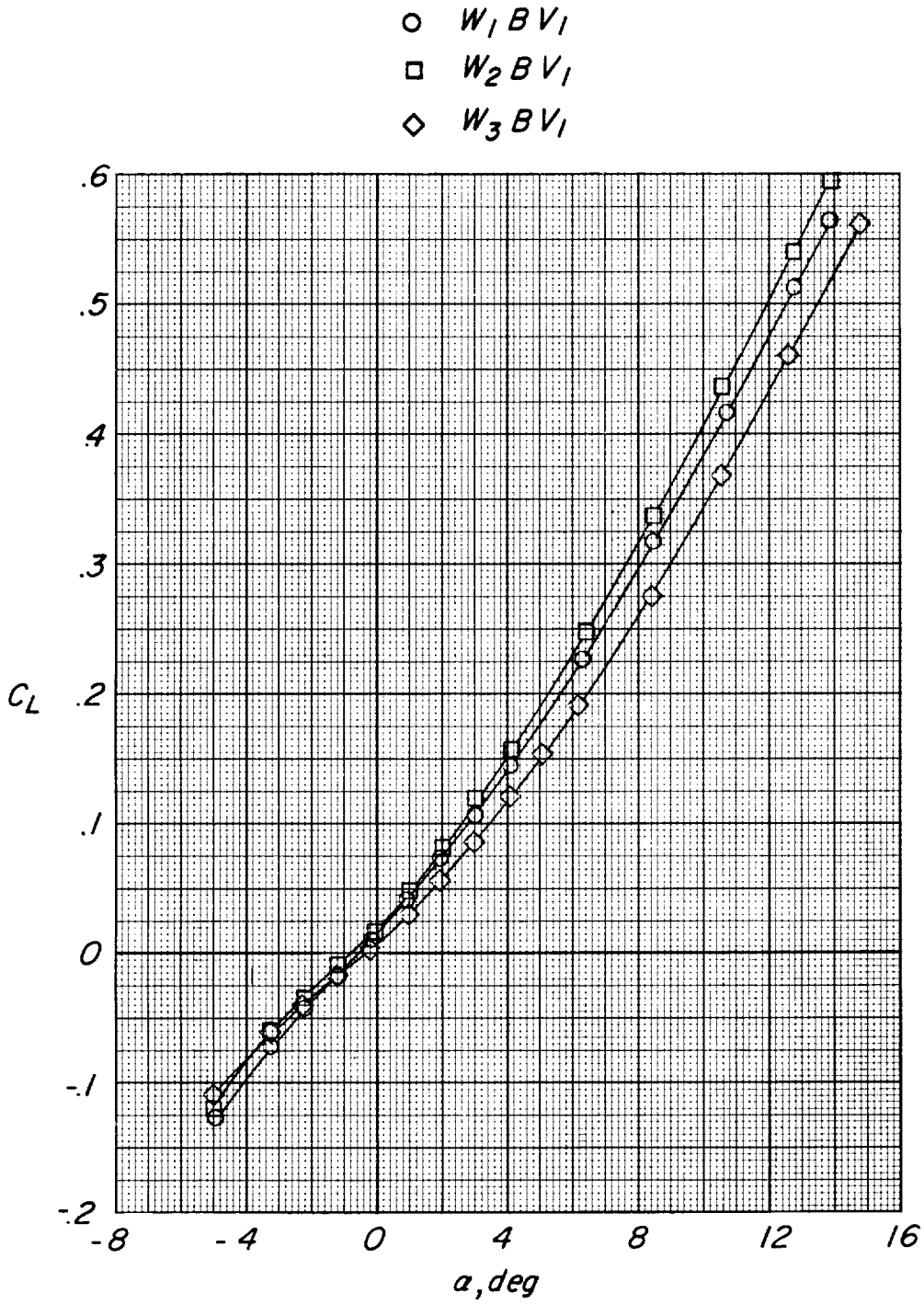

(d) M = 0.90.

Figure 3.- Continued.

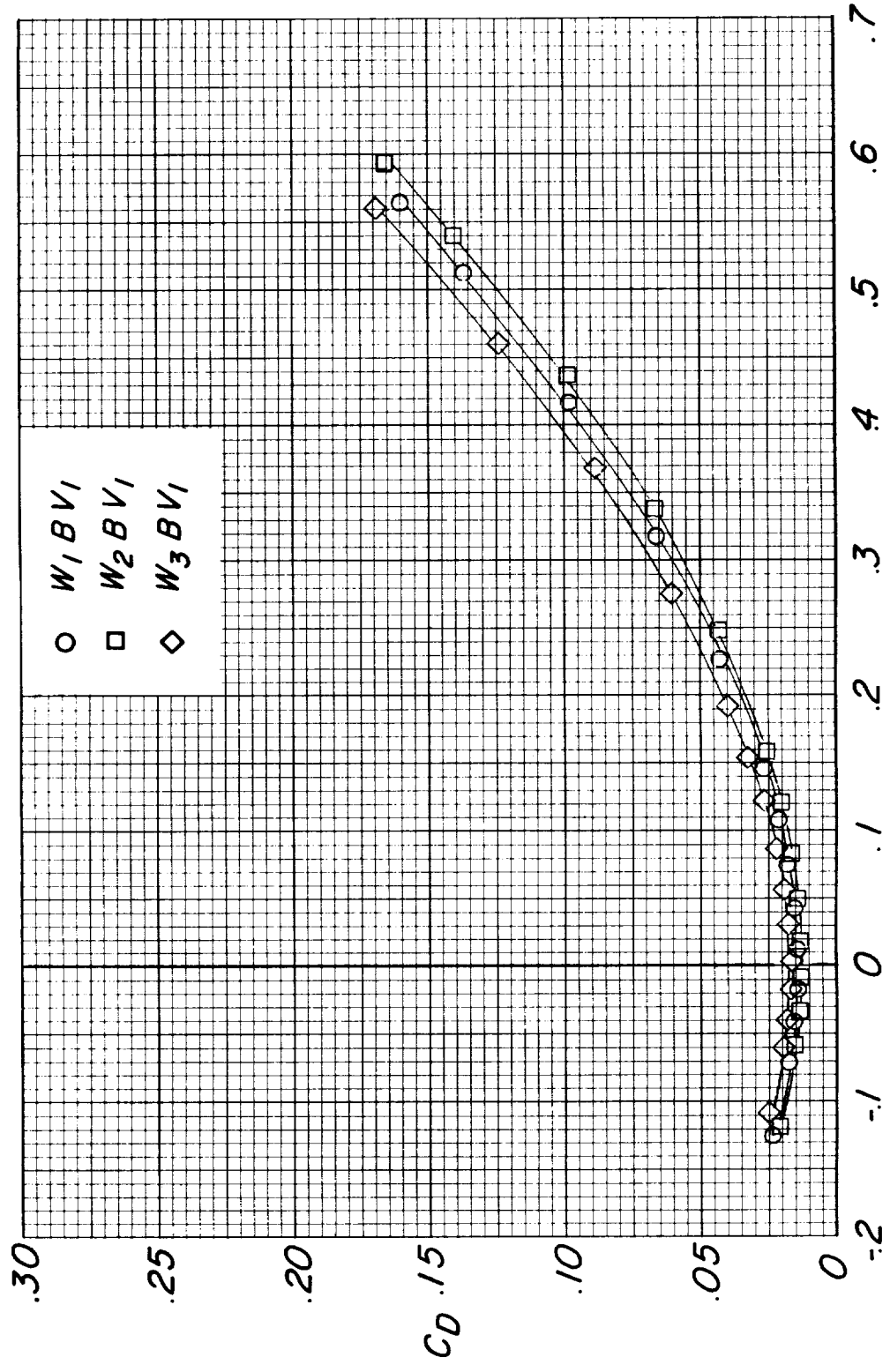

(d) Continued.

Figure 3.- Continued.

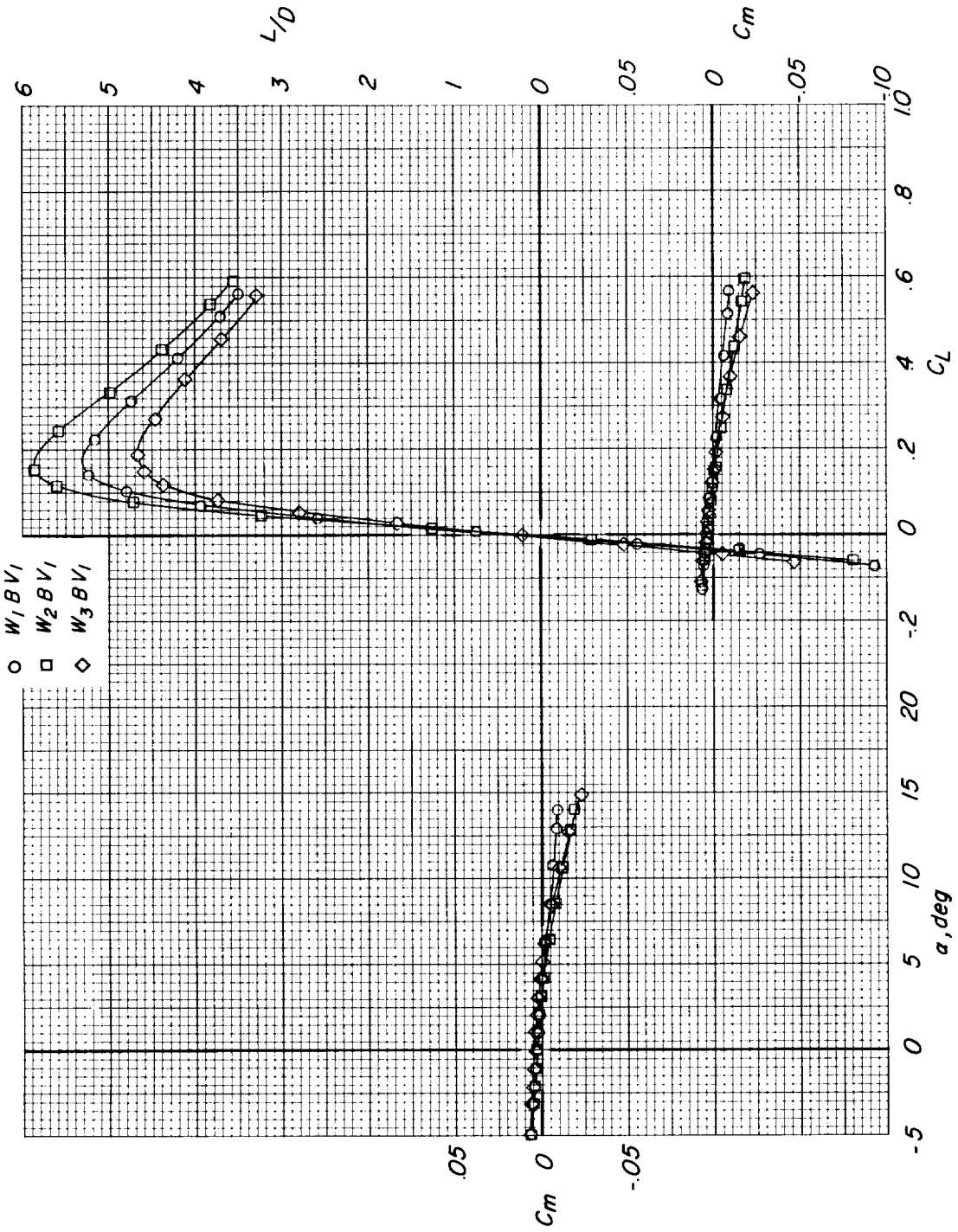

(d) Concluded.

Figure 3.- Continued.

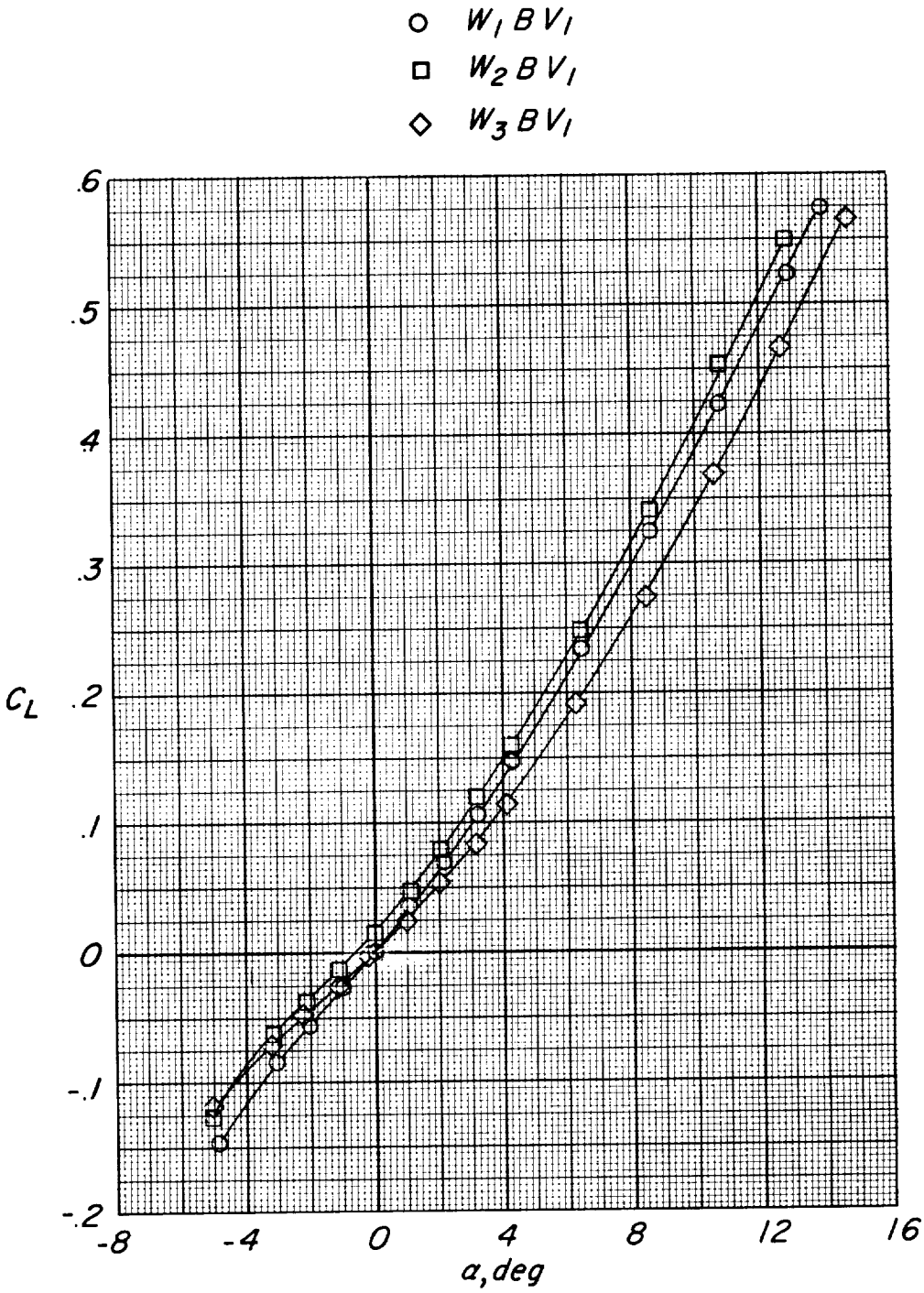

(e) M = 0.95.

Figure 3.- Continued.

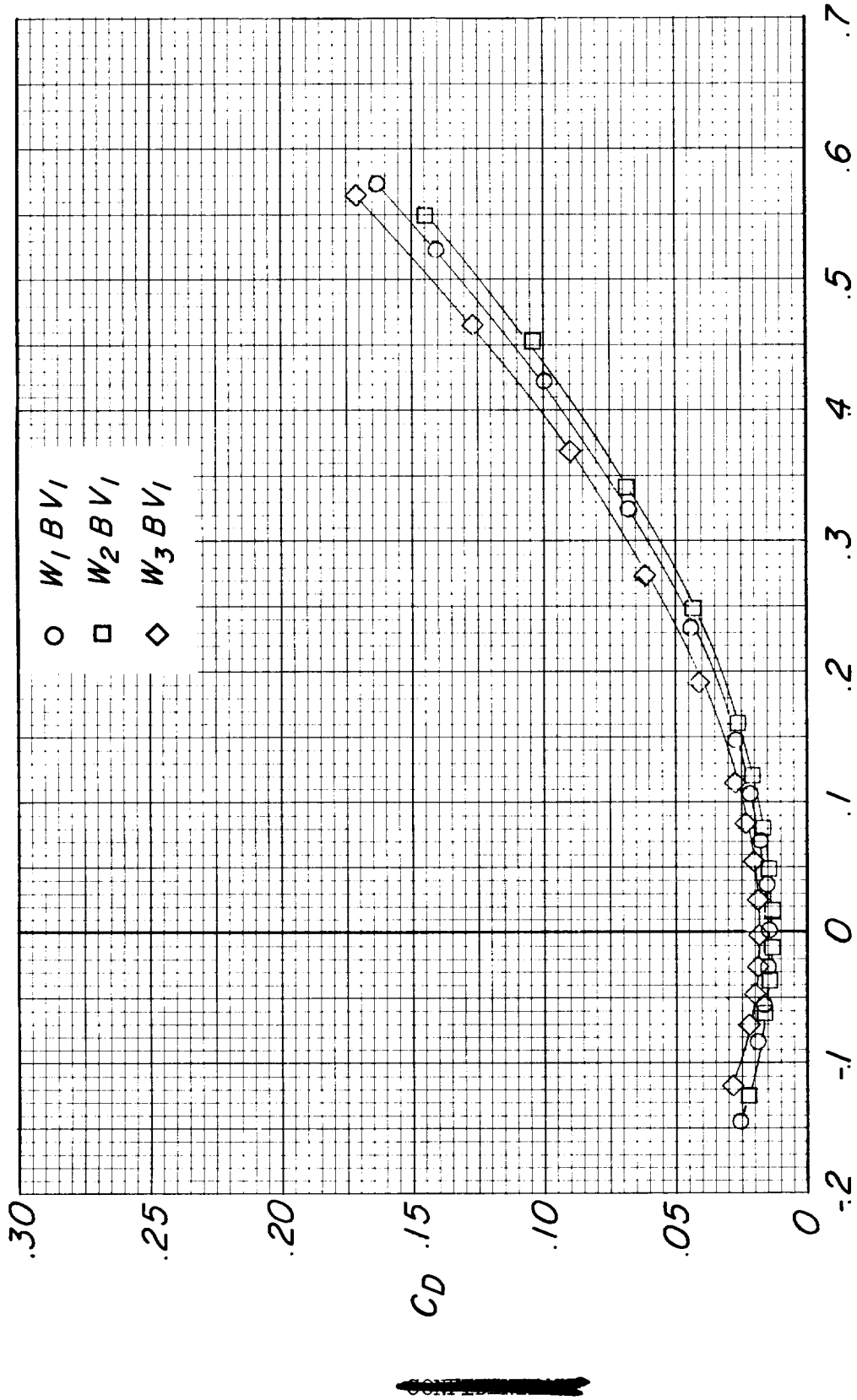

(e) Continued.

Figure 3.- Continued.

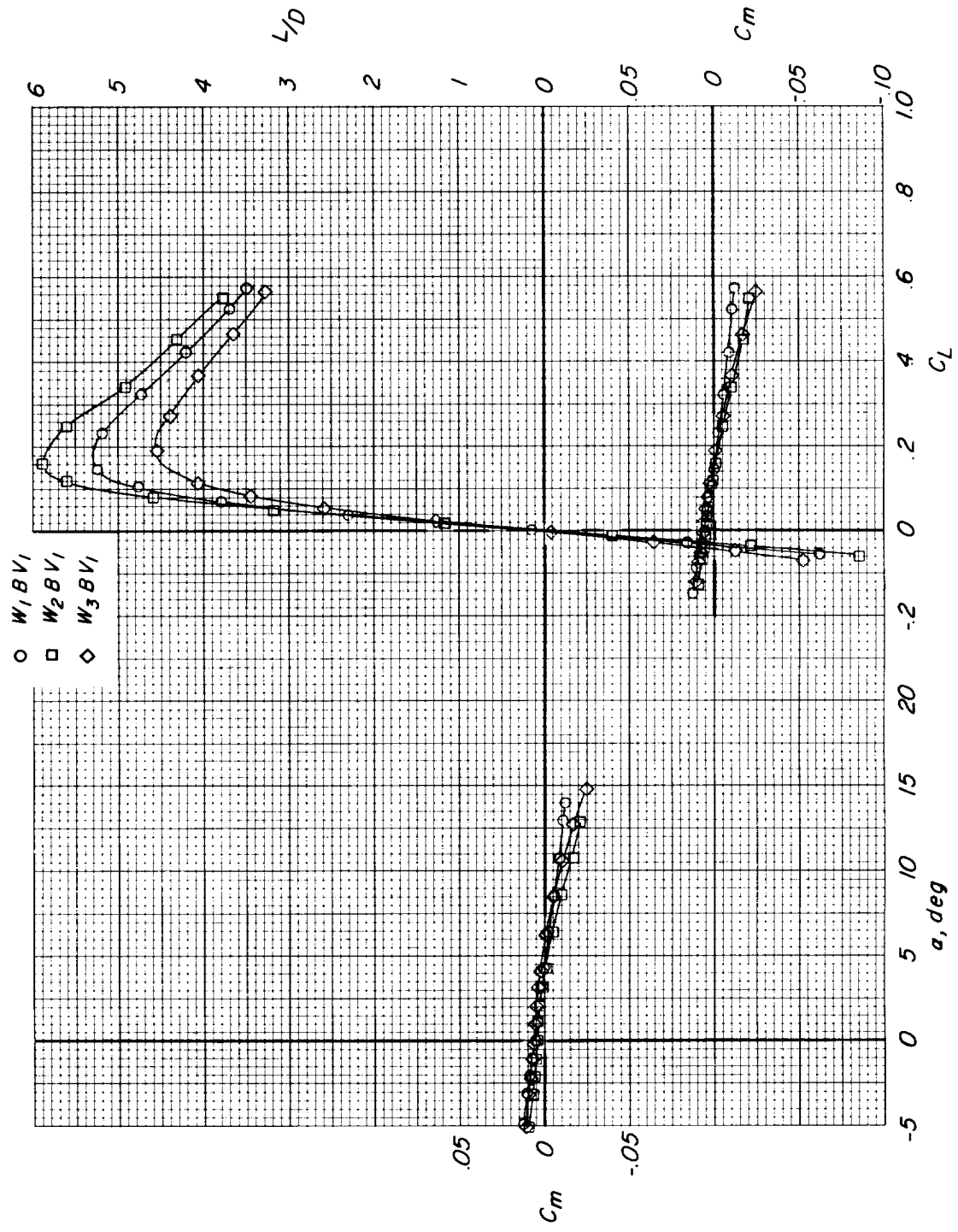

(e) Concluded.

Figure 3.- Continued.

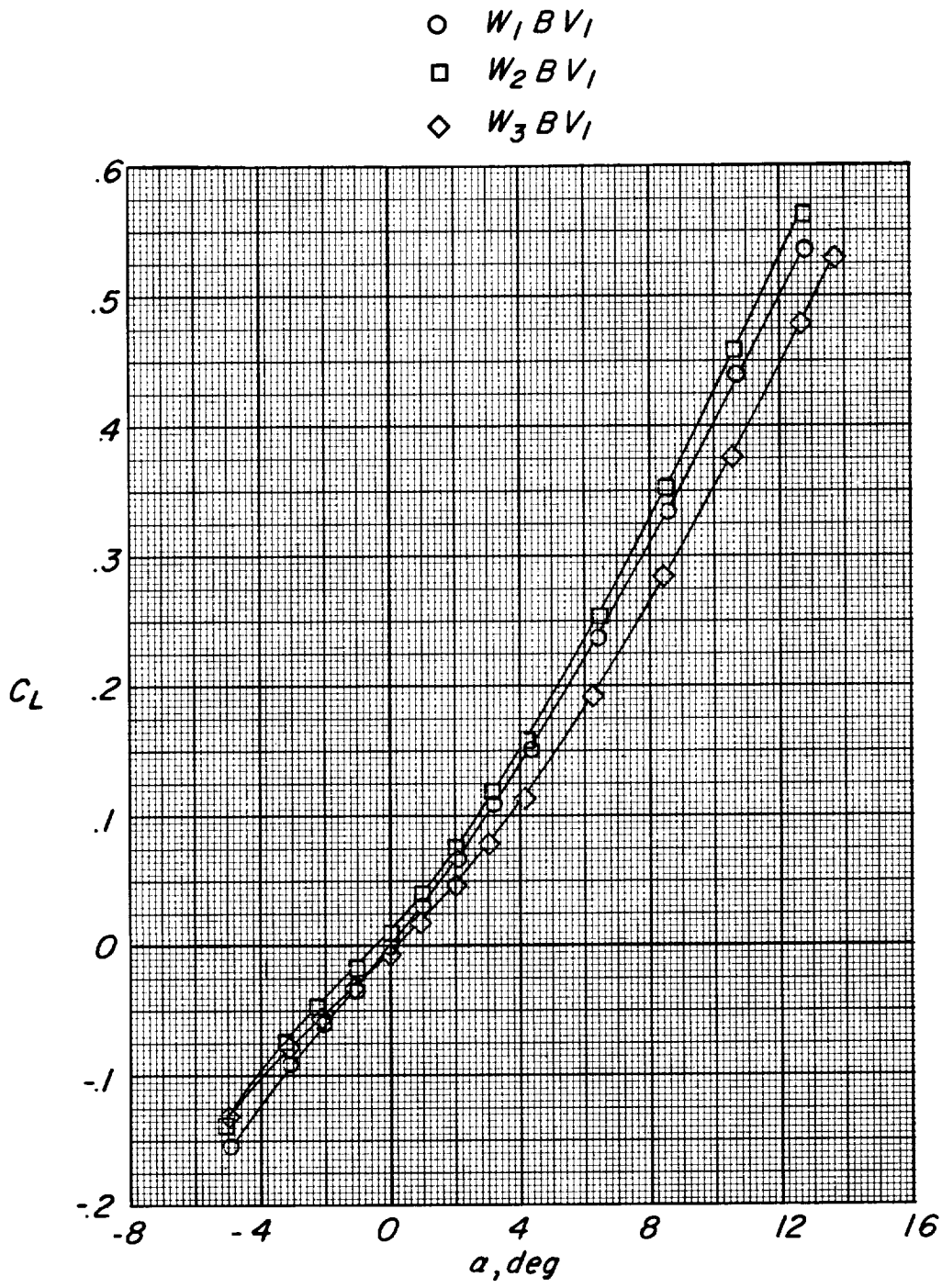

(f) M = 1.00.

Figure 3.- Continued.

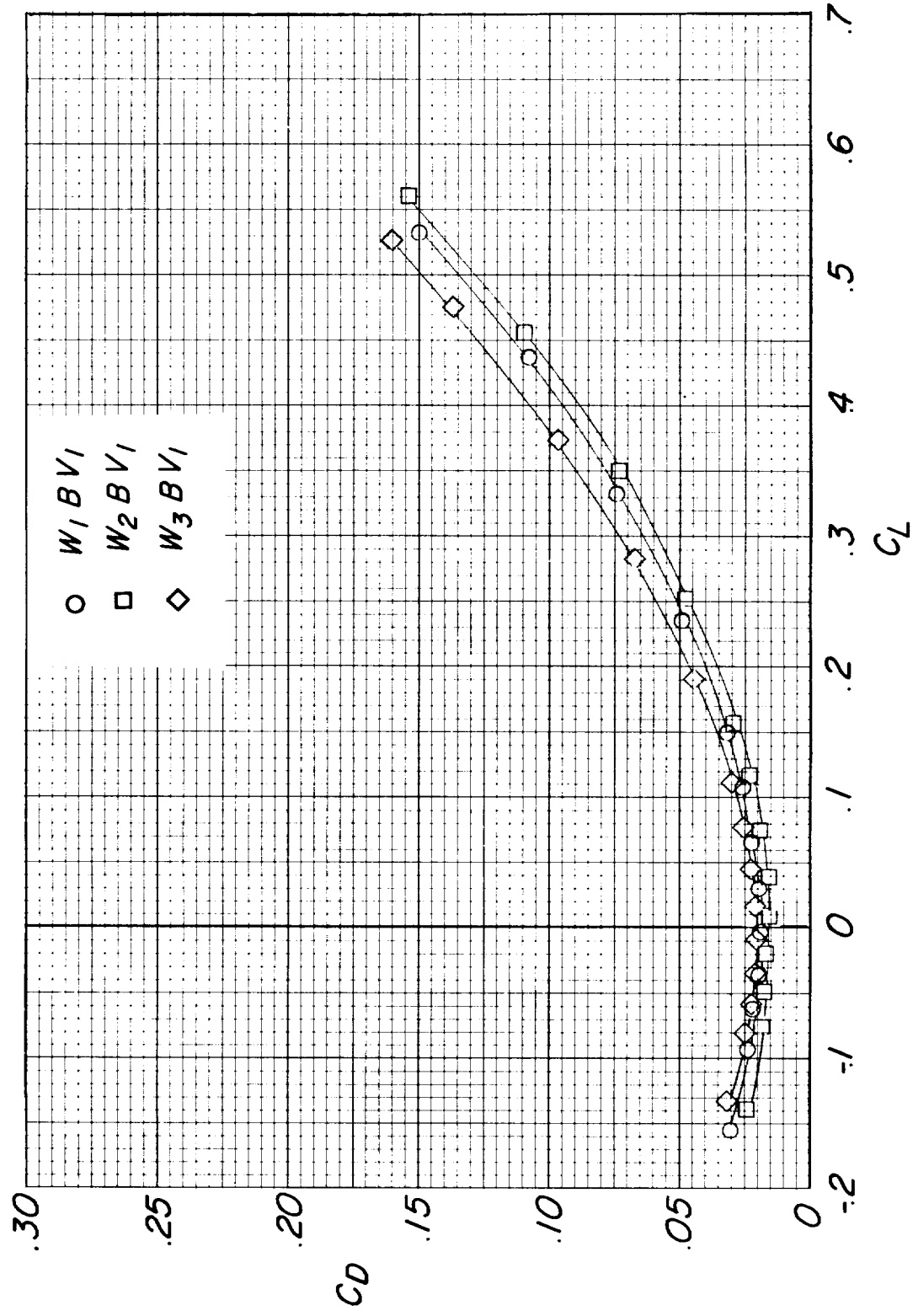

(f) Continued.

Figure 3.- Continued.

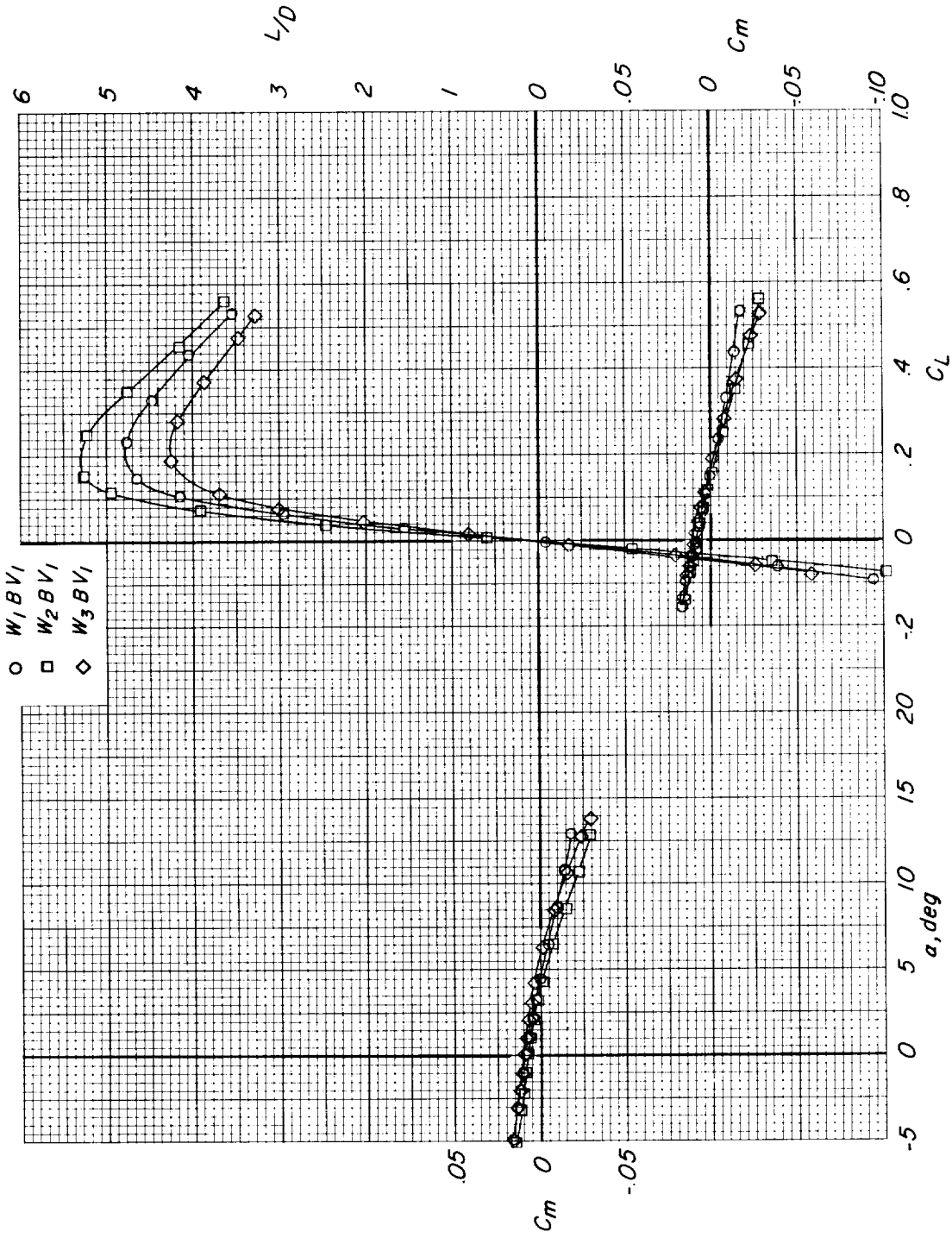

(f) Concluded.

Figure 3.- Continued.

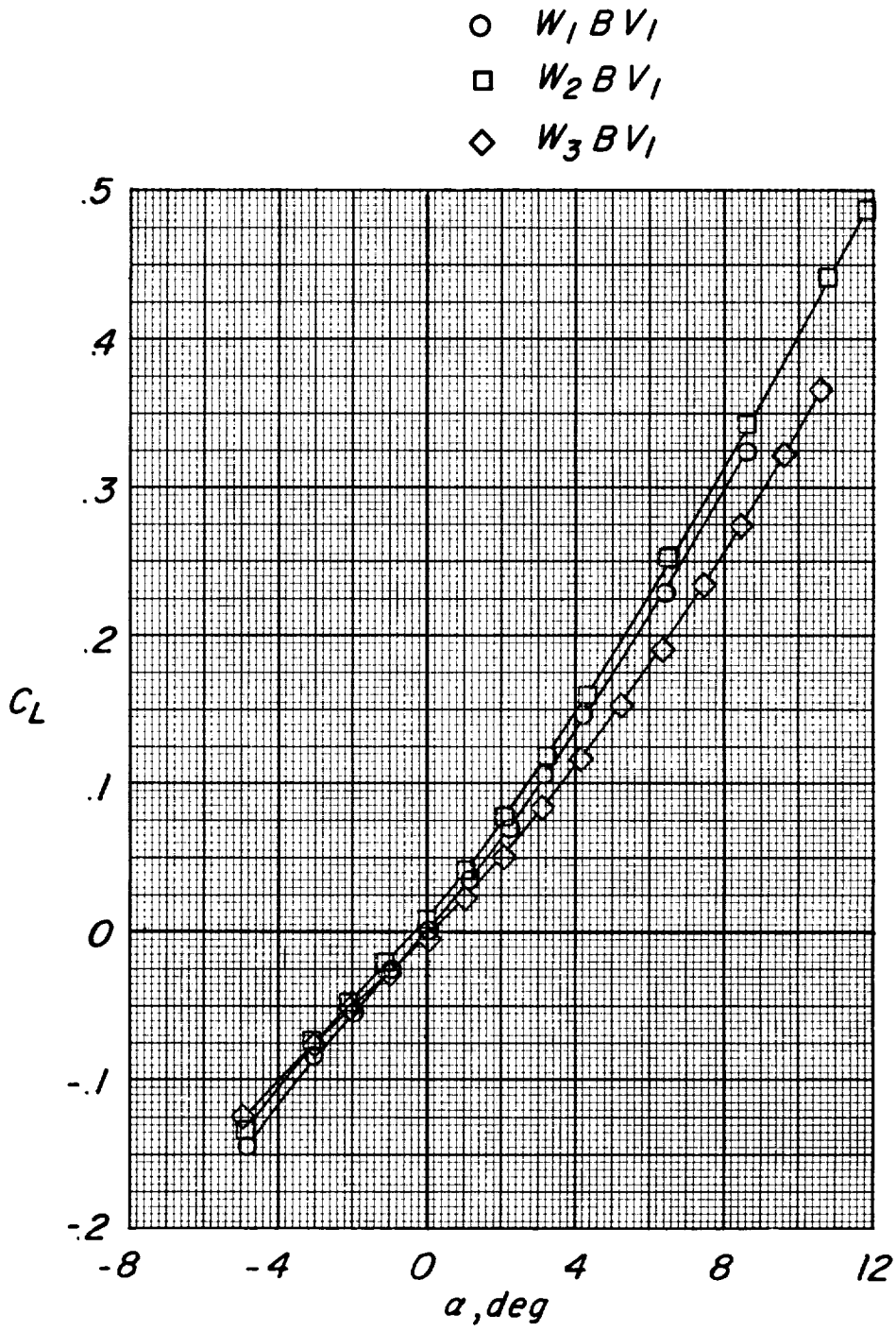

(g) M = 1.13.

Figure 3.- Continued.

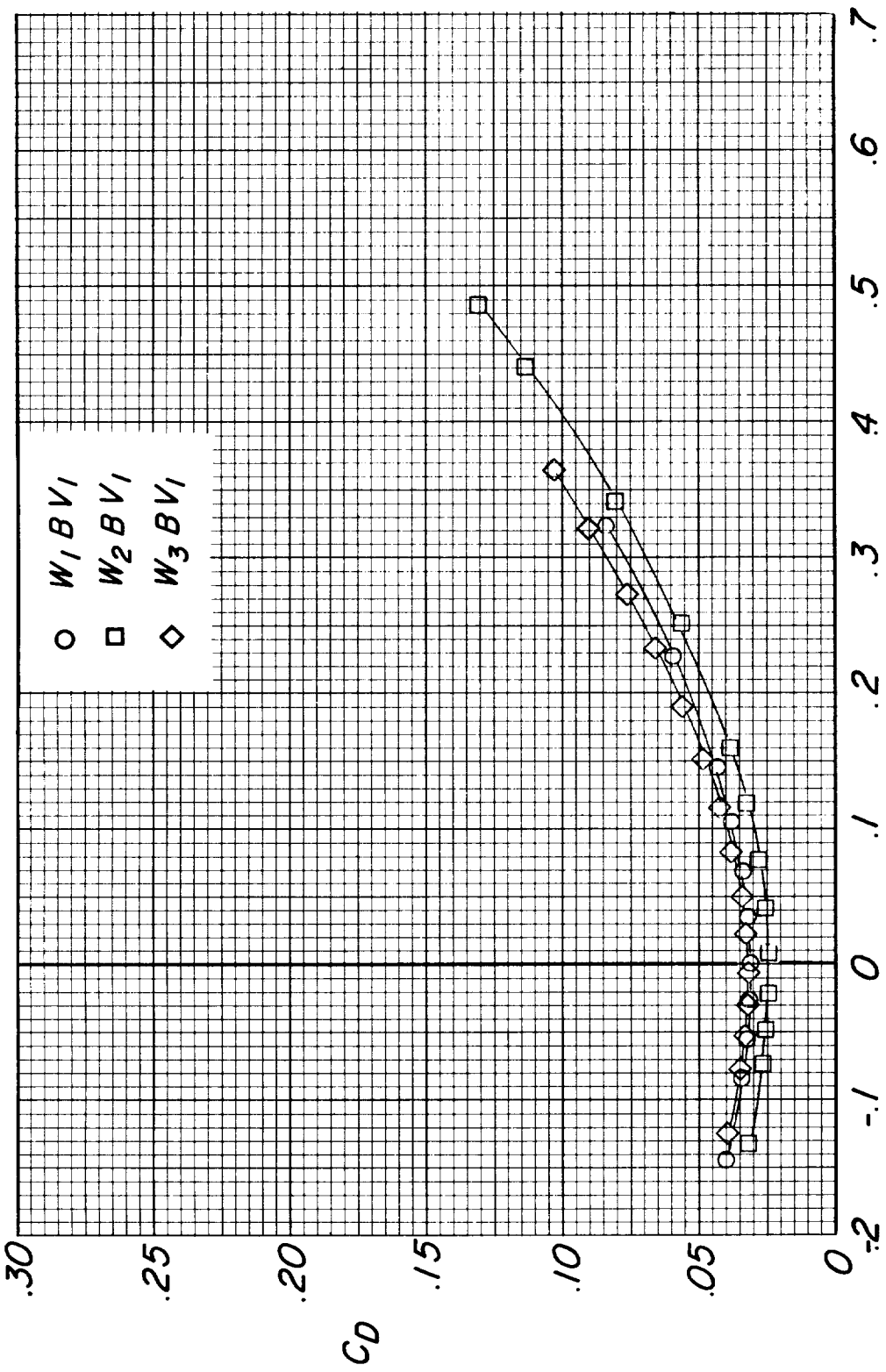

(g) Continued.

Figure 3.- Continued.

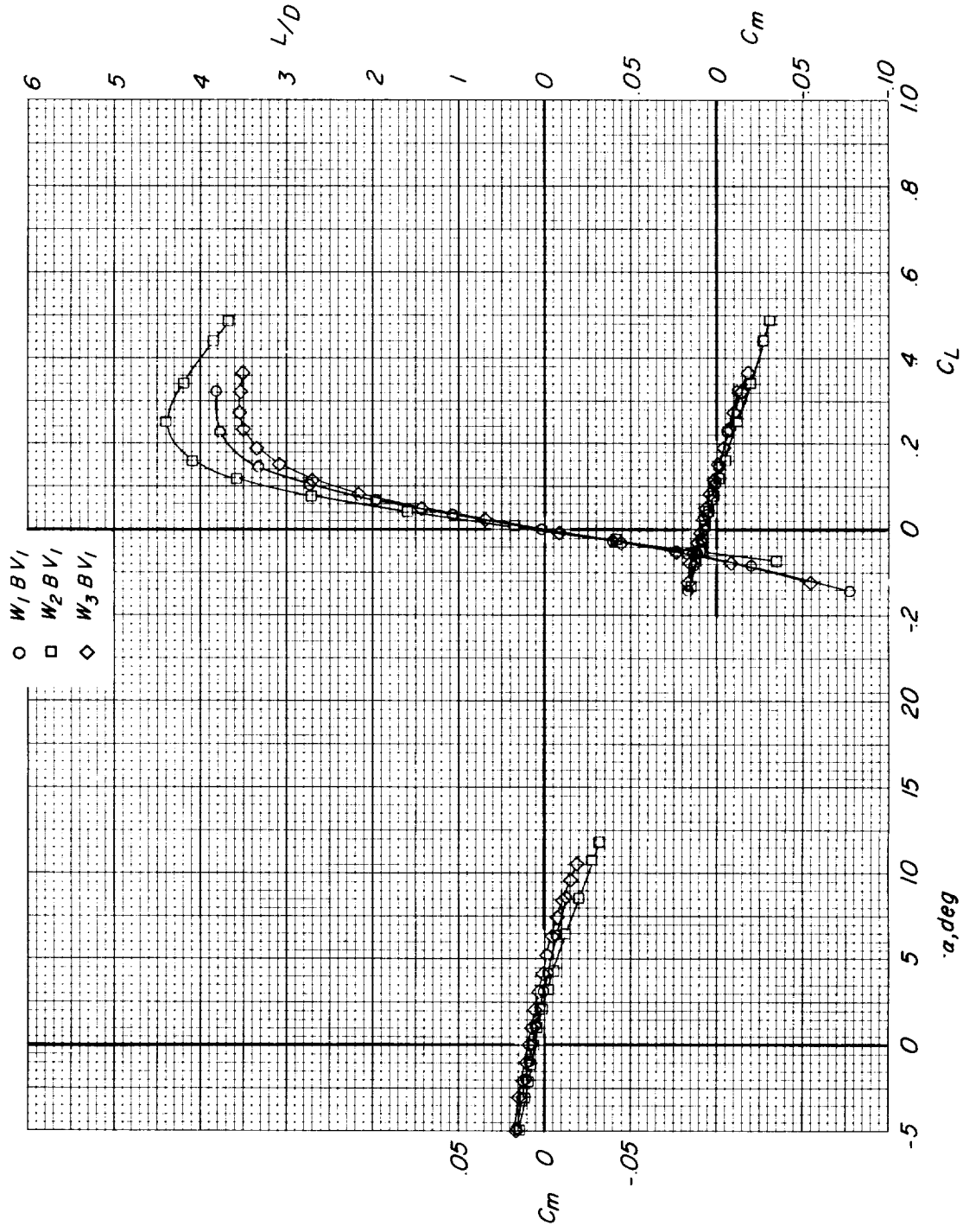

(g) Concluded.

Figure 3.- Concluded.

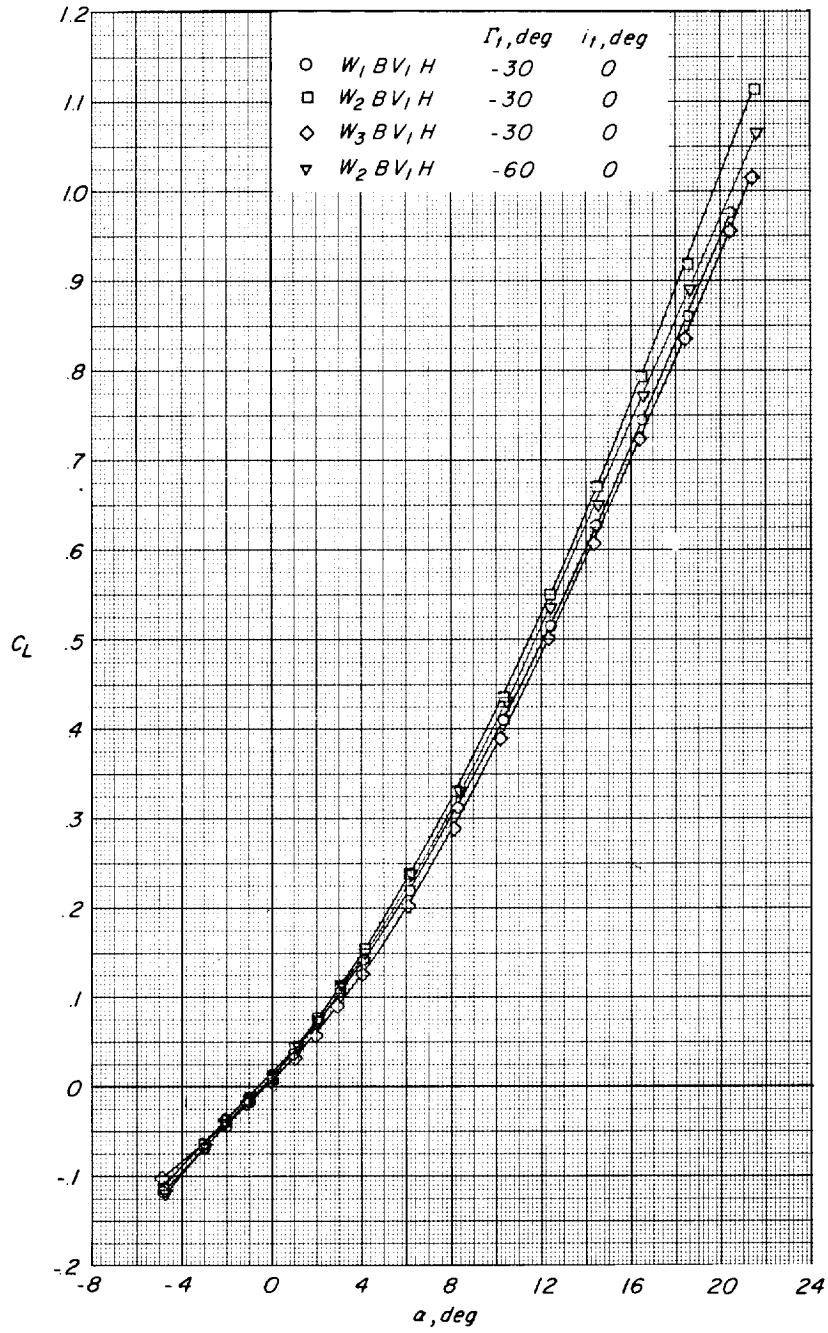

(a) M = 0.40.

Figure 4.- Effects of wing planform on the longitudinal aerodynamic characteristics of the configuration having the horizontal stabilizers on, at various Mach numbers. Small center vertical tail (V_1) on.

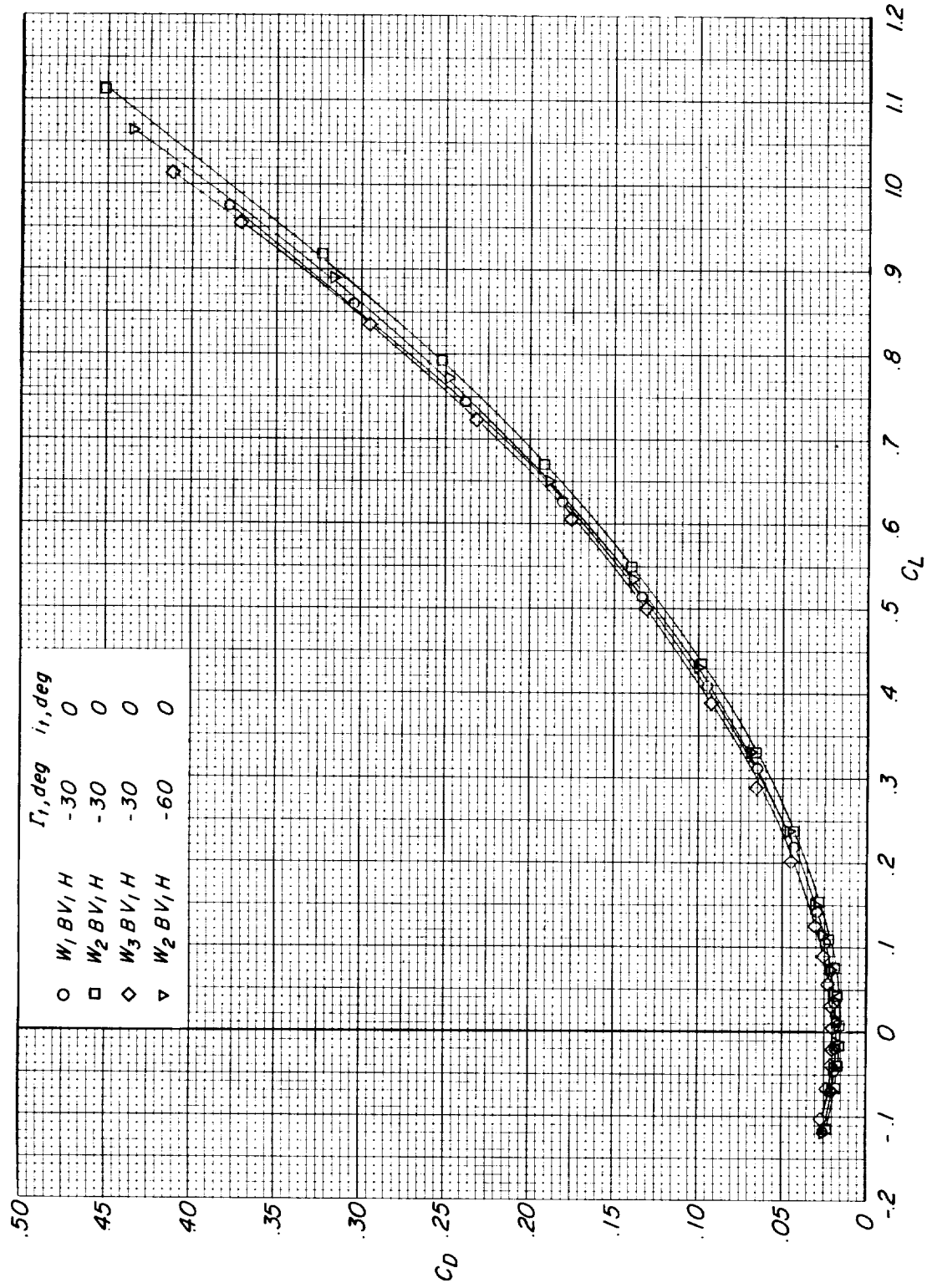

(a) Continued.

Figure 4.- Continued.

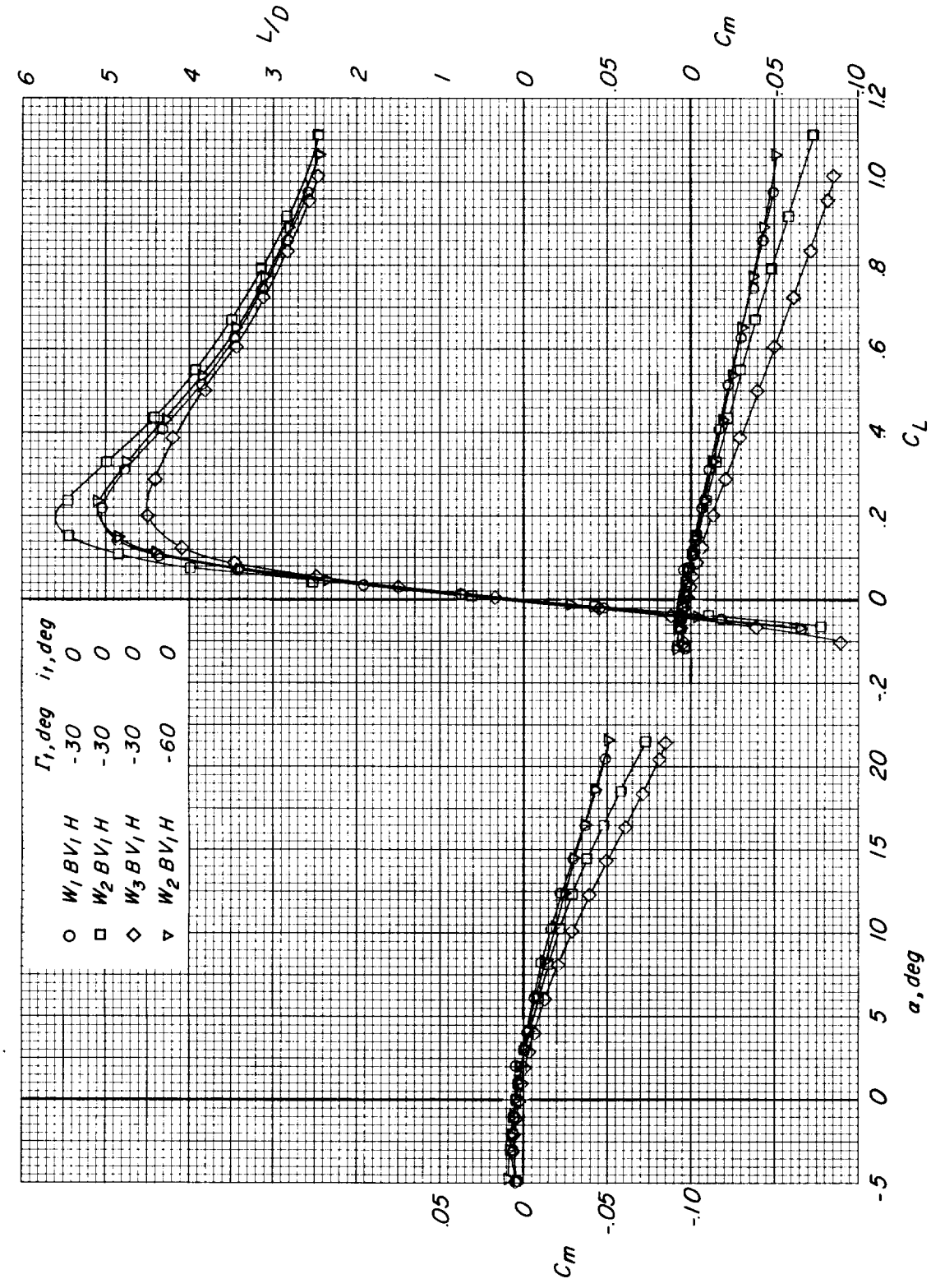

(a) Concluded.

Figure 4.- Continued.

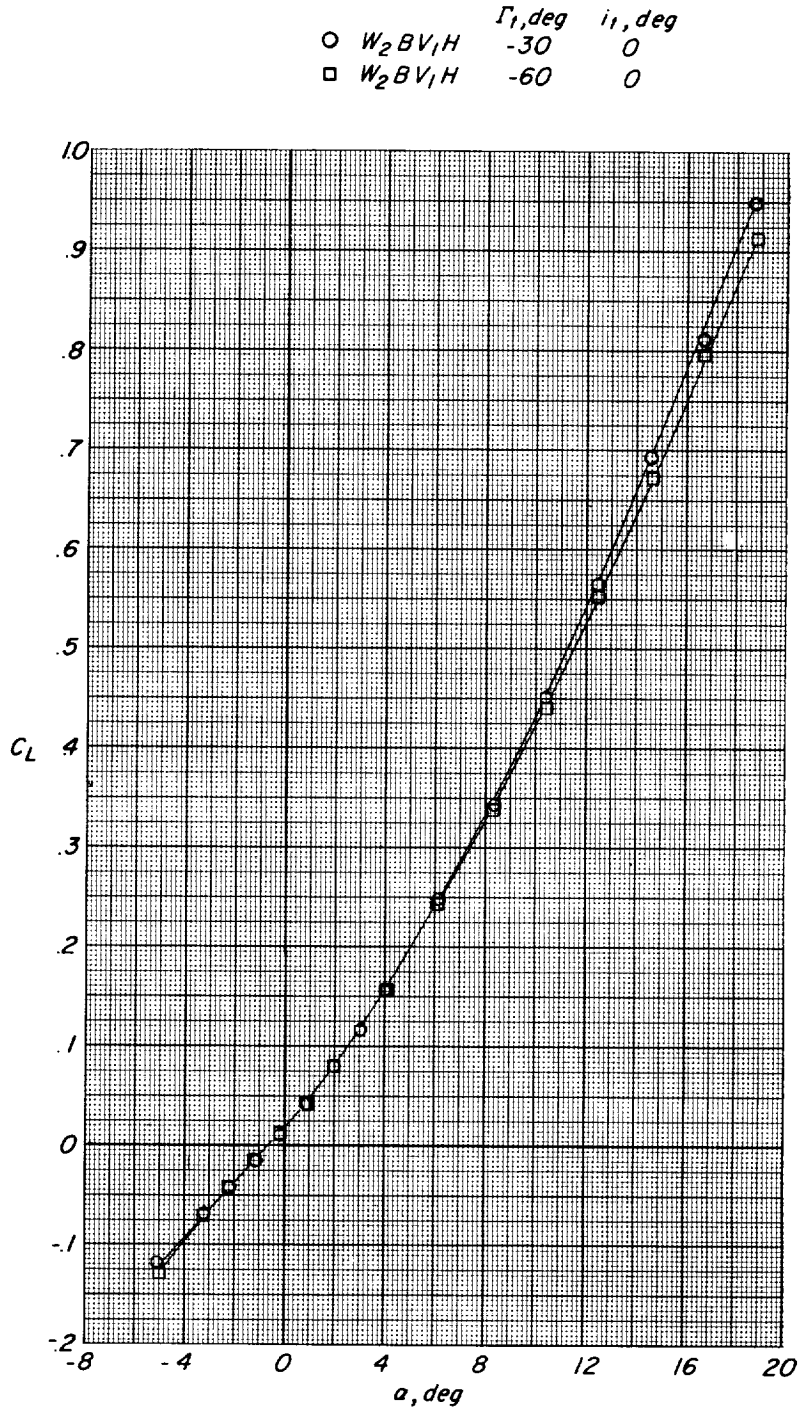

(b) M = 0.60.

Figure 4.- Continued.

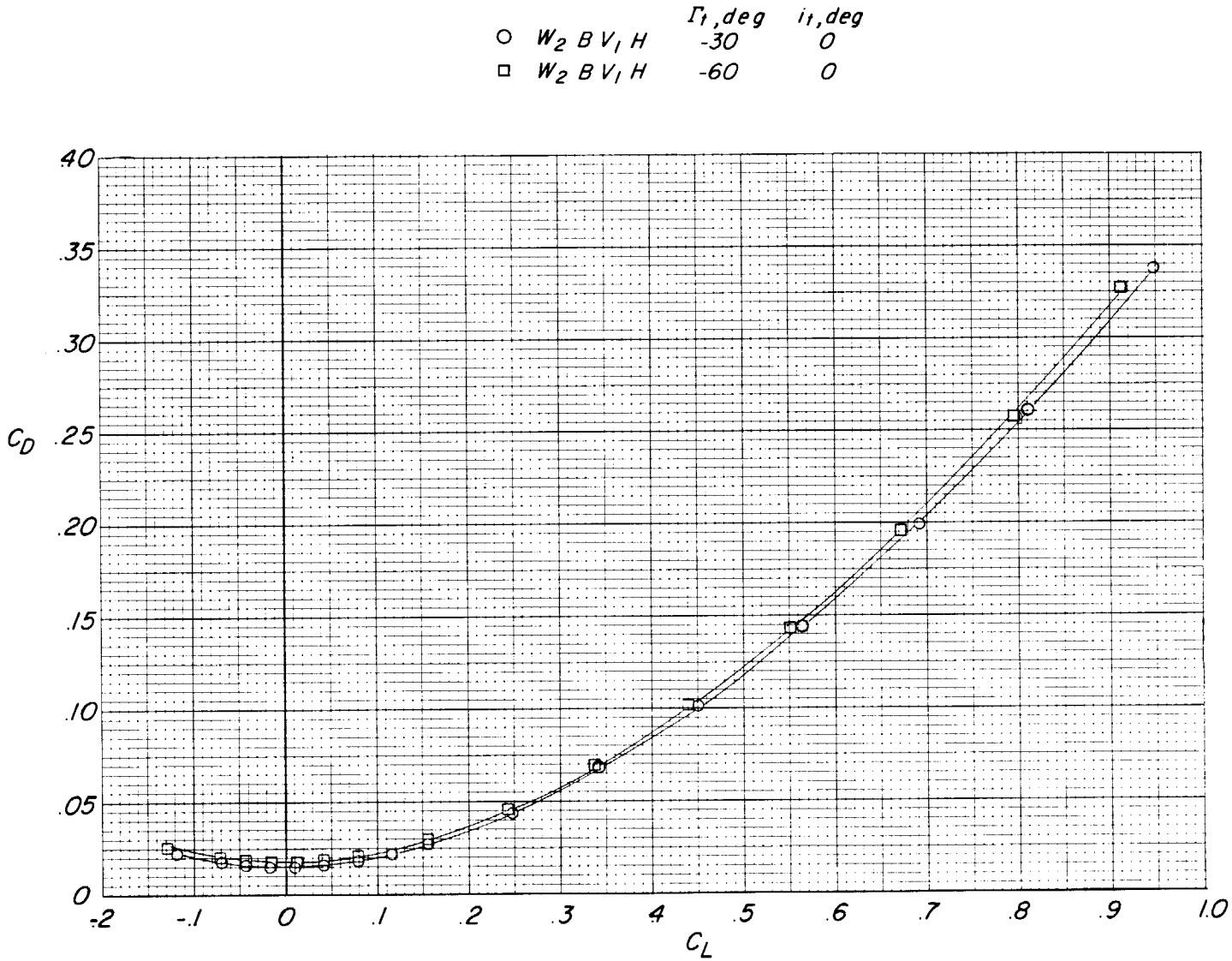

(b) Continued.

Figure 4.- Continued.

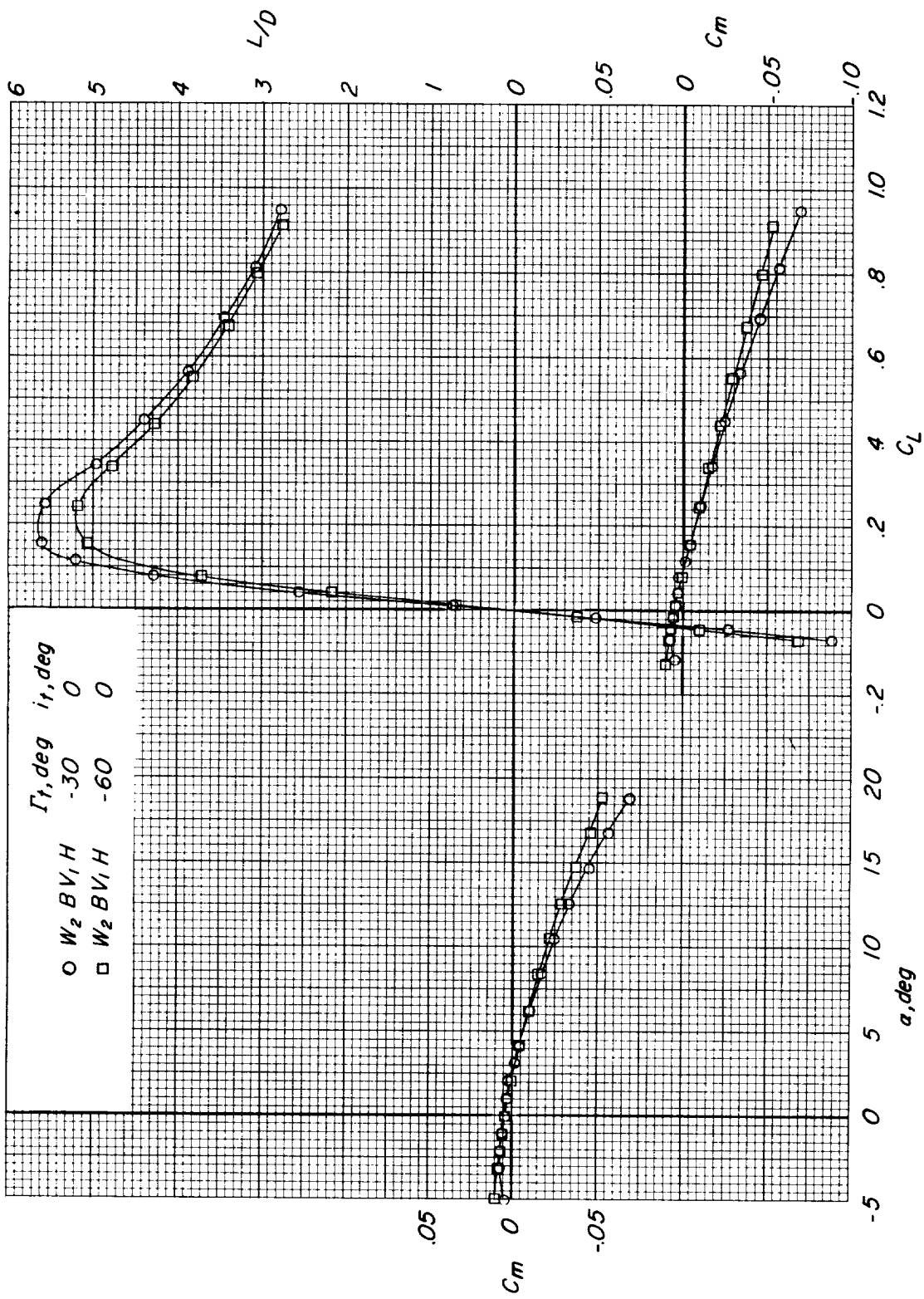

(b) Concluded.

Figure 4.- Continued.

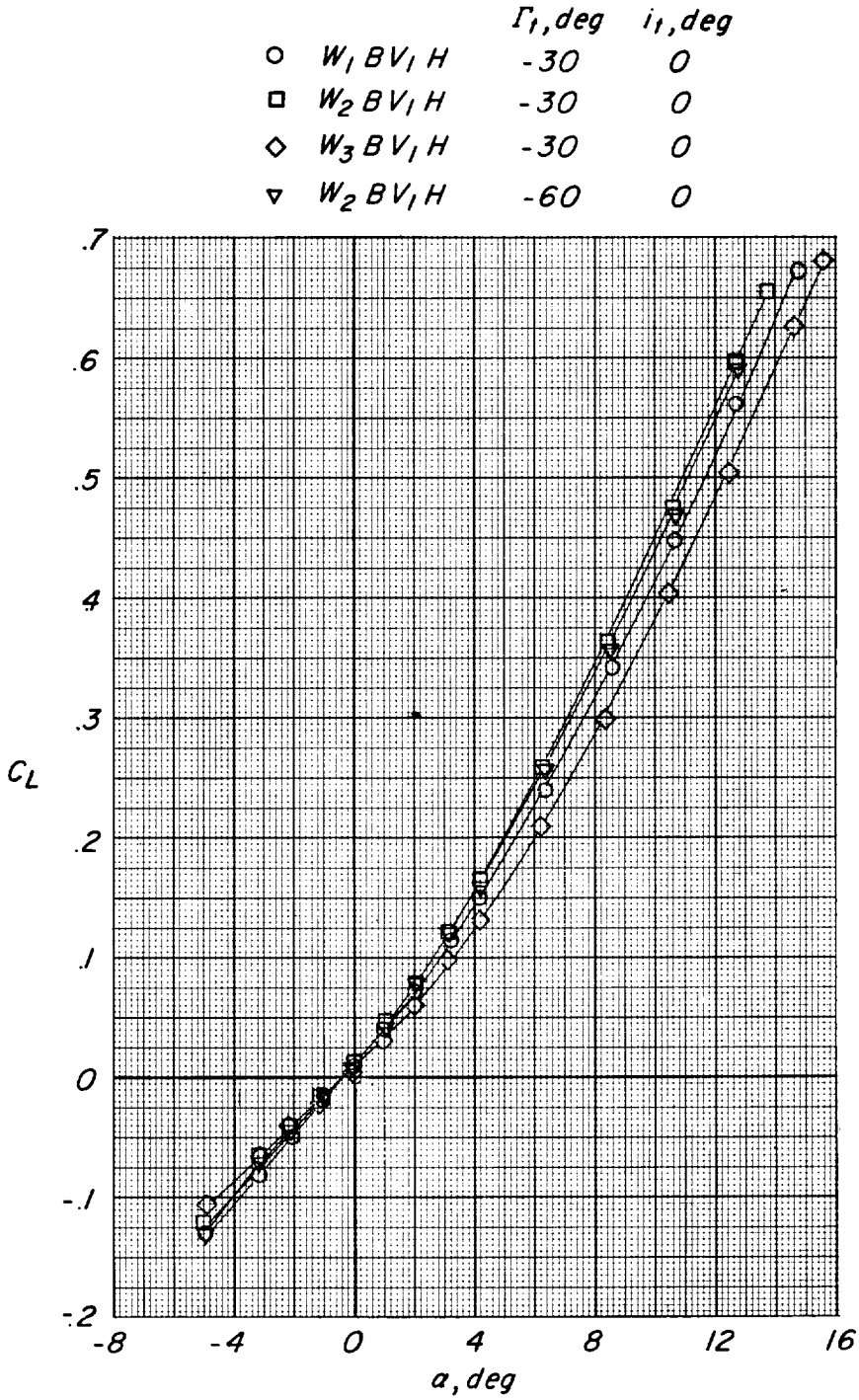

(c) M = 0.80.

Figure 4.- Continued.

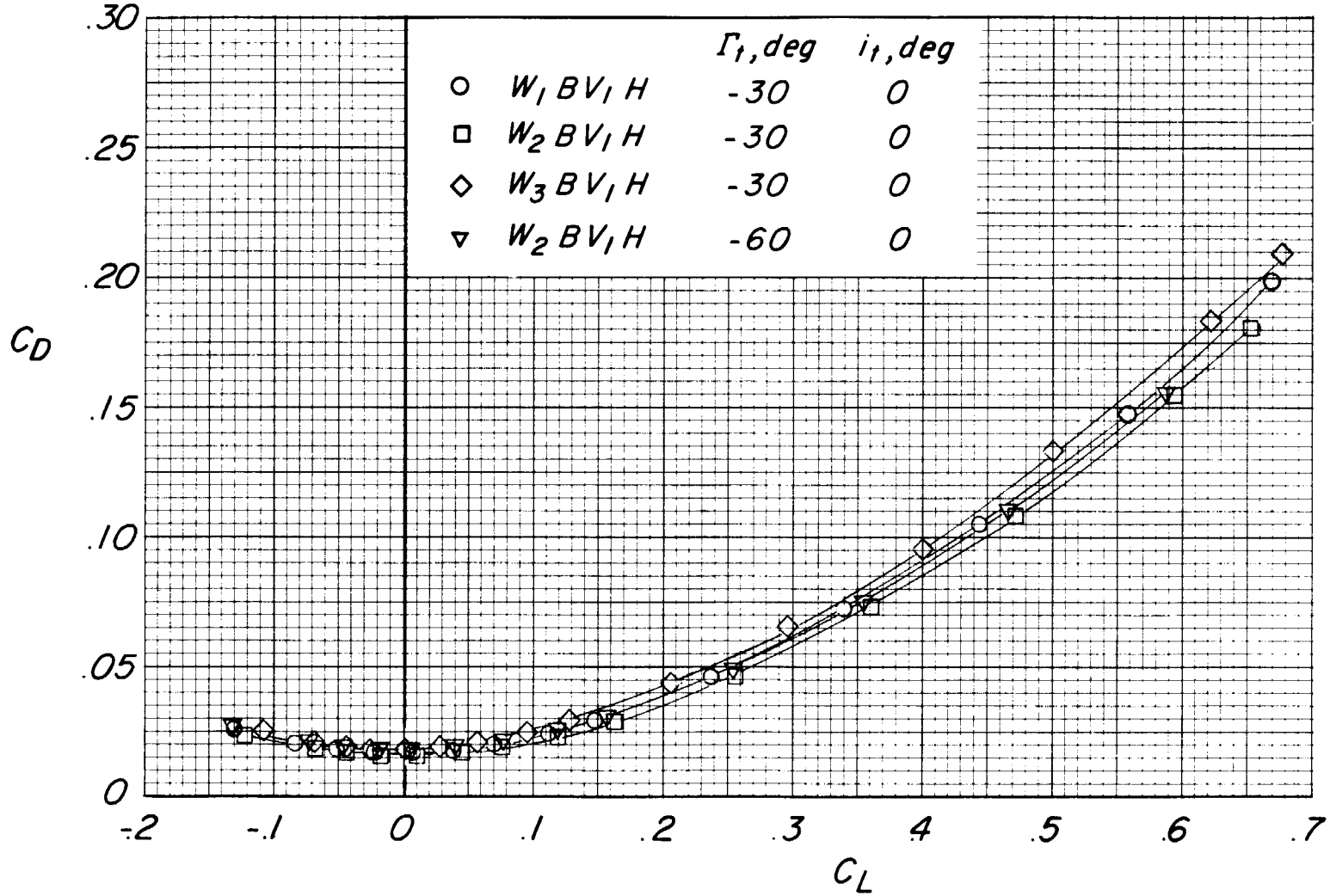

(c) Continued.

Figure 4.- Continued.

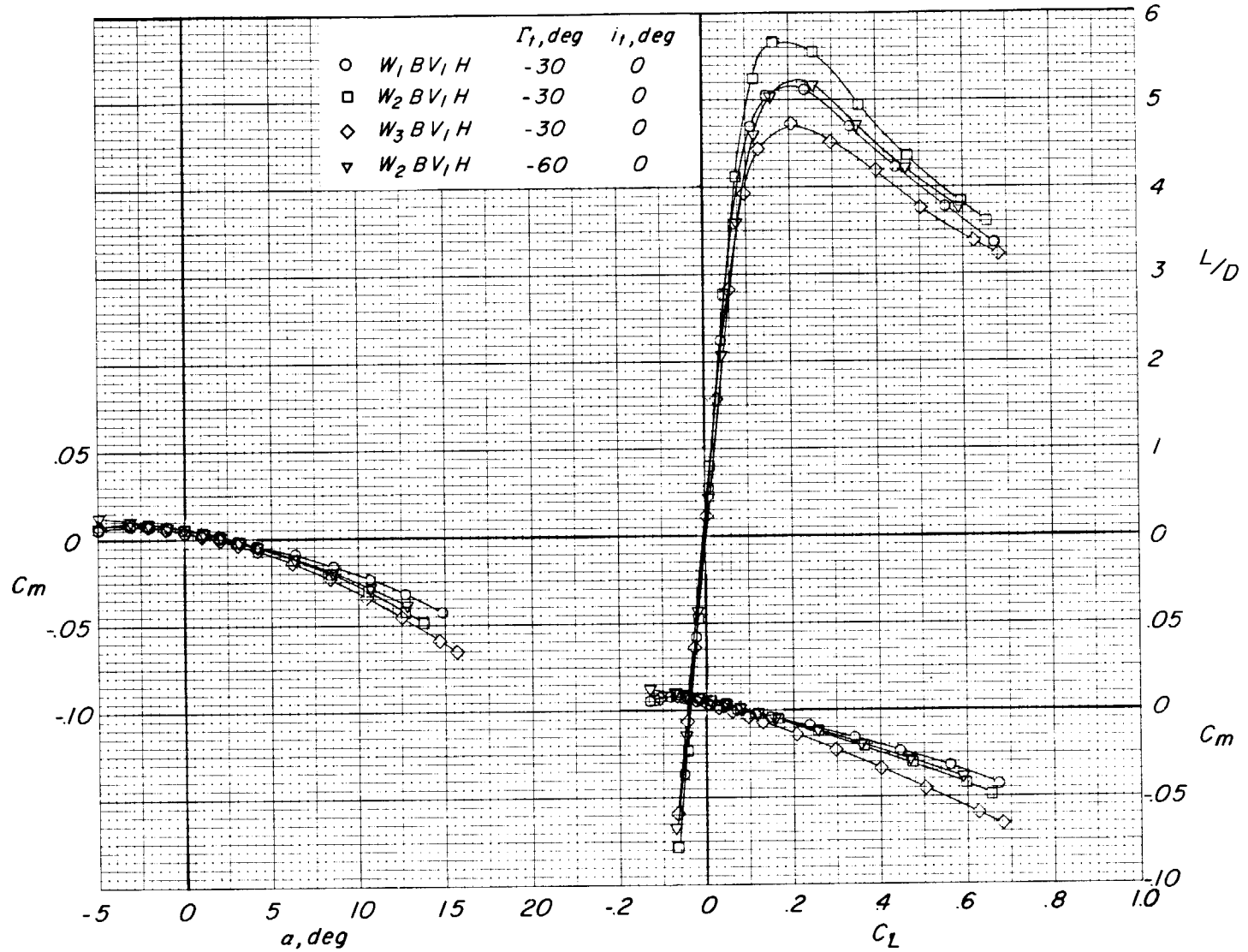

(c) Concluded.

Figure 4.- Continued.

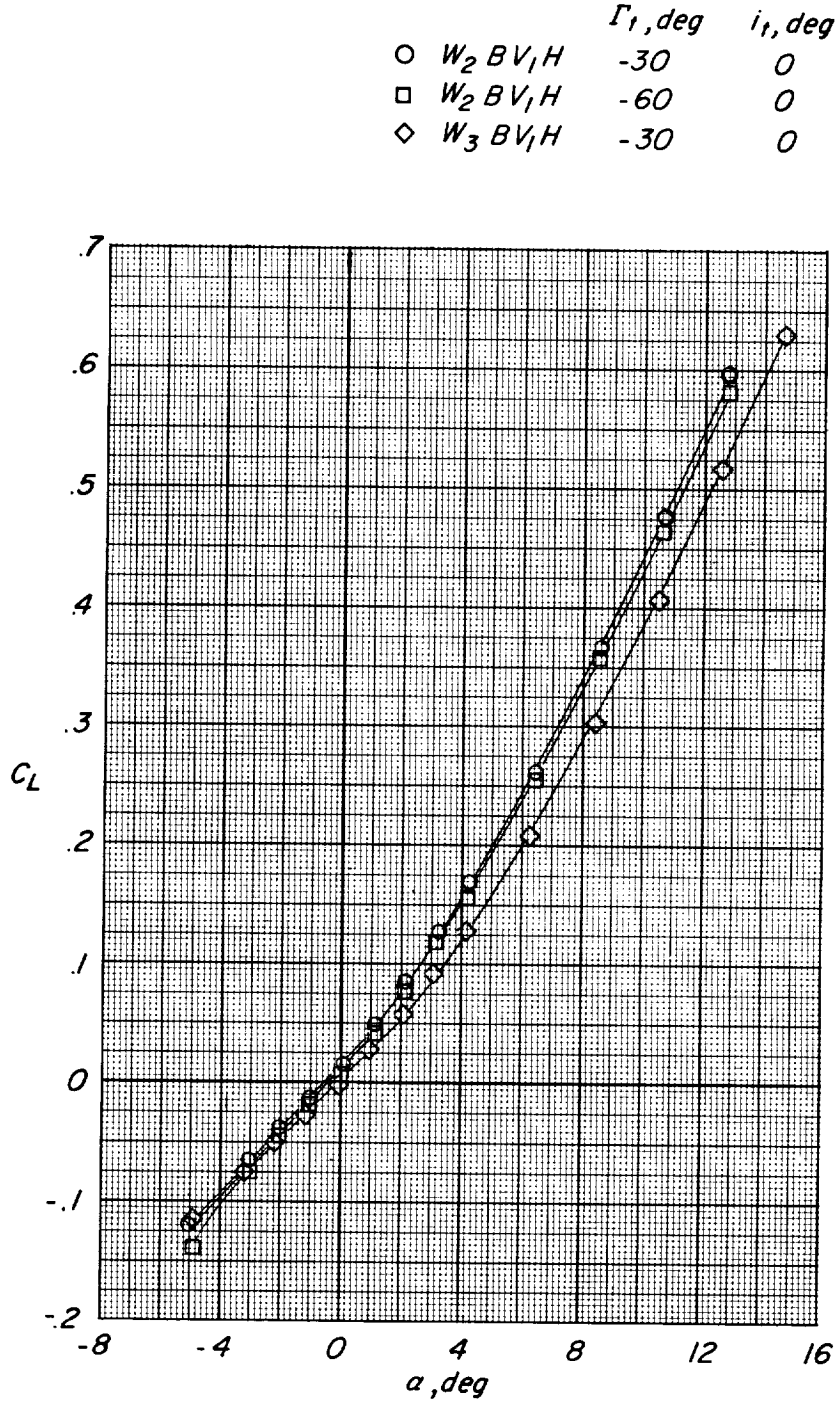

(d) M = 0.90.

Figure 4.- Continued.

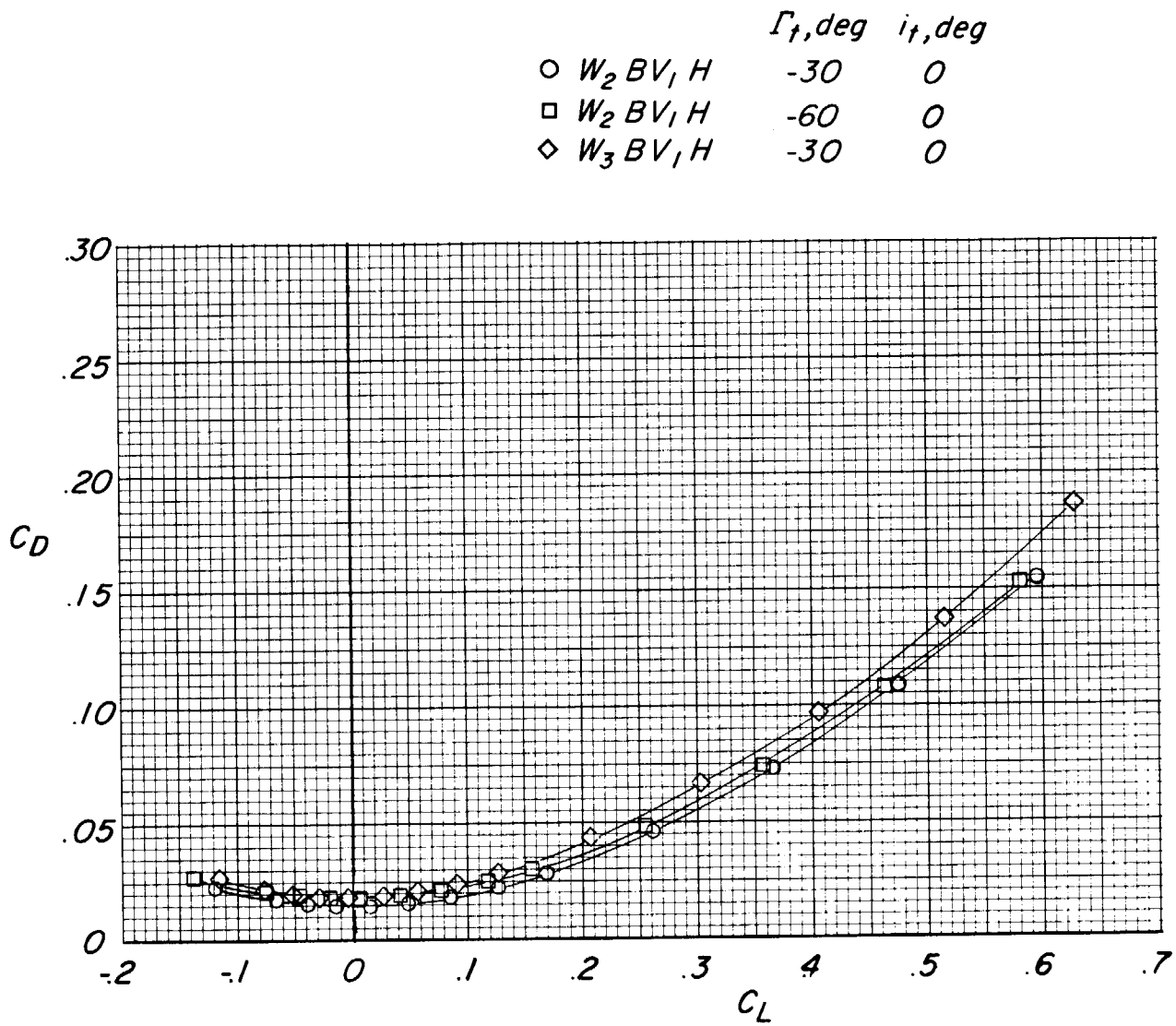

(d) Continued.

Figure 4.- Continued.

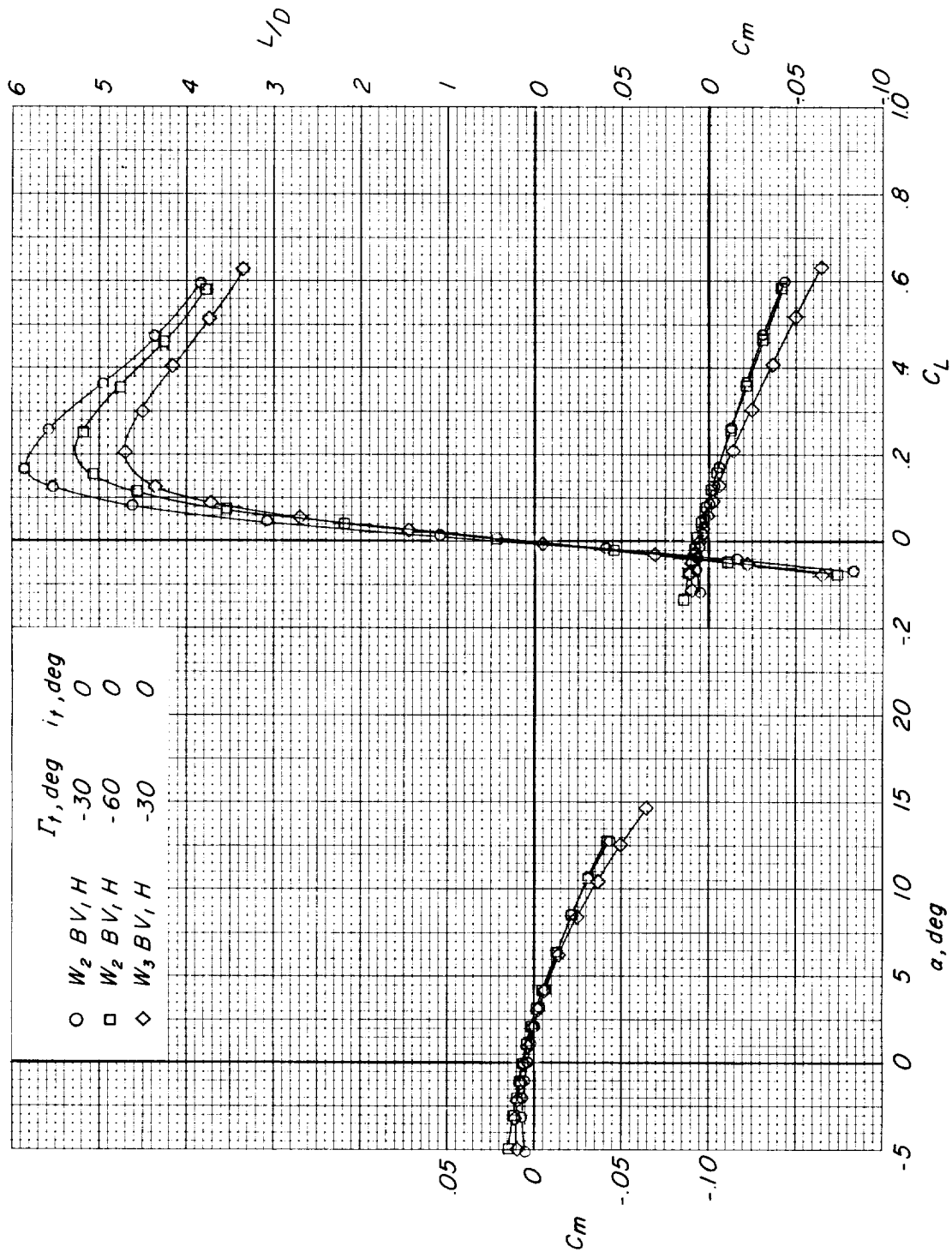

(d) Concluded.

Figure 4.- Continued.

		Γ_t, deg	i_t, deg
○	$W_2 B V_1 H$	-30	0
□	$W_2 B V_1 H$	-60	0
◇	$W_3 B V_1 H$	-30	0

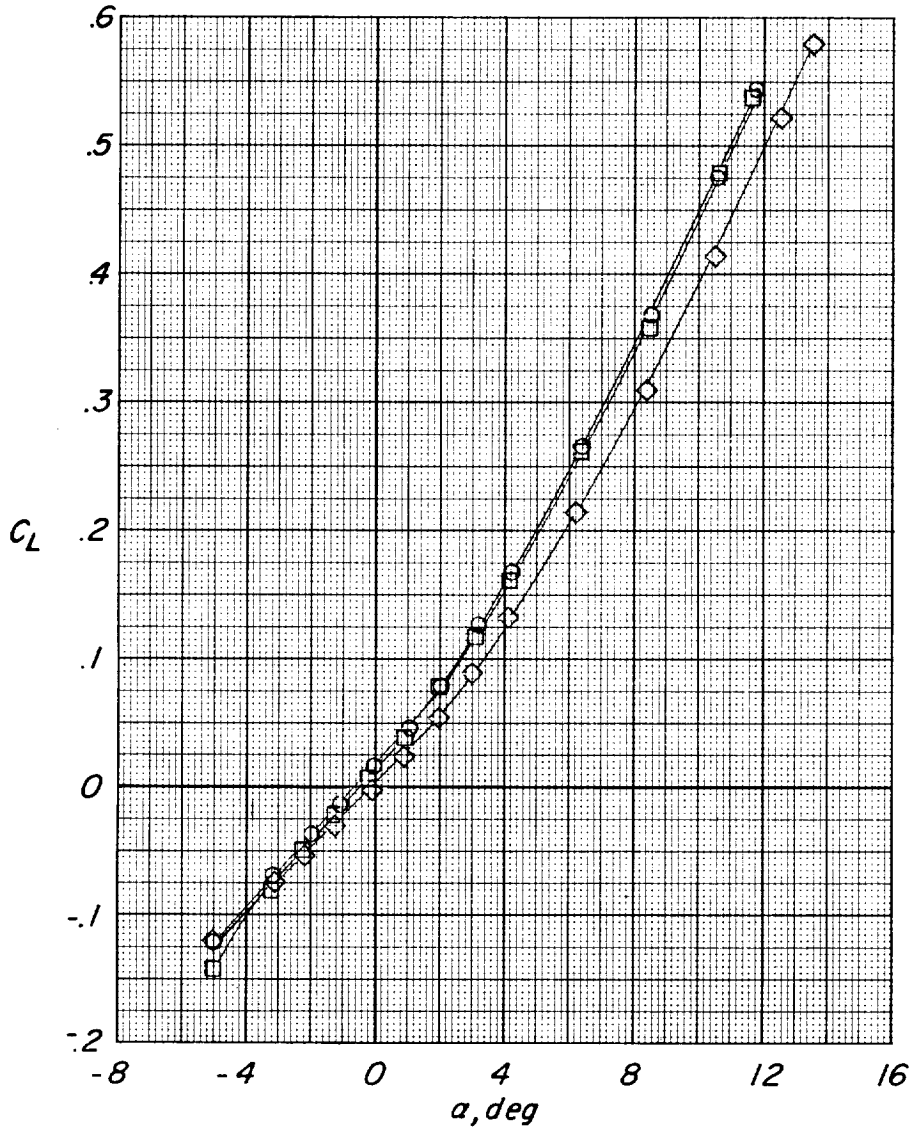

(e) M = 0.95.

Figure 4.- Continued.

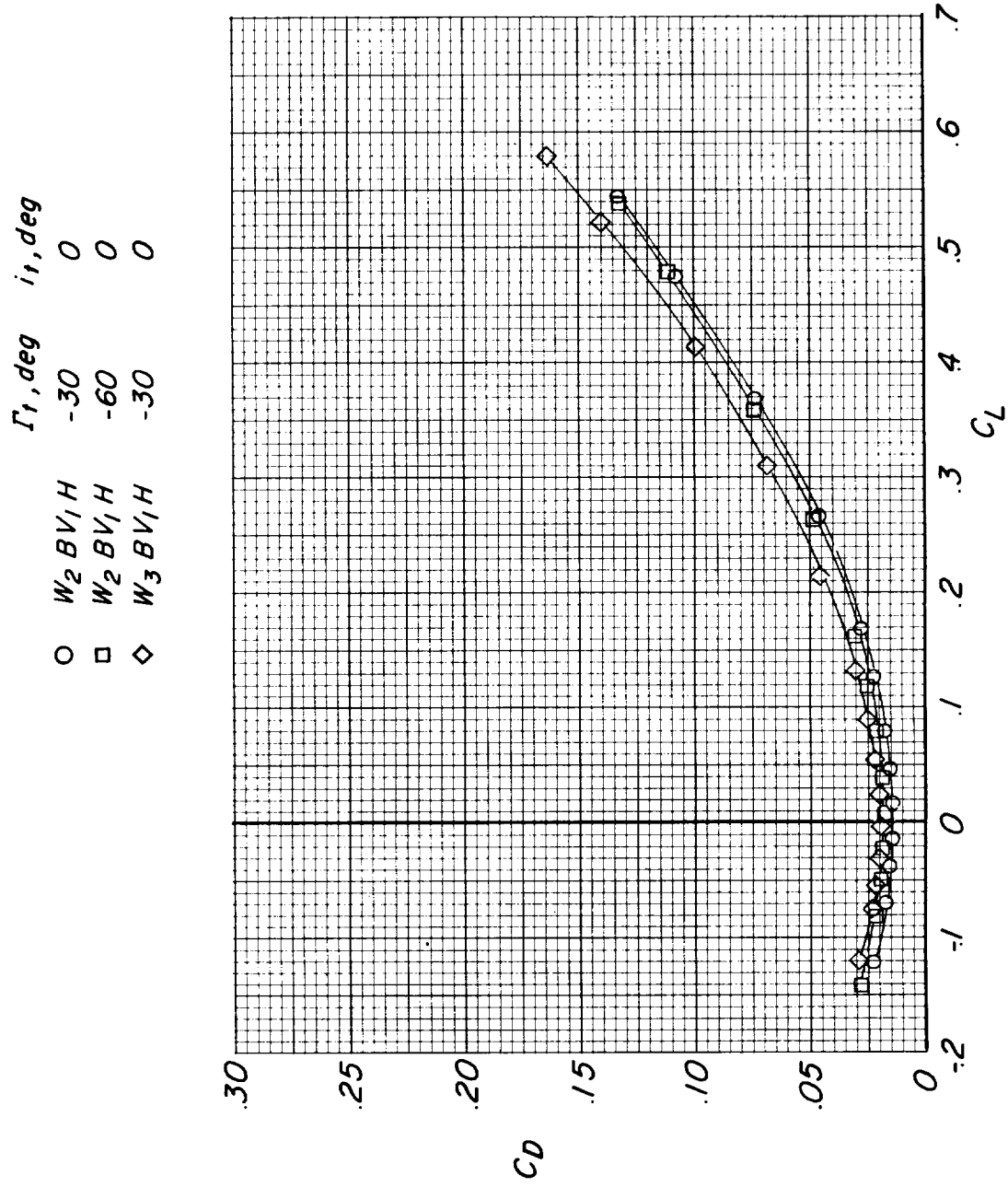

(e) Continued.

Figure 4.- Continued.

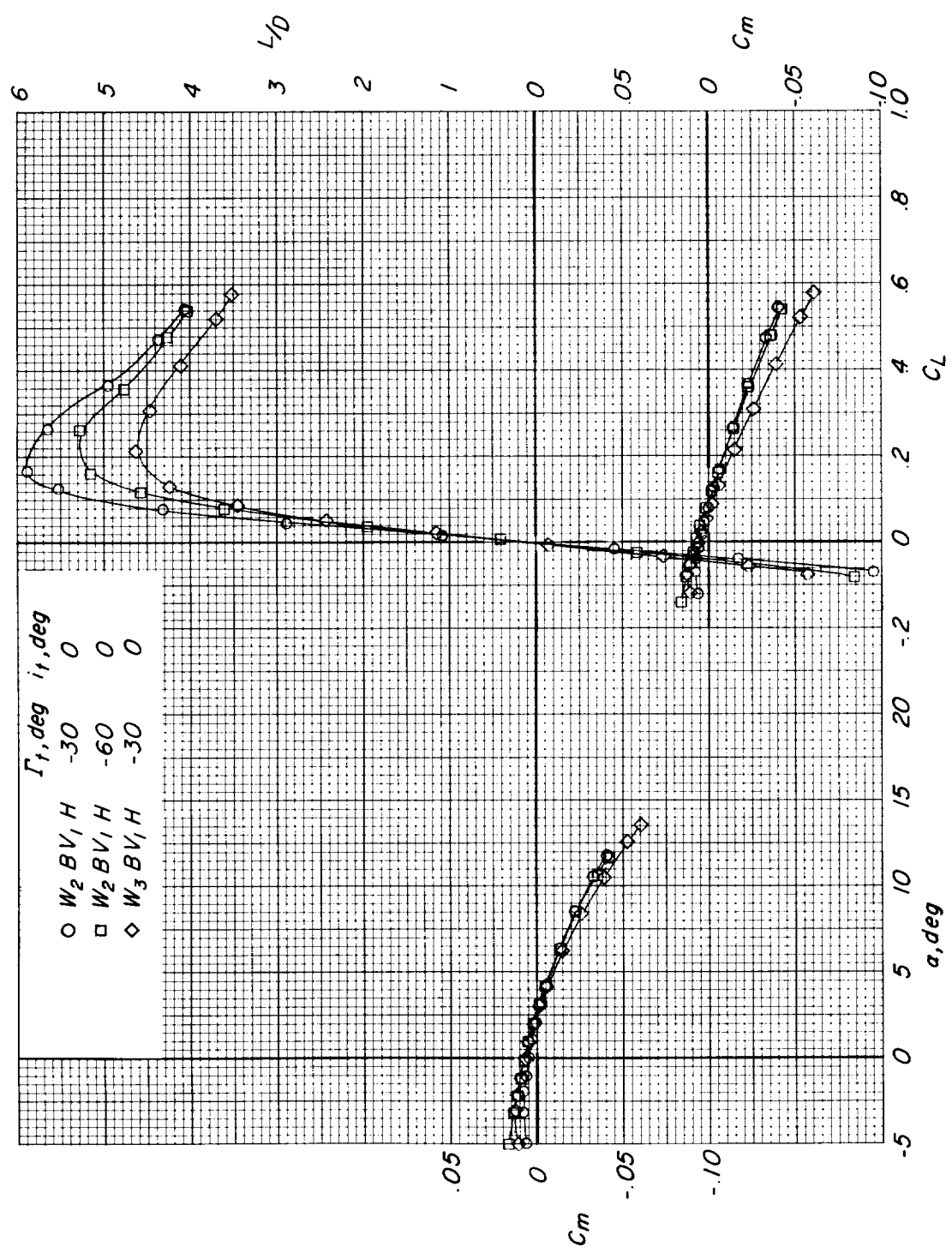

(e) Concluded.

Figure 4.- Continued.

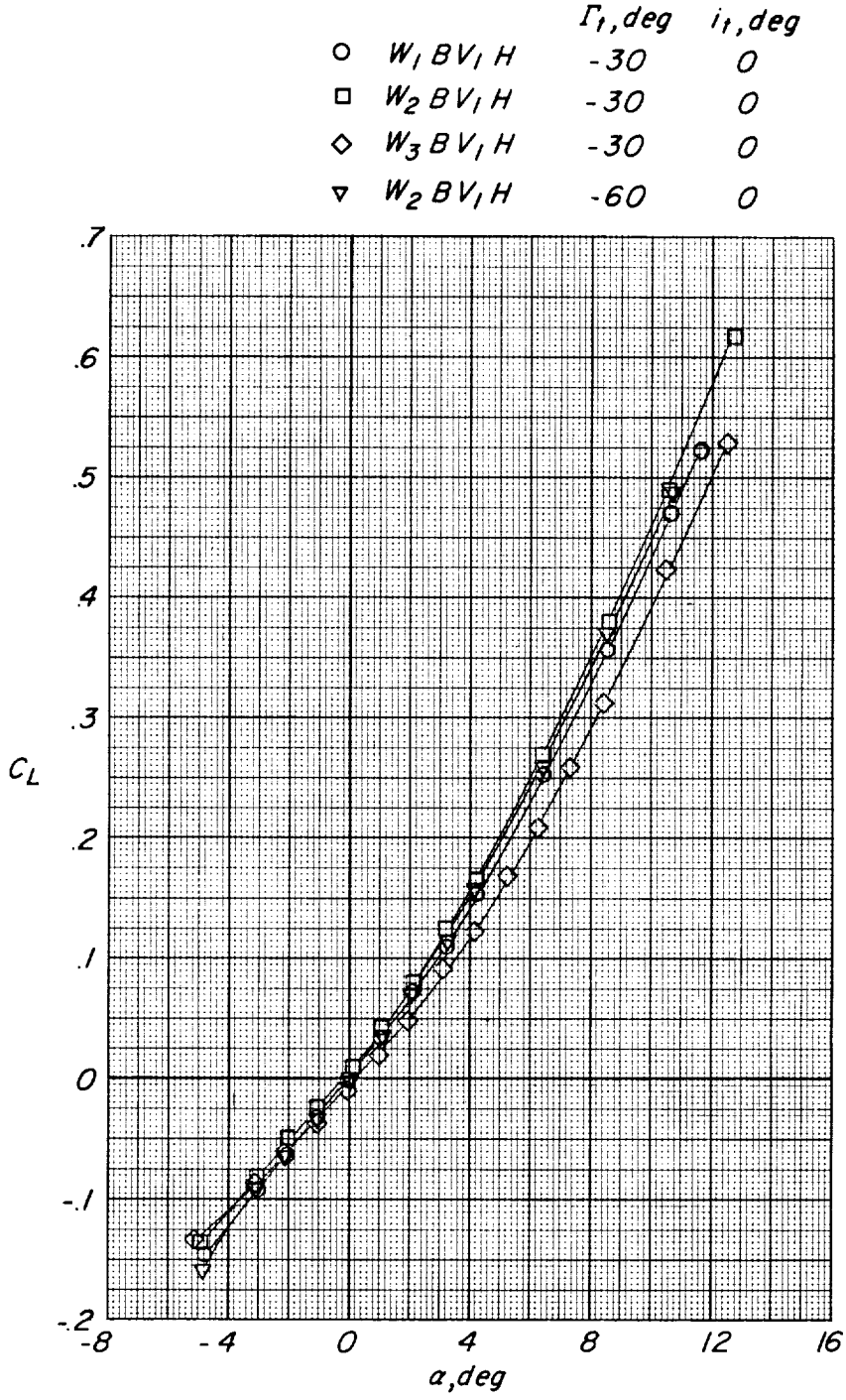

(f) M = 1.00.

Figure 4.- Continued.

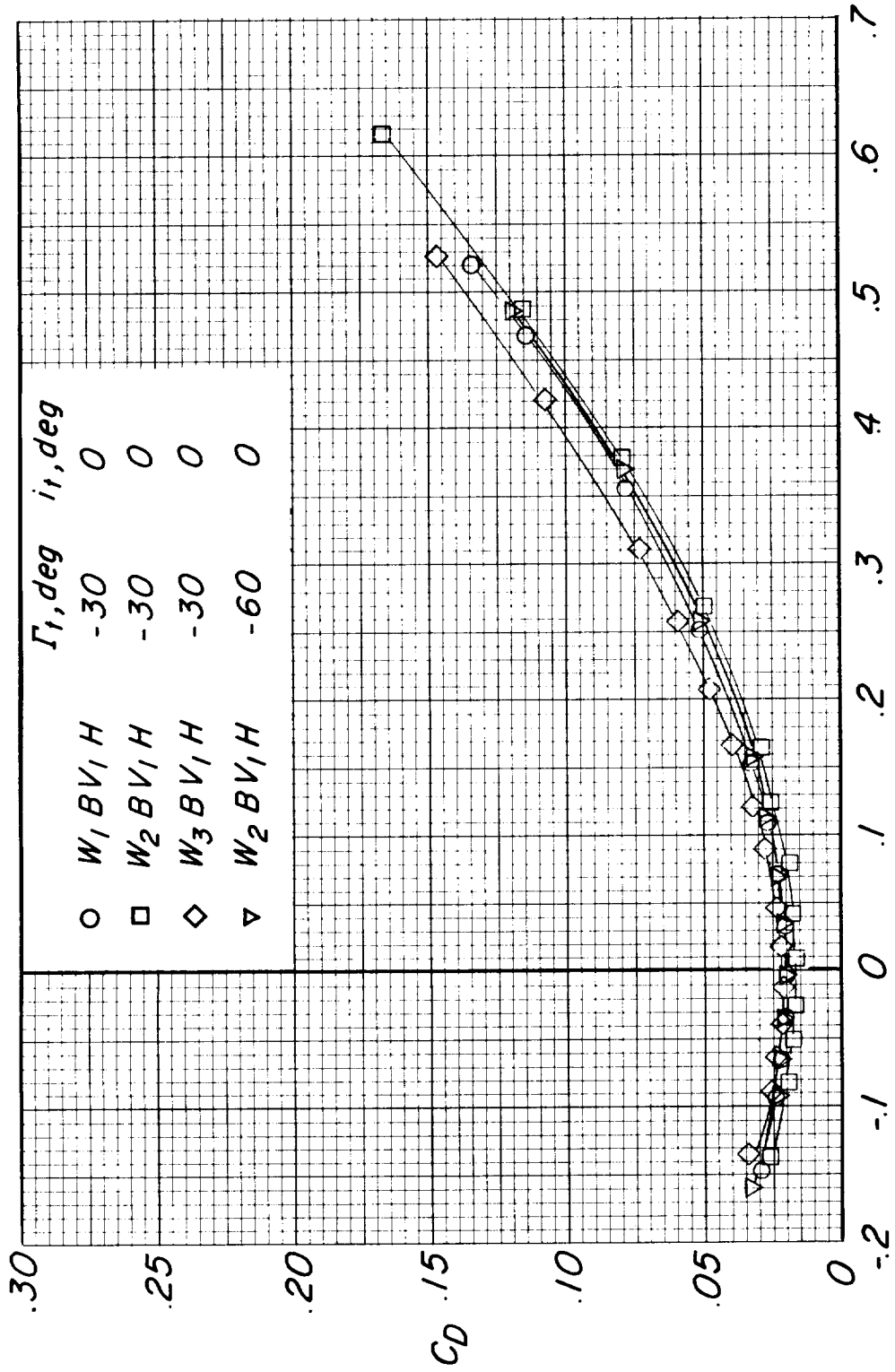

(f) Continued.

Figure 4.- Continued.

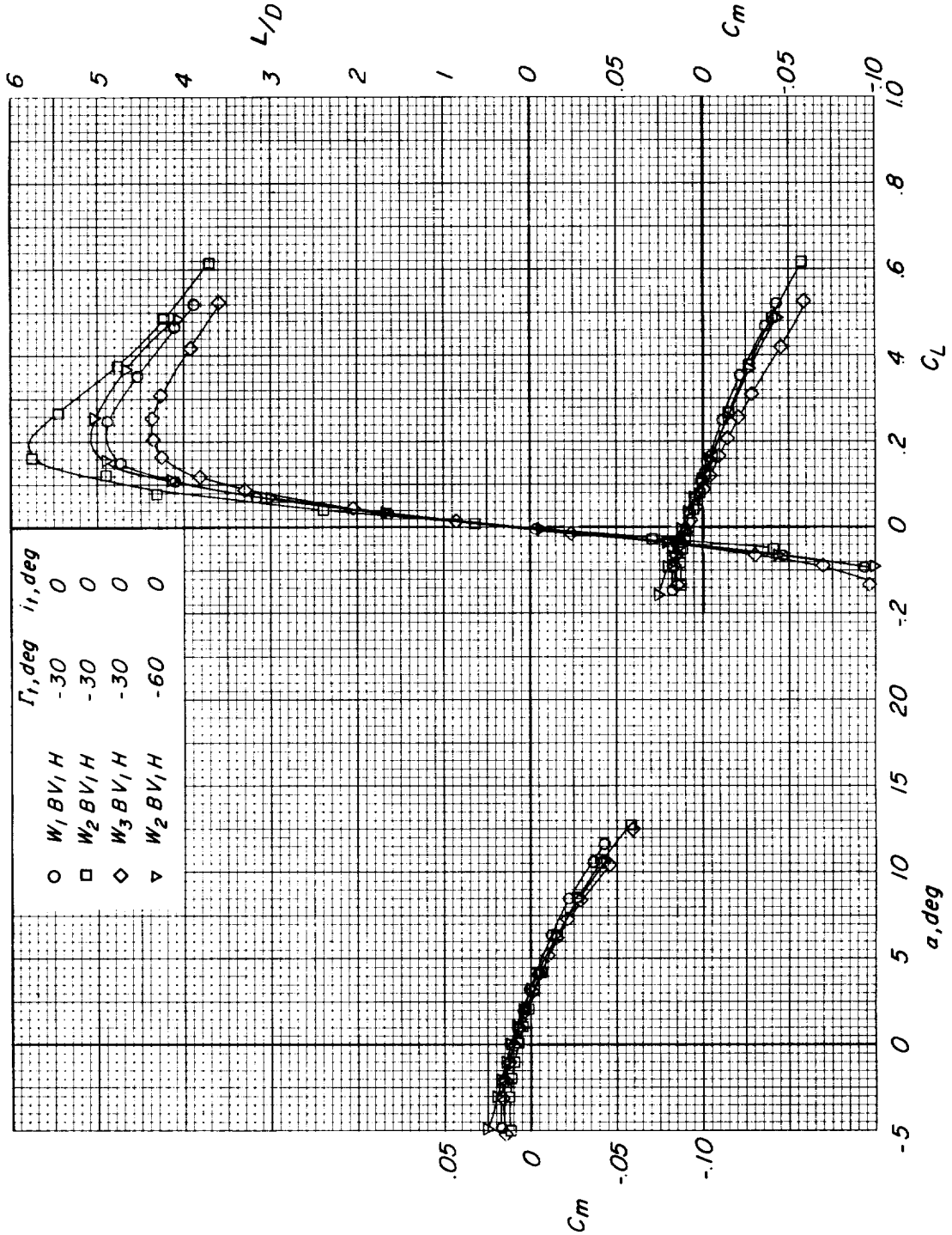

(f) Concluded.

Figure 4.- Continued.

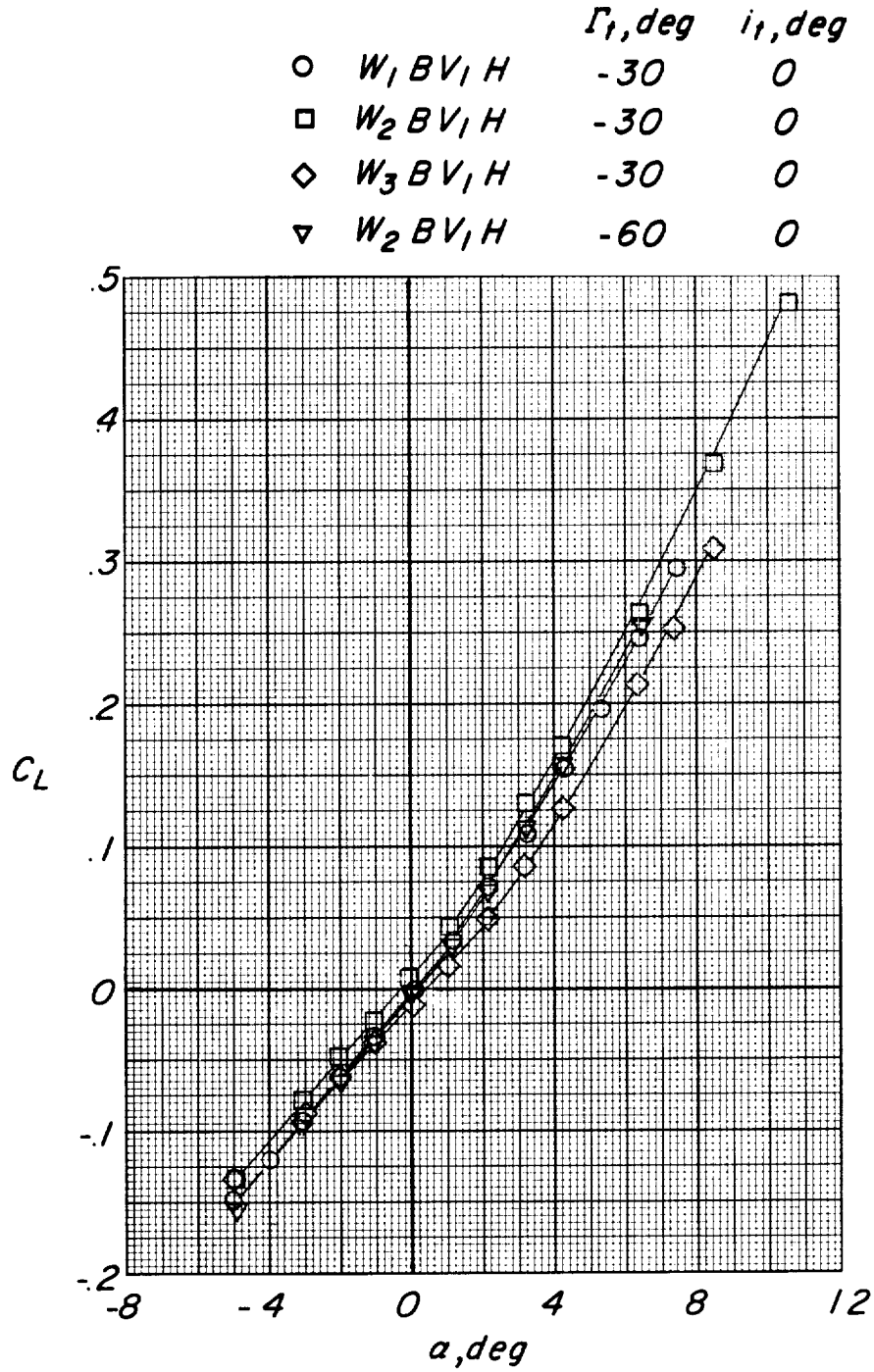

(g) M = 1.13.

Figure 4.- Continued.

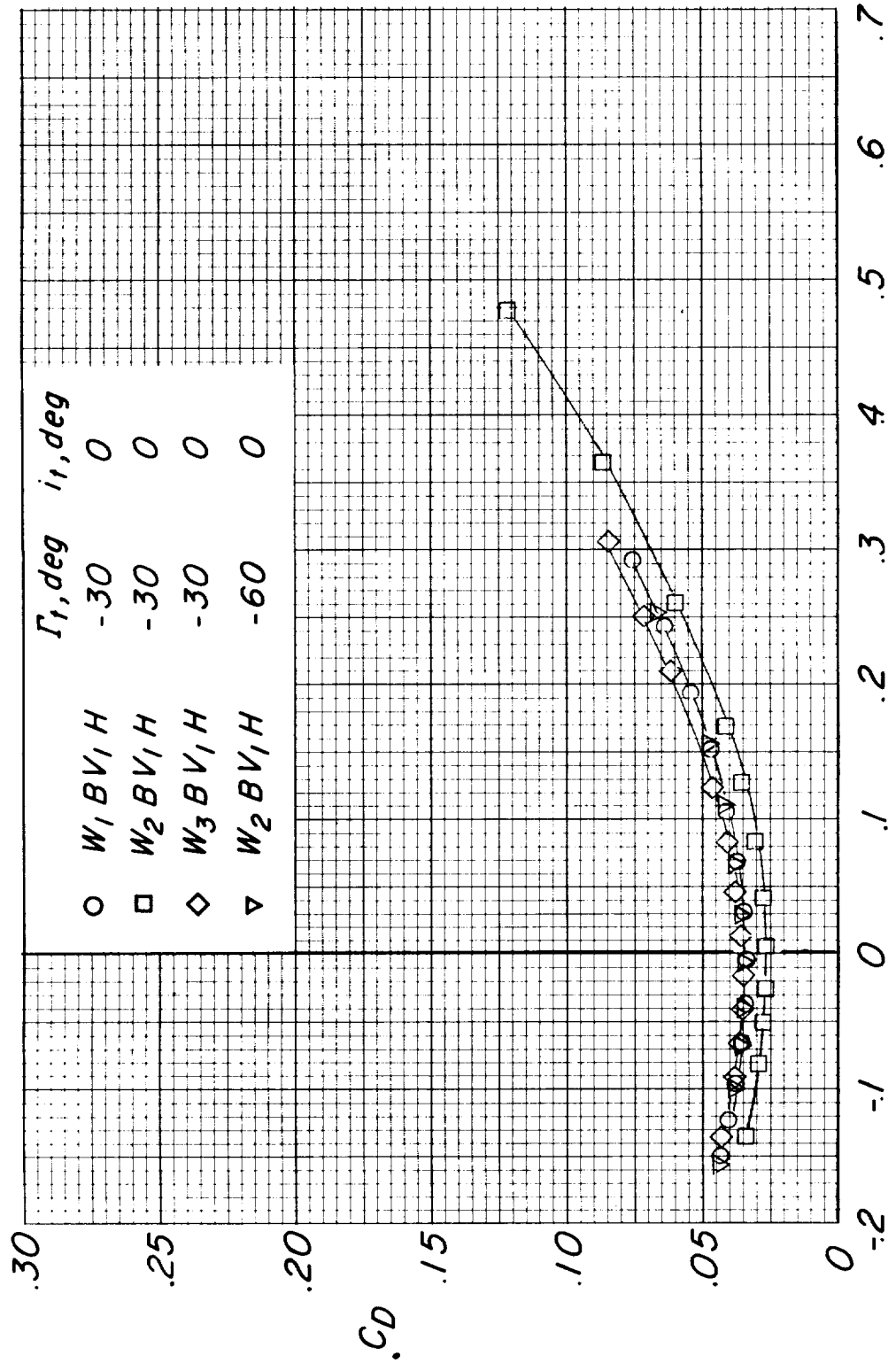

(g) Continued.

Figure 4.- Continued.

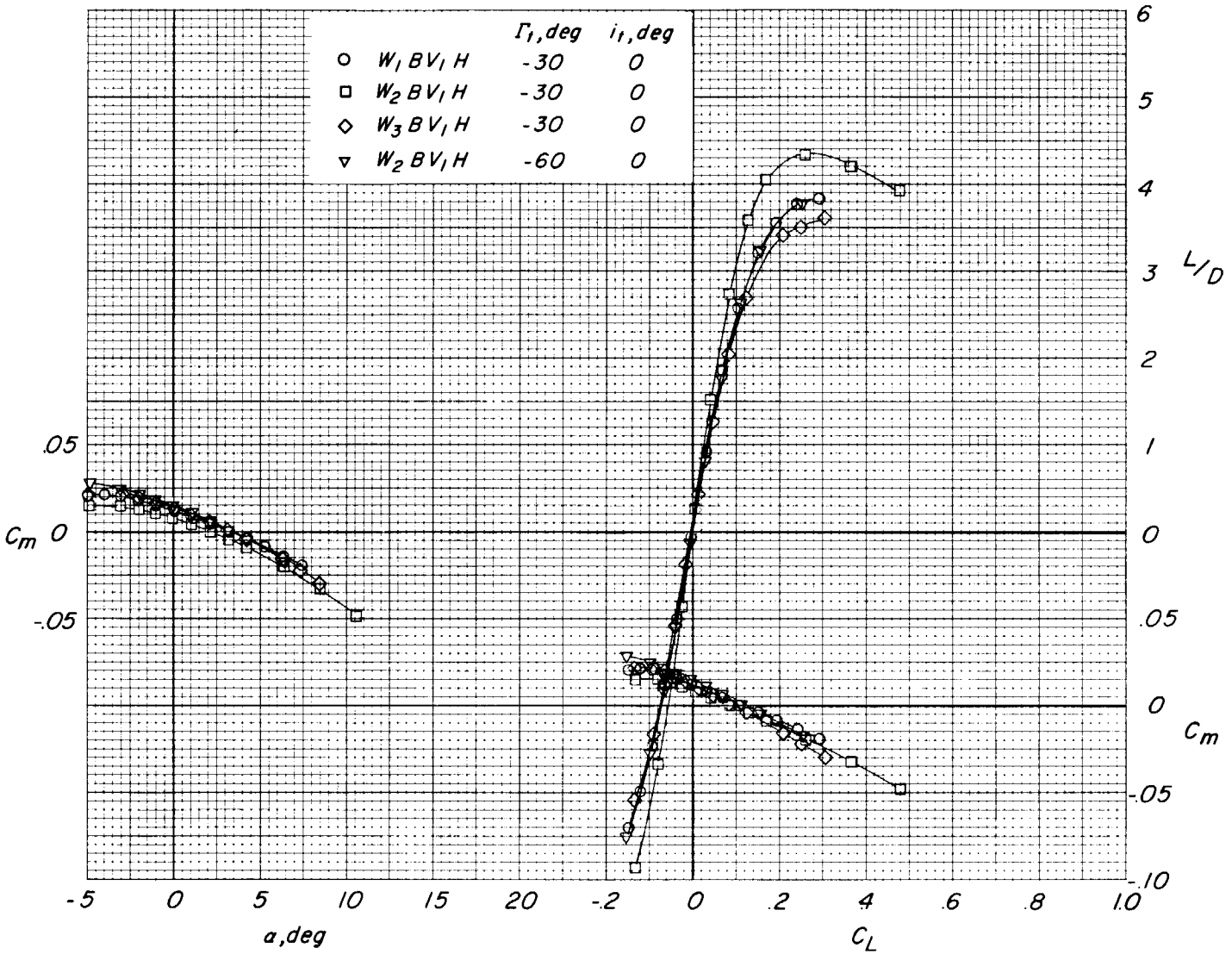

(g) Concluded.

Figure 4.- Concluded.

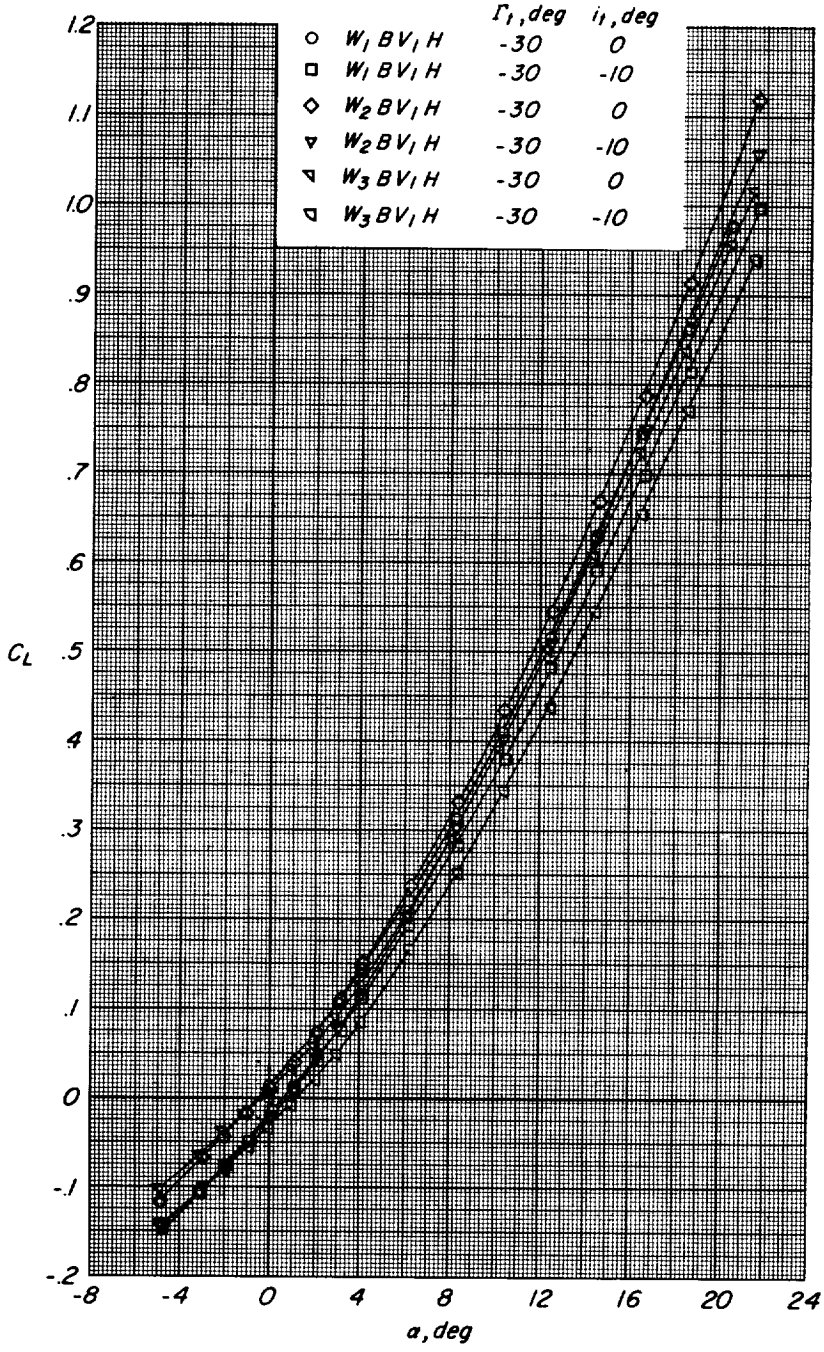

(a) M = 0.40.

Figure 5.- Longitudinal control characteristics at various Mach numbers associated with deflection of the horizontal stabilizers, for the configurations having the 75° delta, 75° modified arrow, or 70°-80° cranked wing. Small center vertical tail (V_1) on.

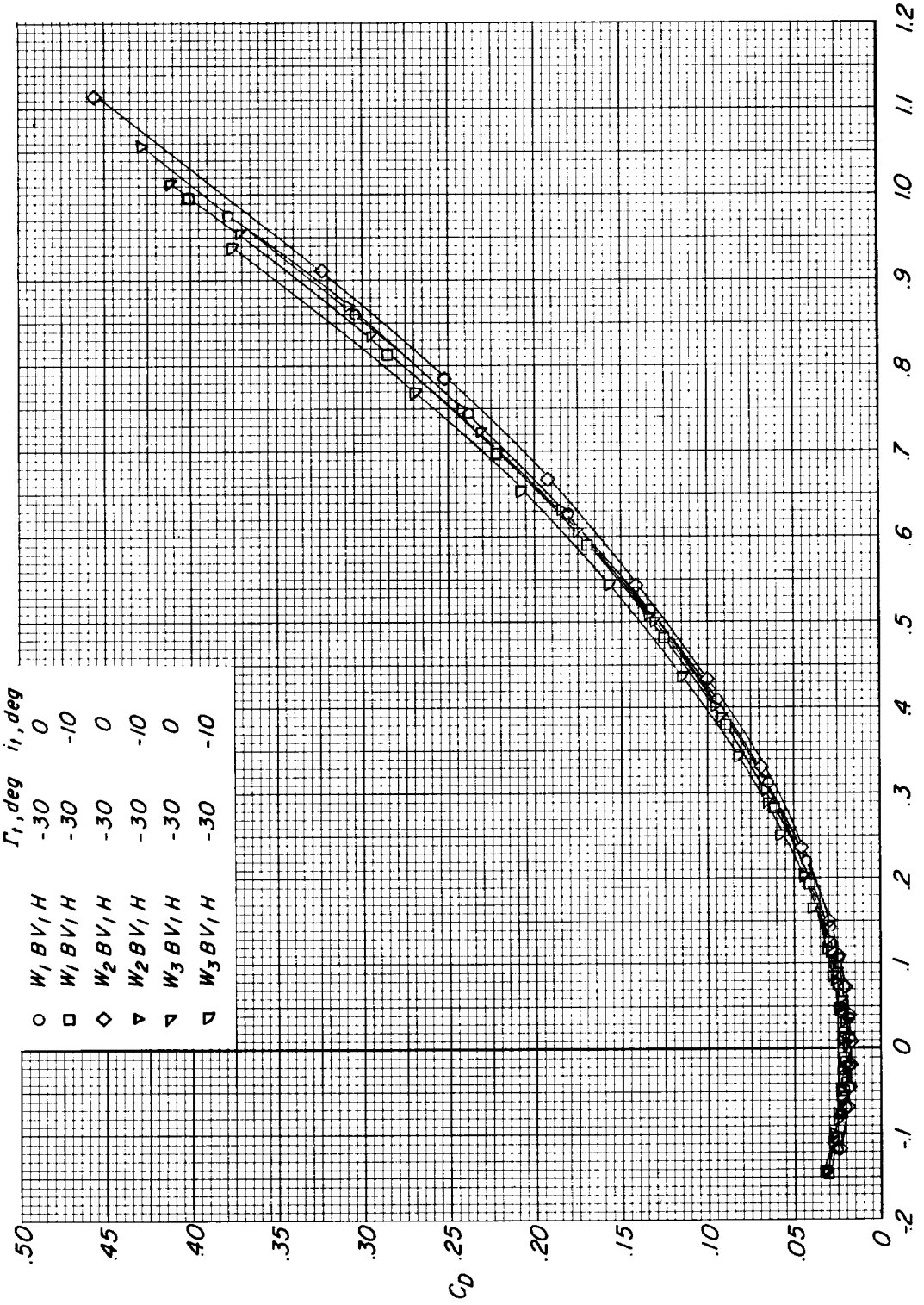

(a) Continued.

Figure 5.- Continued.

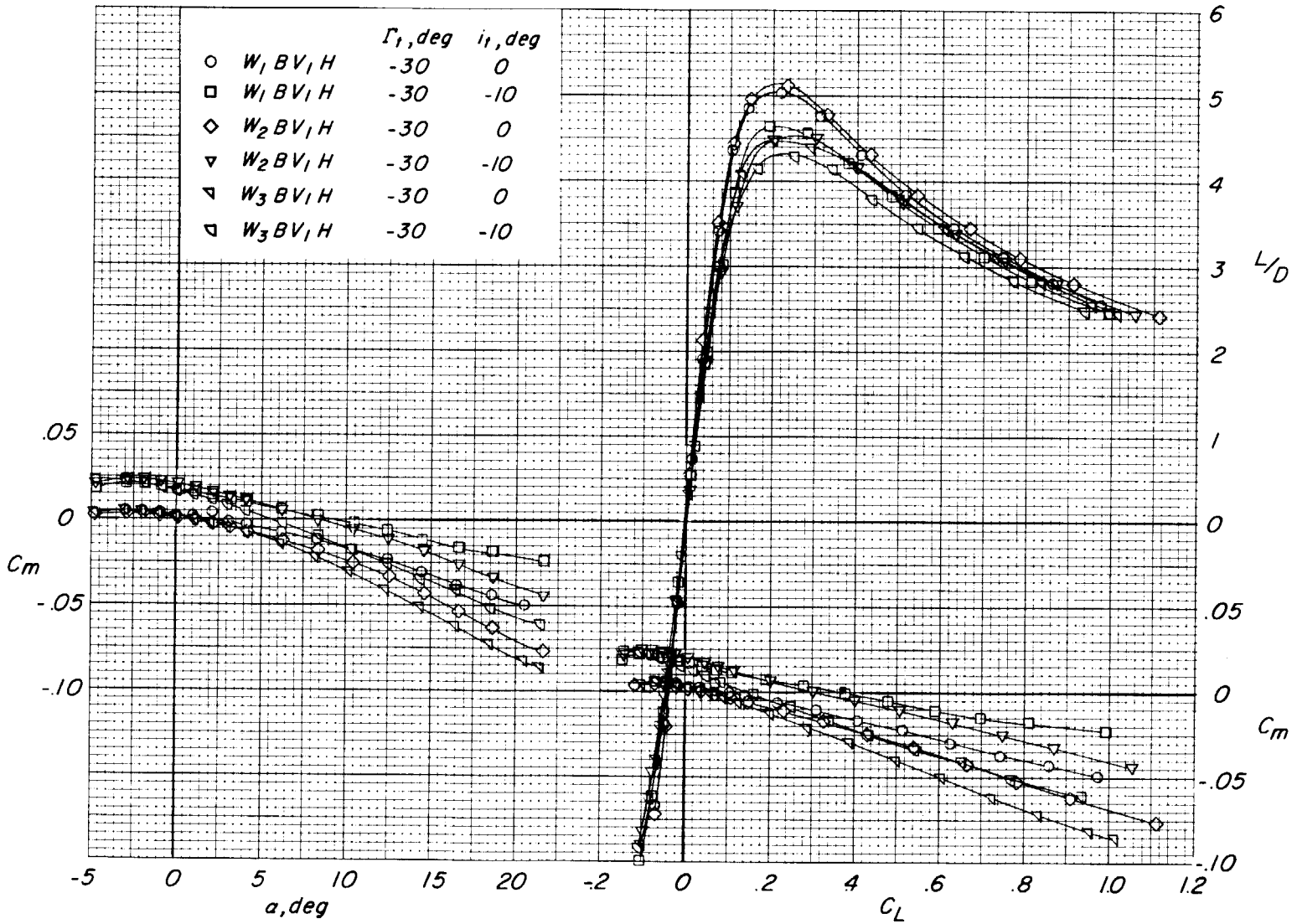

(a) Concluded.

Figure 5.- Continued.

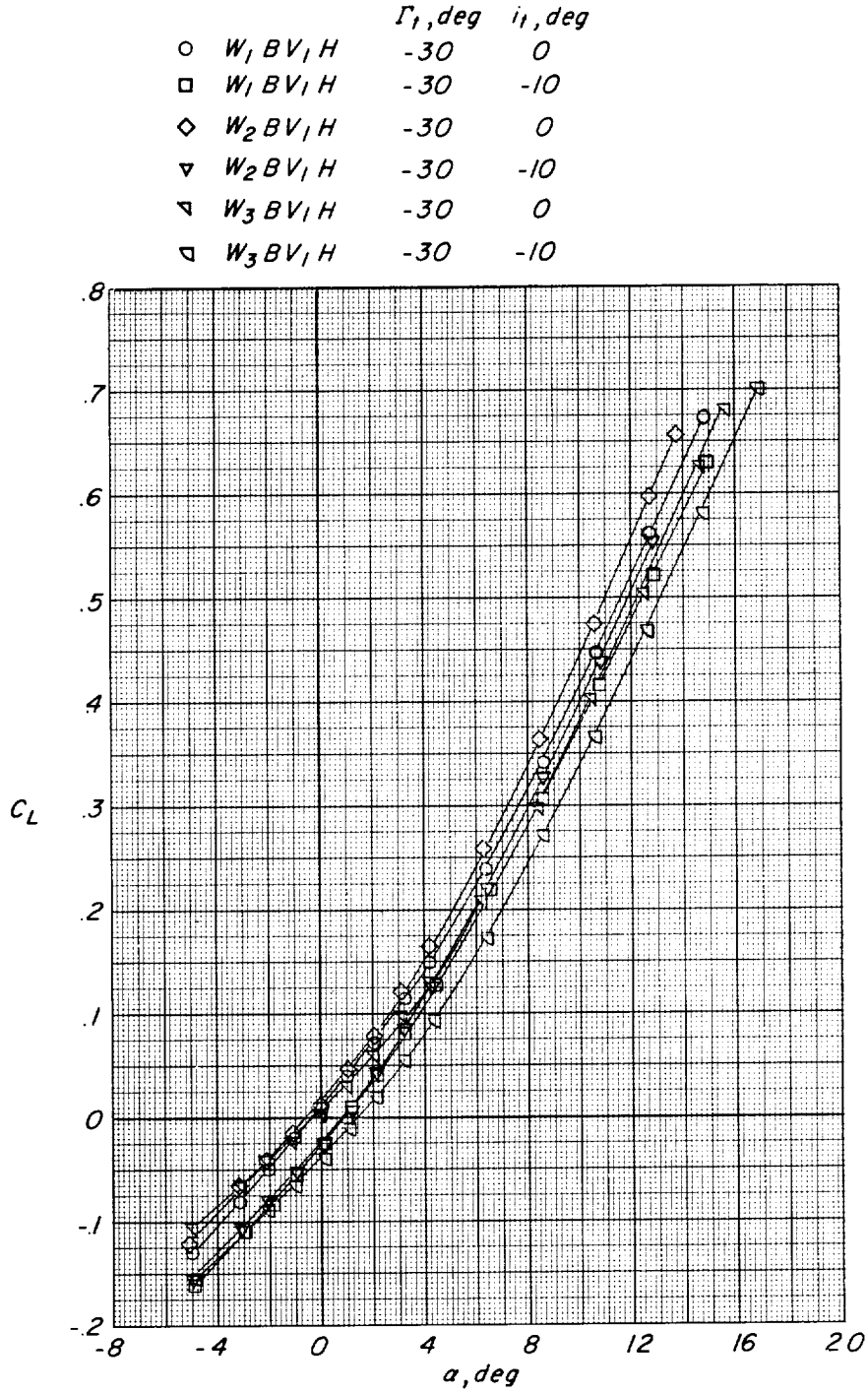

(b) M = 0.80.

Figure 5.- Continued.

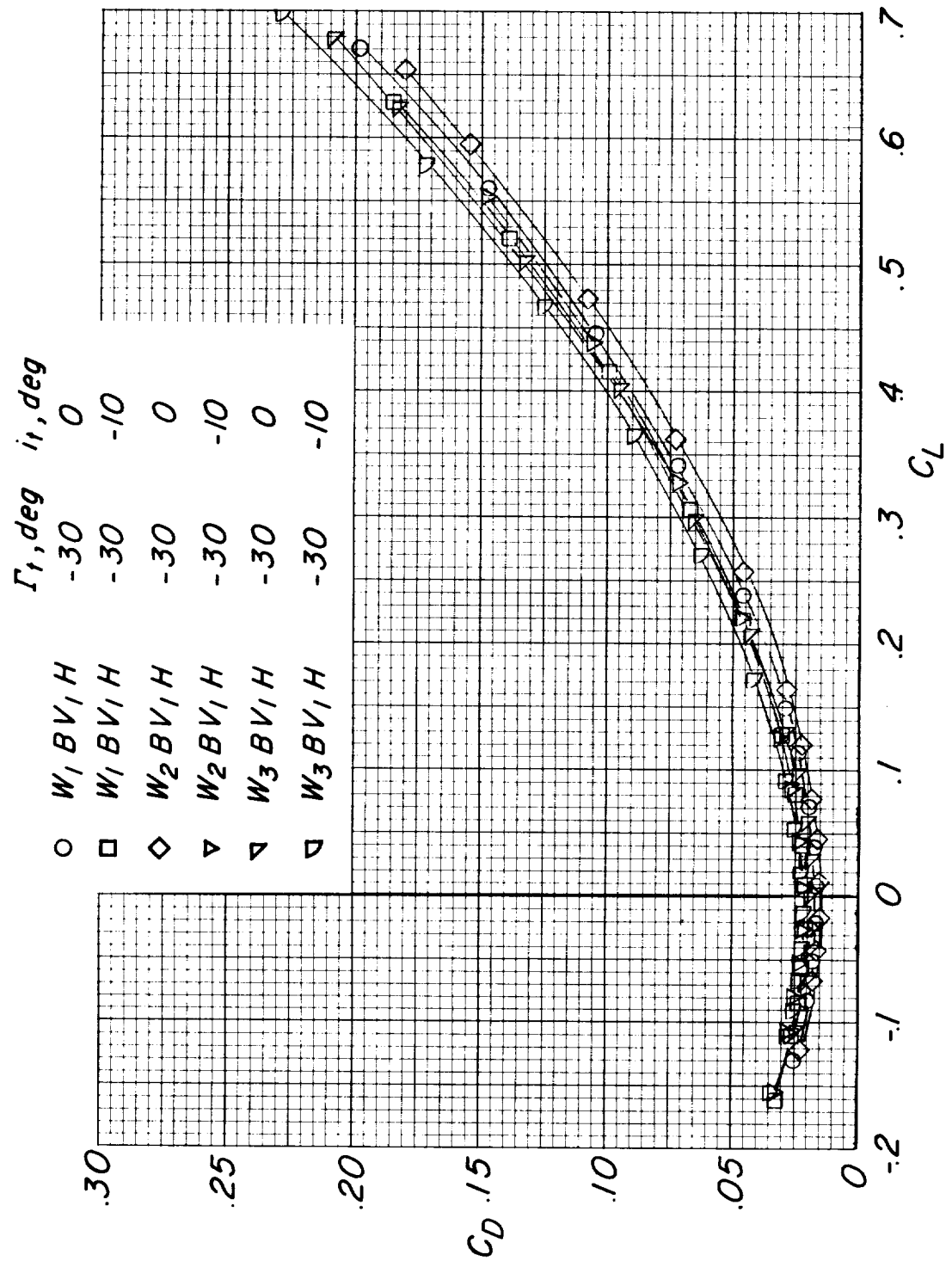

(b) Continued.

Figure 5.- Continued.

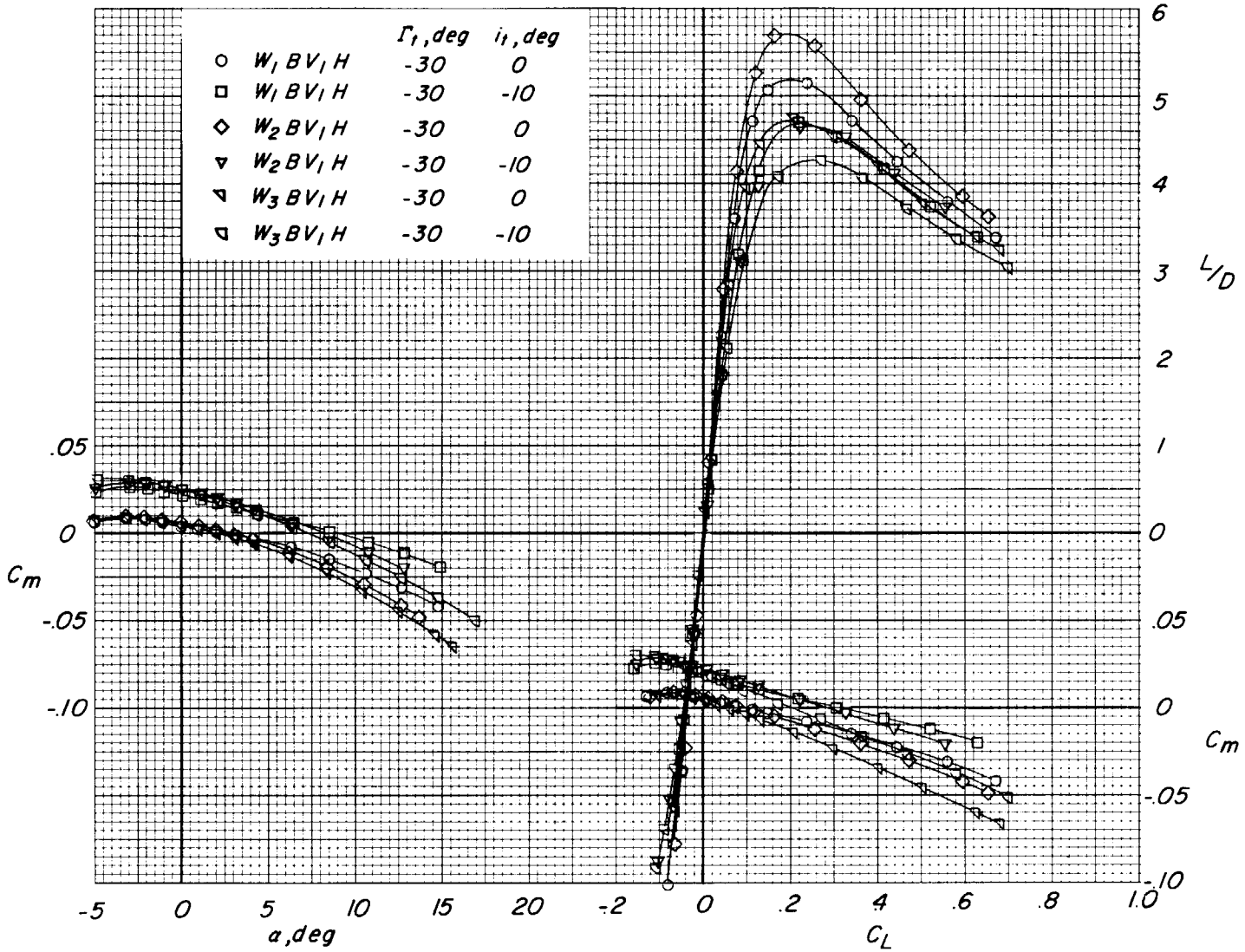

(b) Concluded.

Figure 5.- Continued.

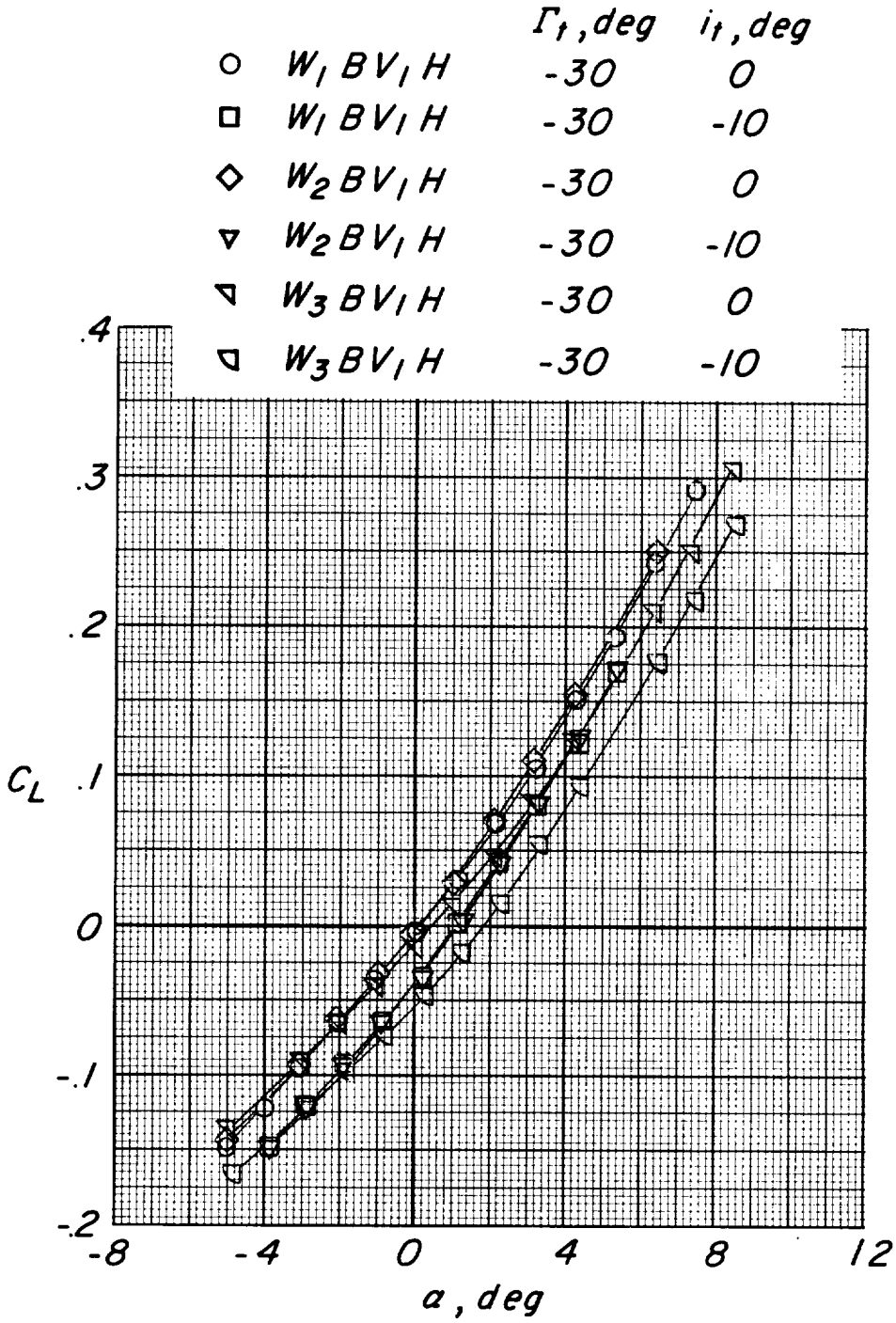

(c) M = 1.13.

Figure 5.- Continued.

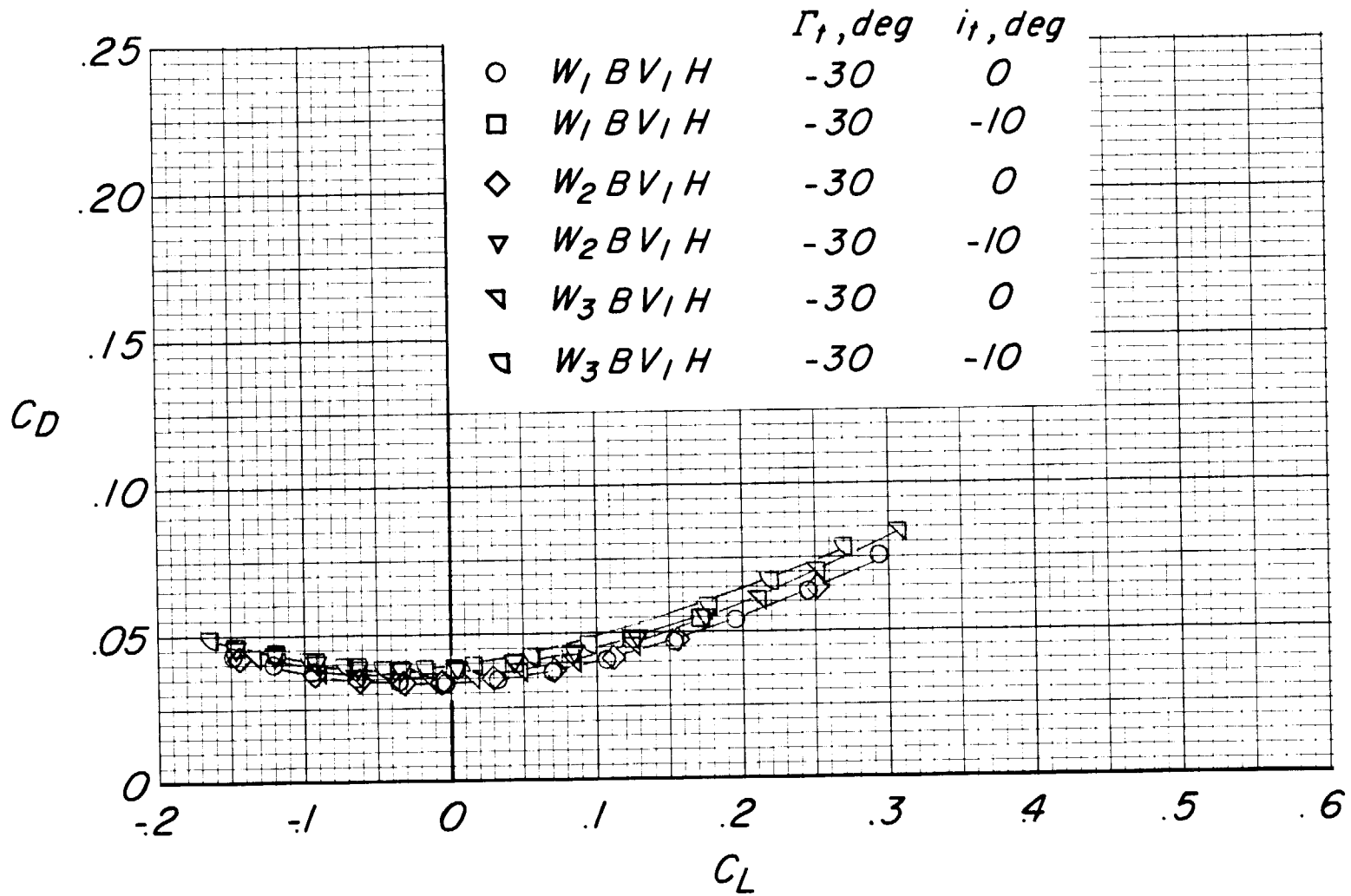

(c) Continued.

Figure 5.- Continued.

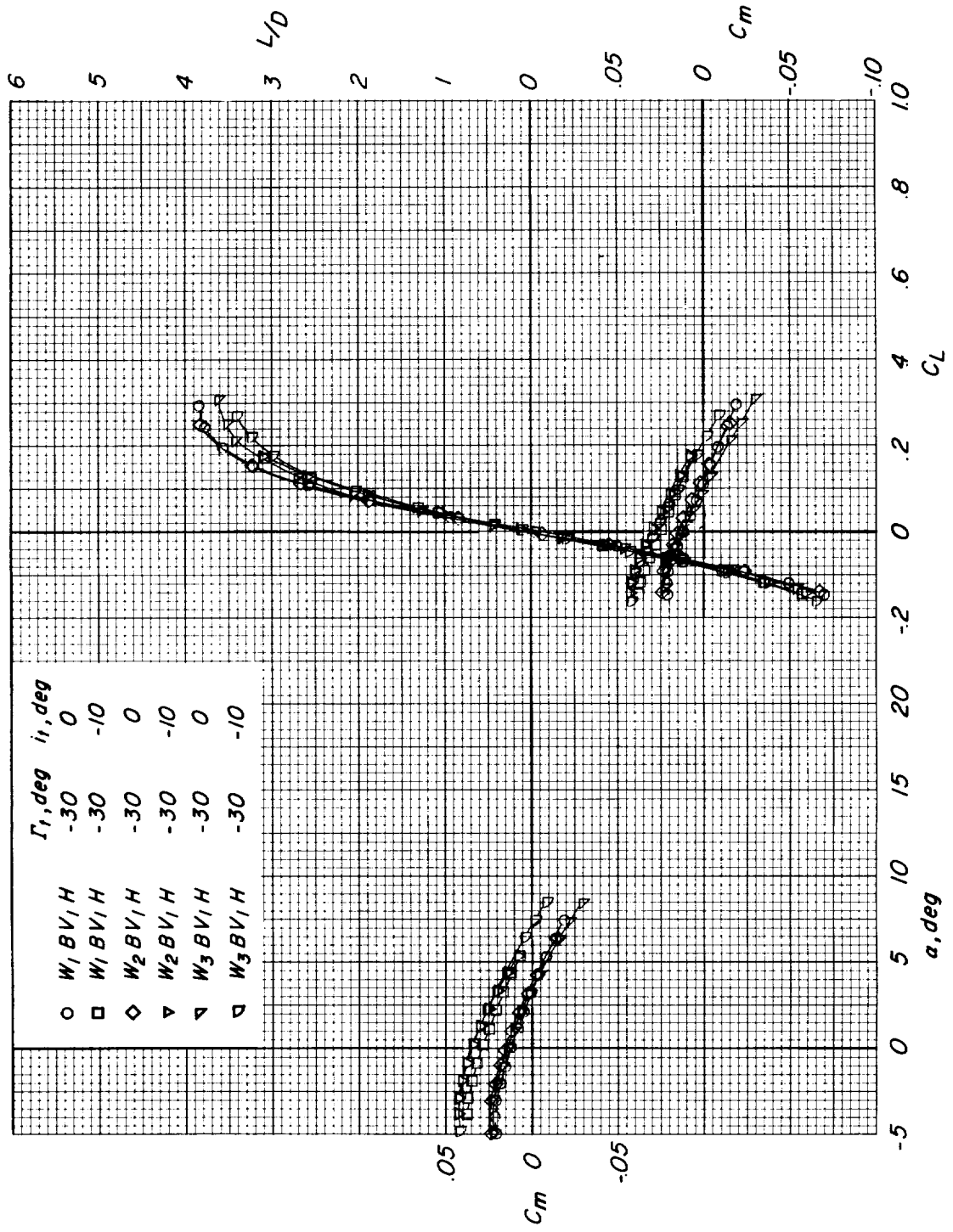

(c) Concluded.

Figure 5.- Concluded.

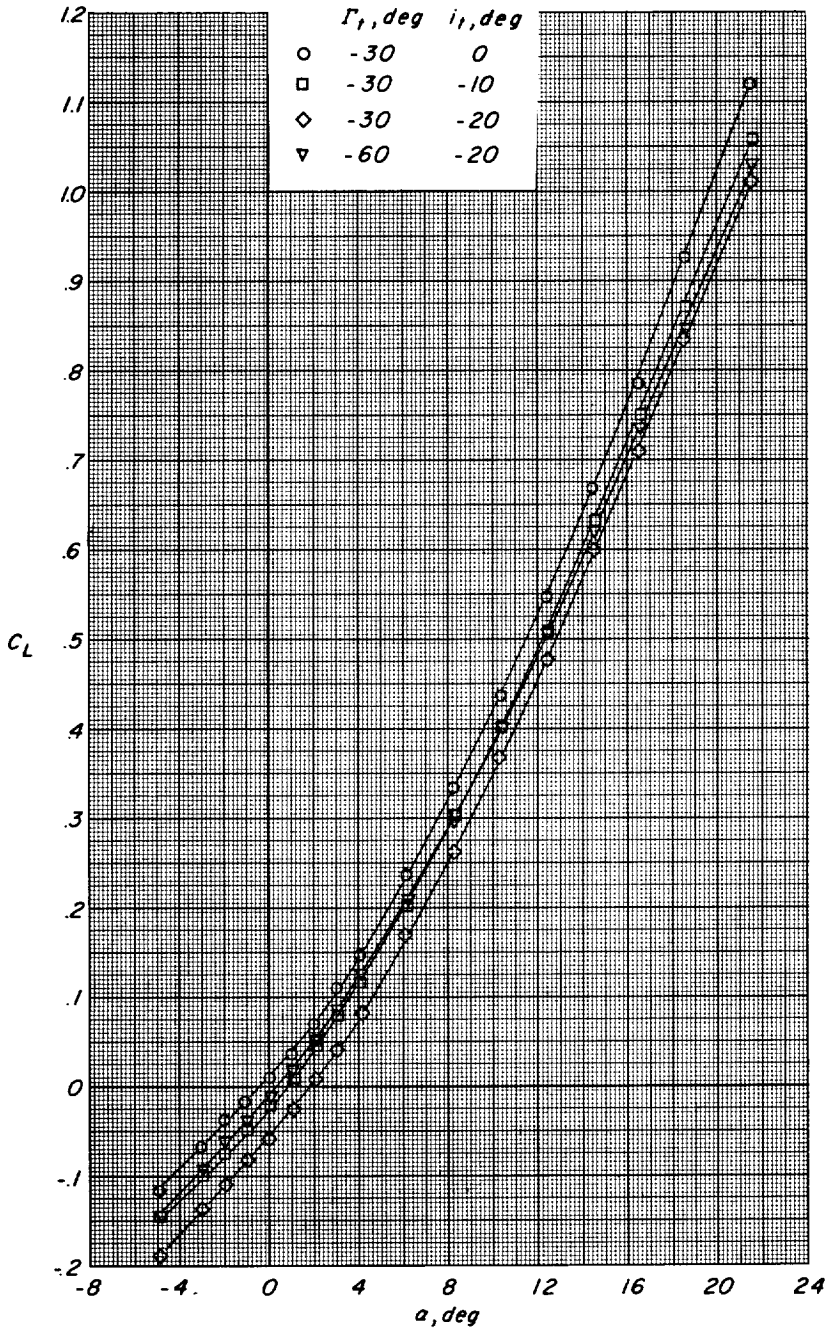

(a) M = 0.40.

Figure 6.- Effects of horizontal-stabilizer incidence and dihedral on the longitudinal aerodynamic characteristics of the configurations having the 75° modified arrow wing (W_2) at various Mach numbers. Small center vertical tail (V_1) on.

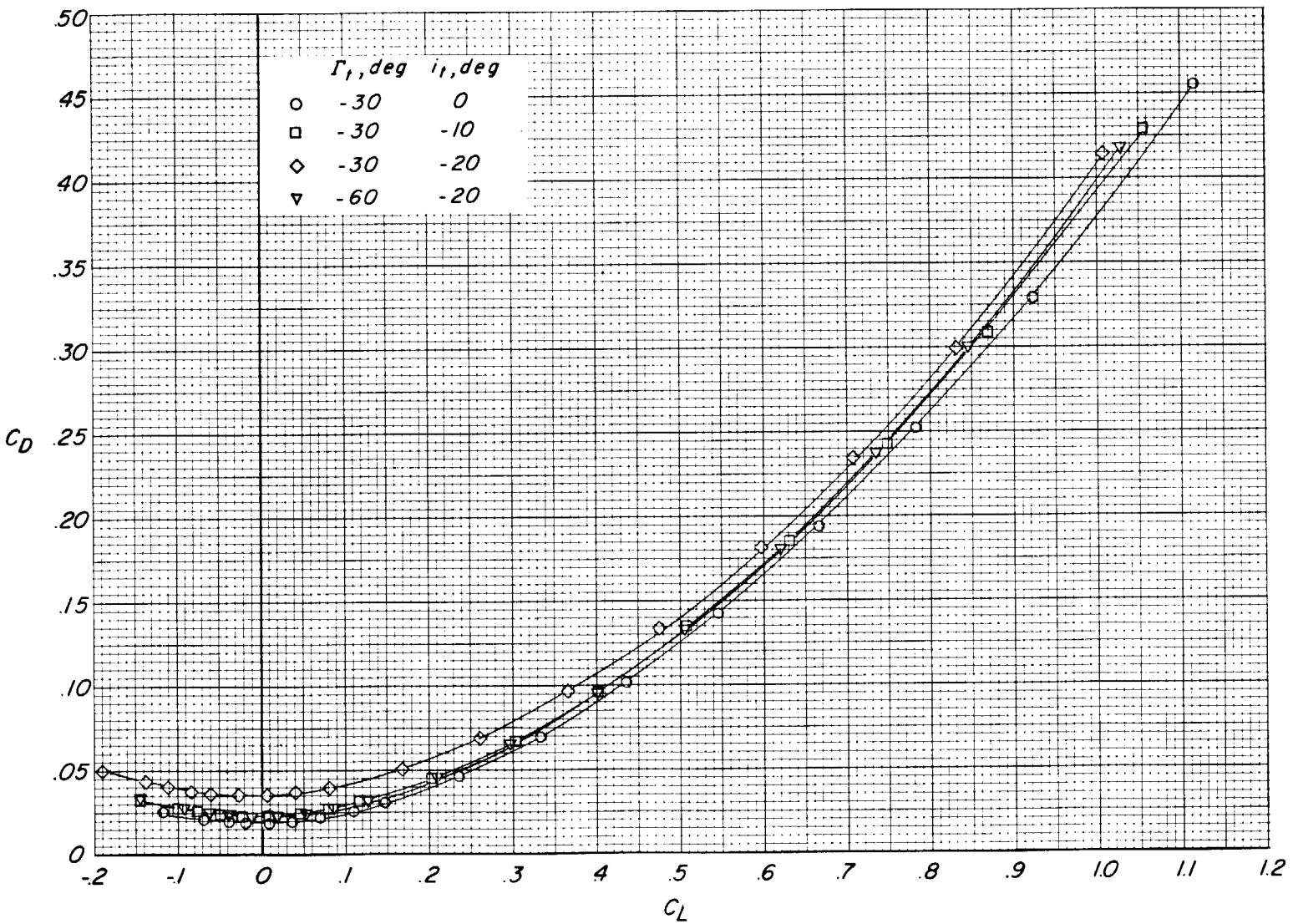

(a) Continued.

Figure 6.- Continued.

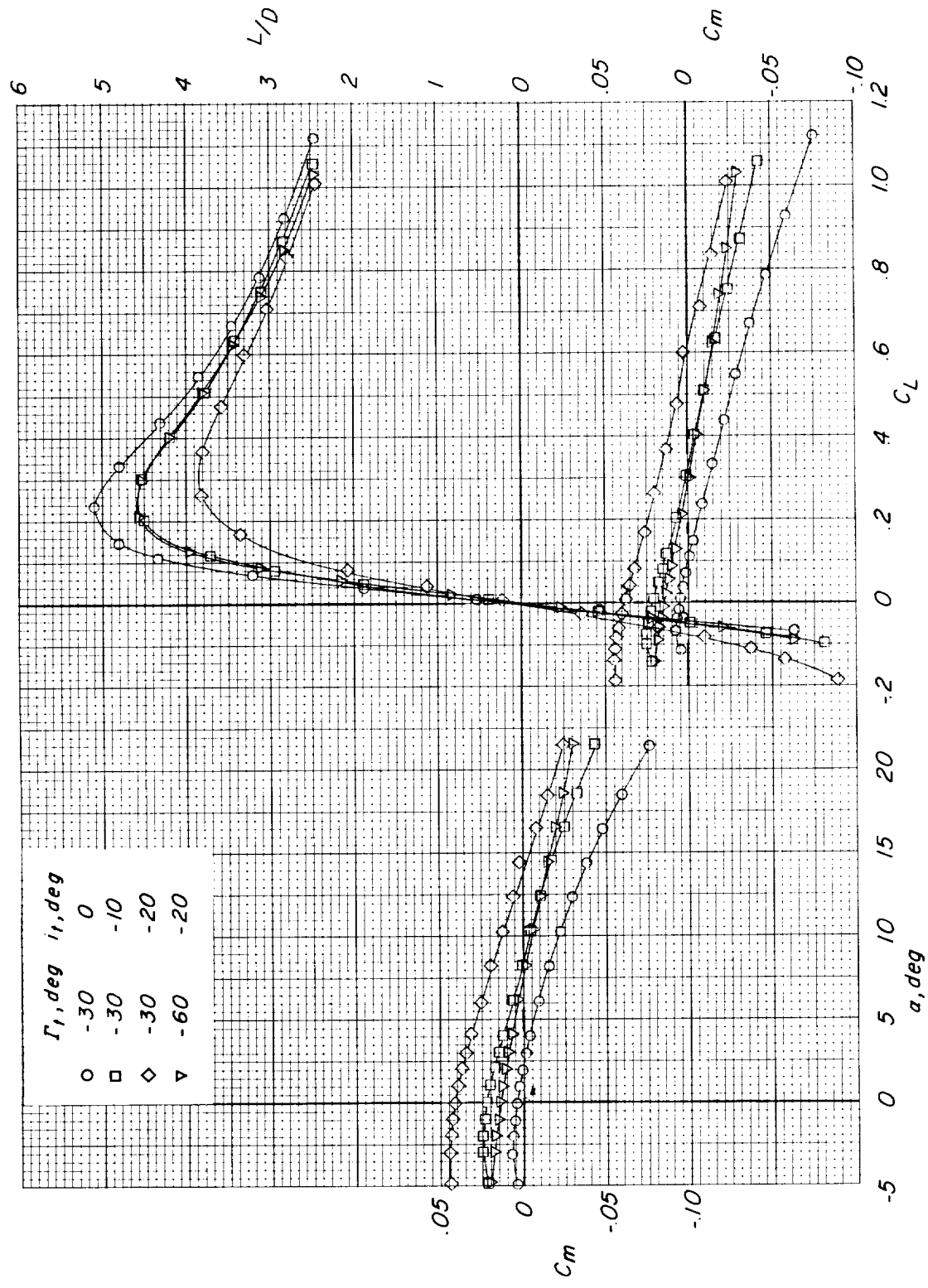

(a) Concluded.

Figure 6.- Continued.

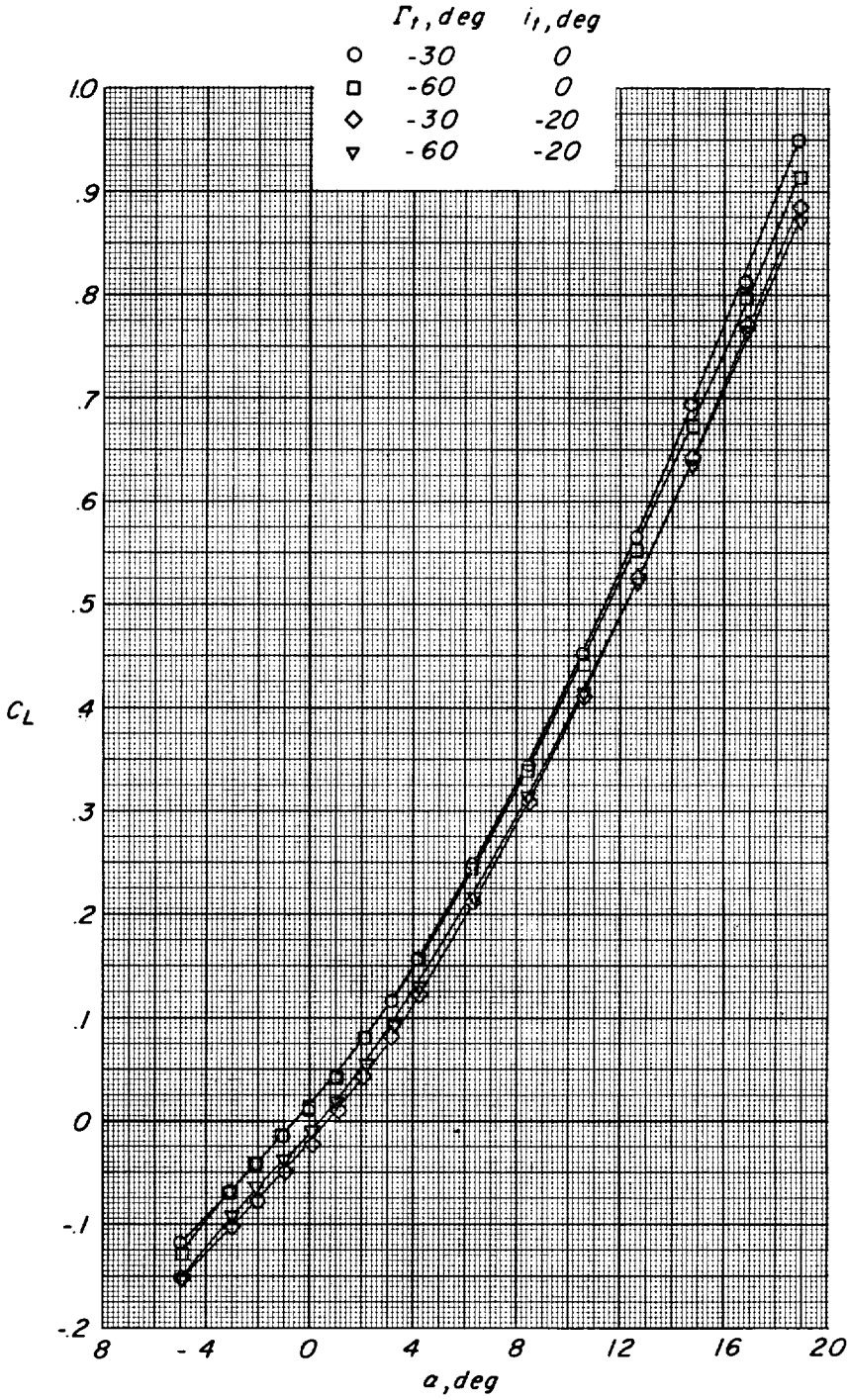

(b) M = 0.60.

Figure 6.- Continued.

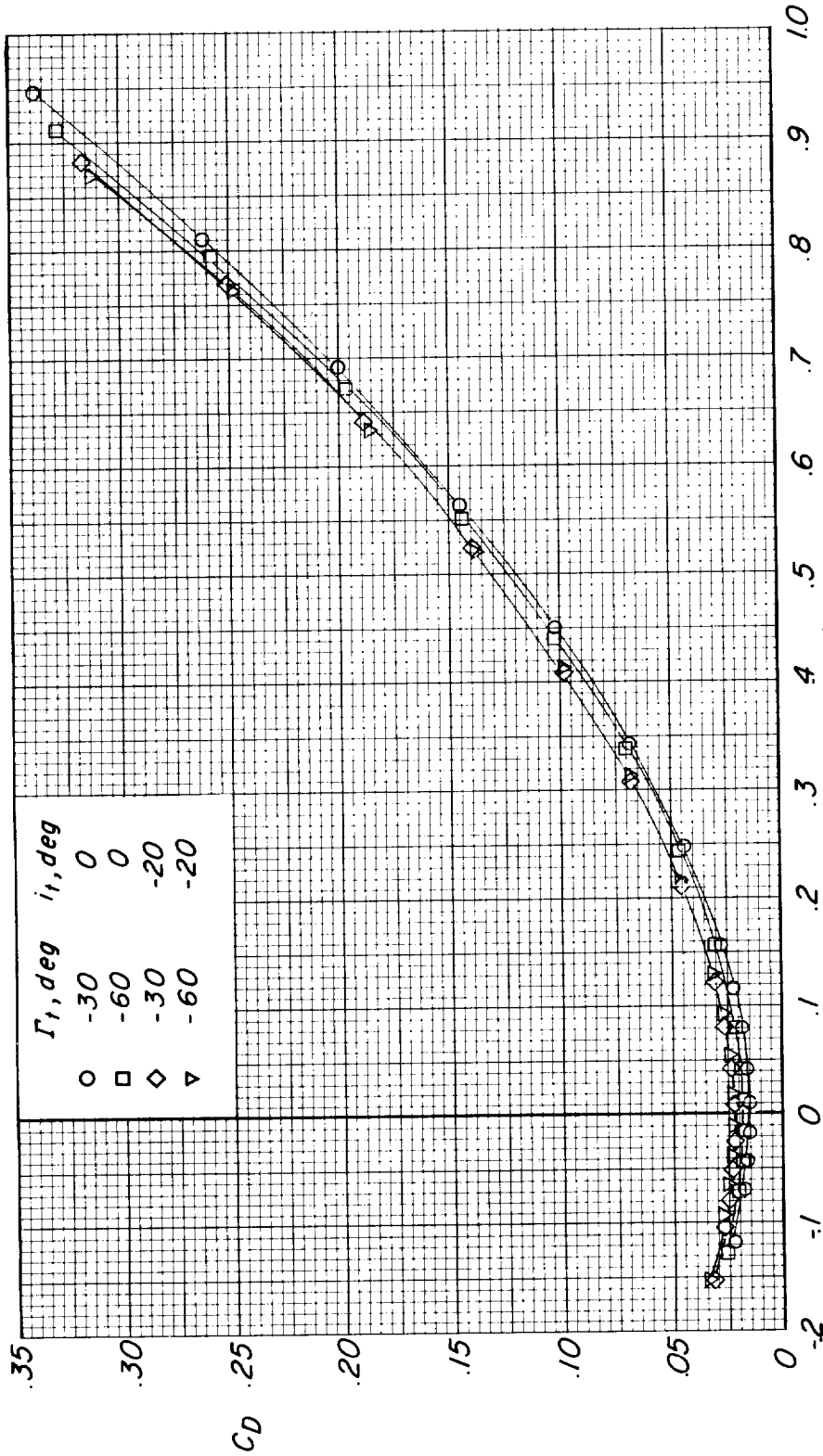

(b) Continued.

Figure 6.- Continued.

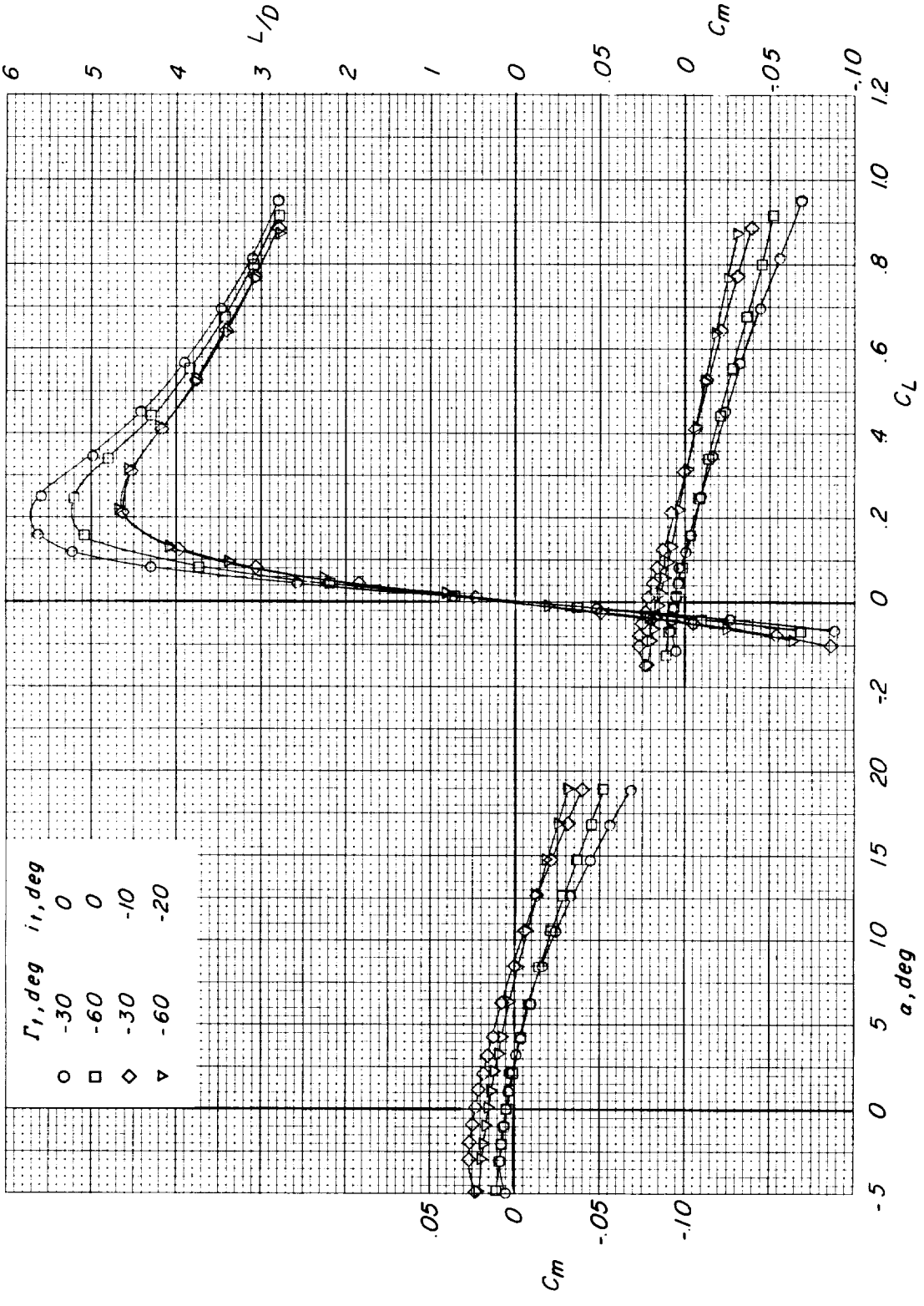

(b) Concluded.

Figure 6.- Continued.

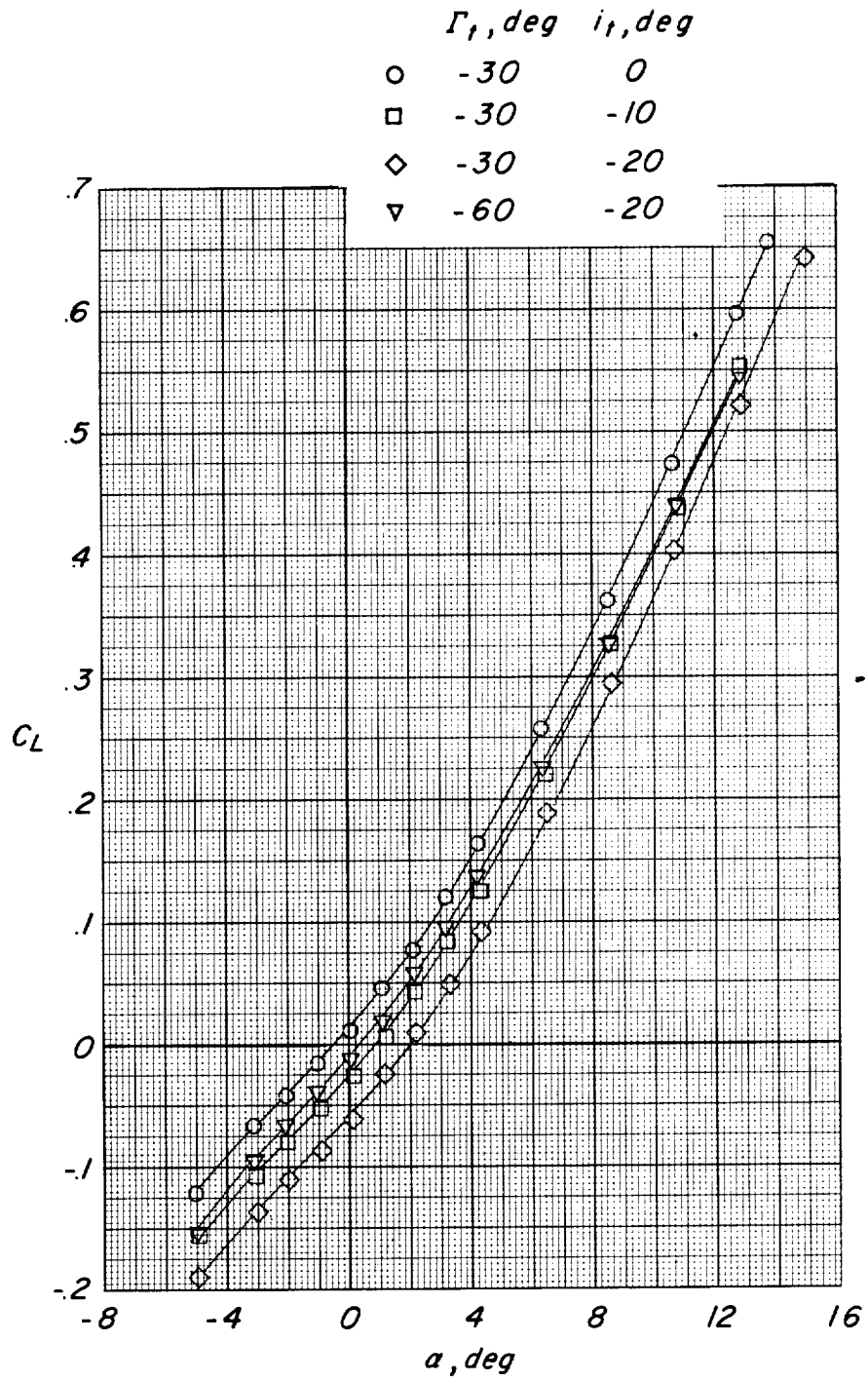

(c) M = 0.80.

Figure 6.- Continued.

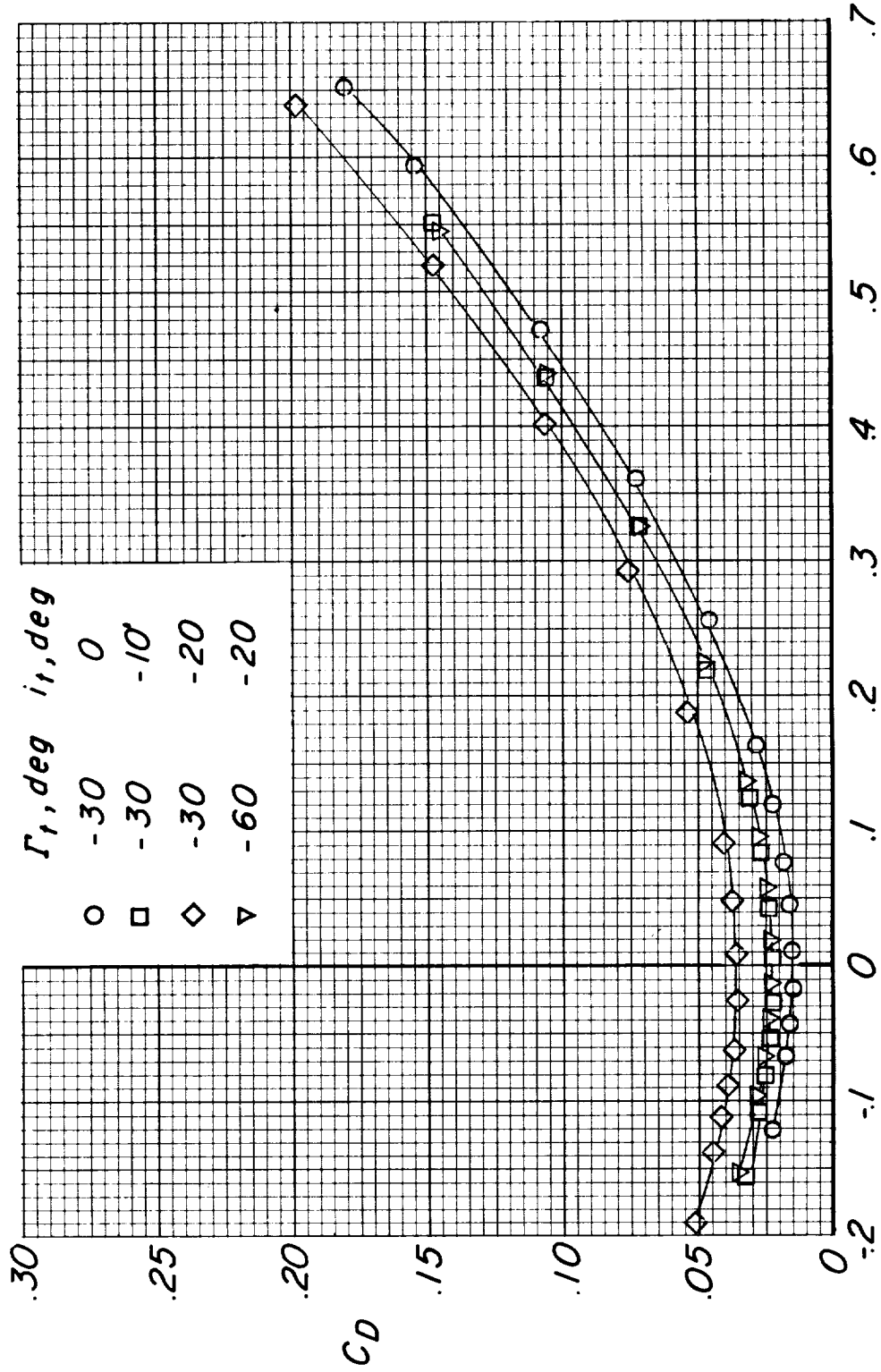

(c) Continued.

Figure 6.- Continued.

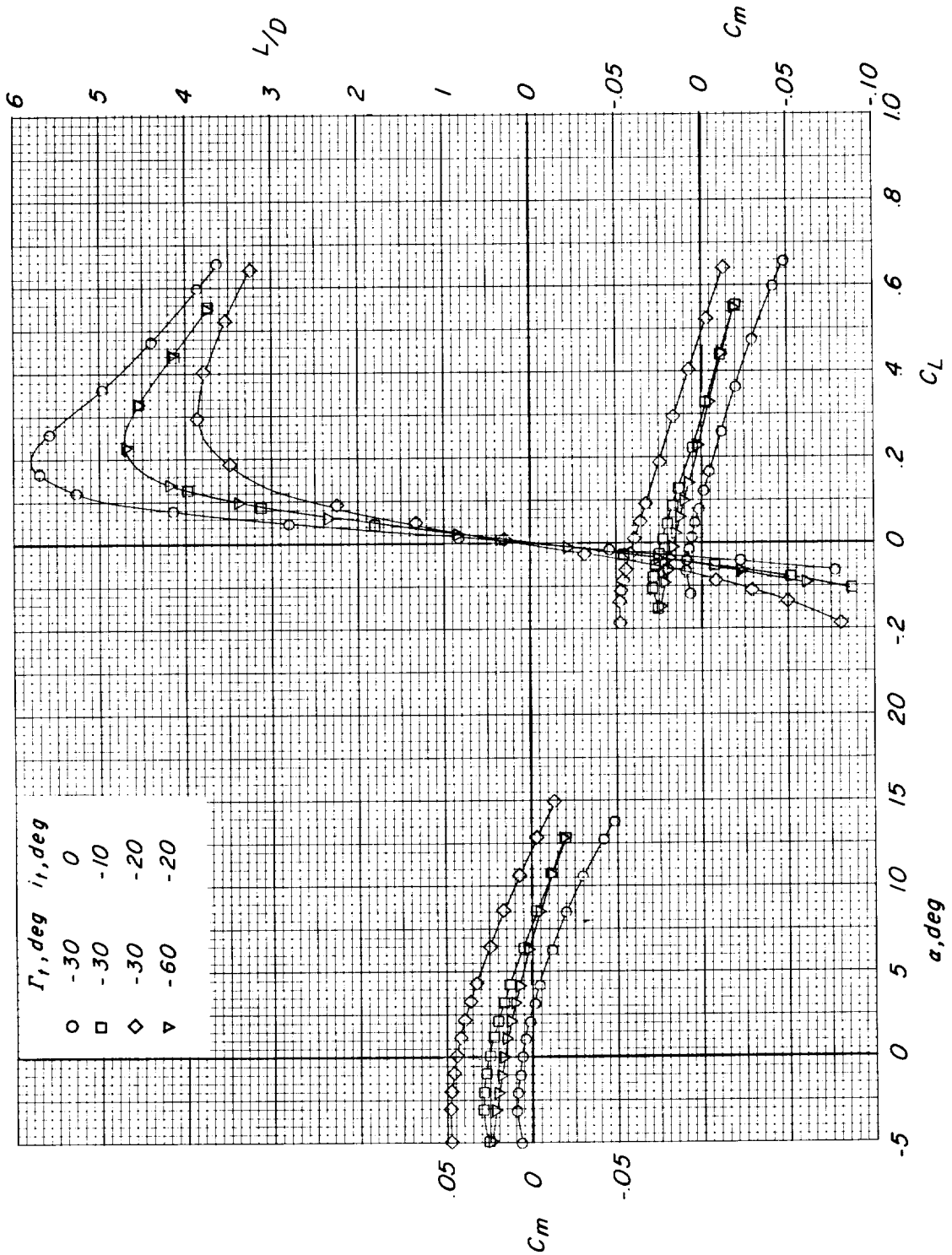

(c) Concluded.

Figure 6.- Continued.

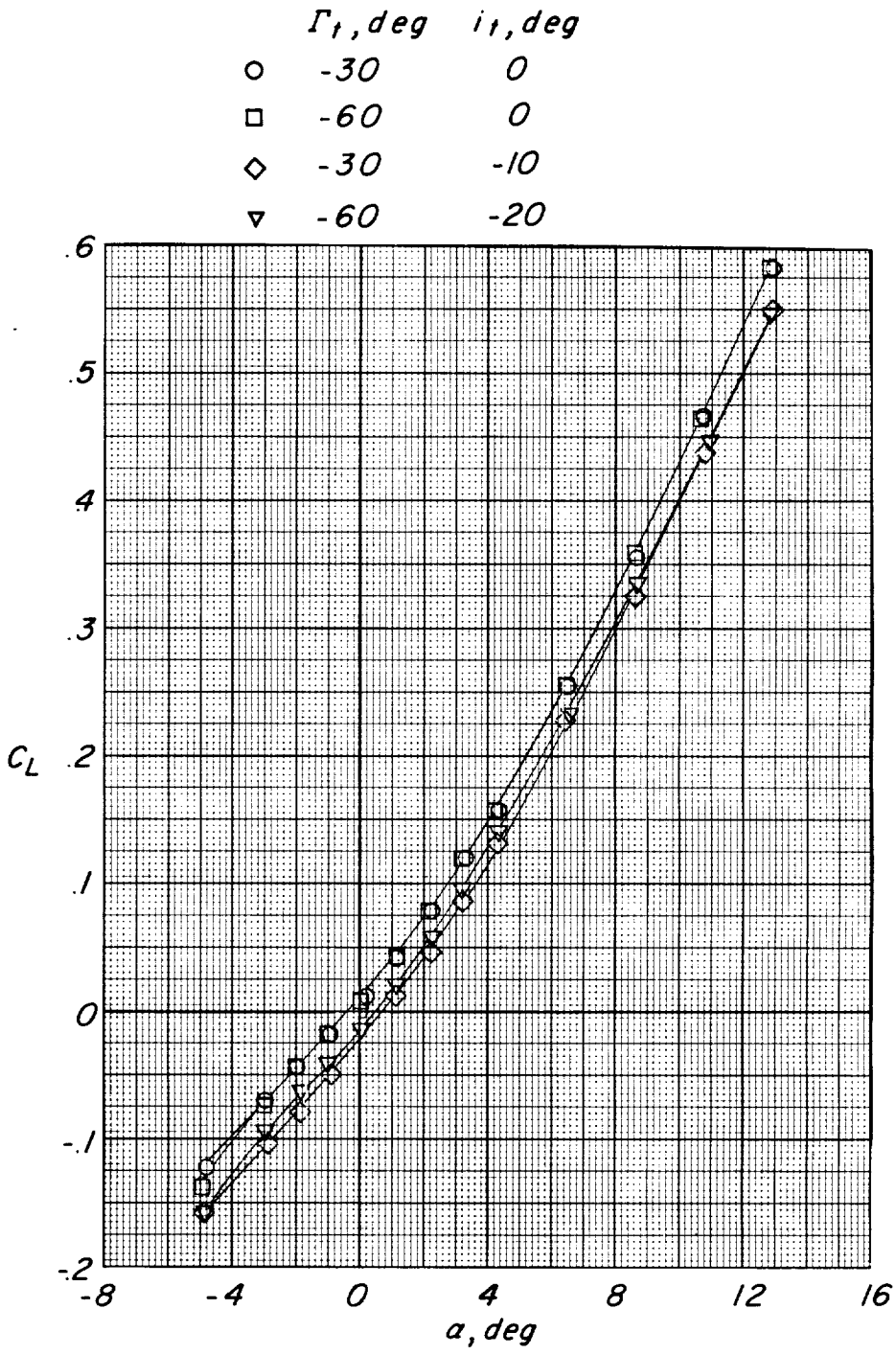

(d) M = 0.90.

Figure 6.- Continued.

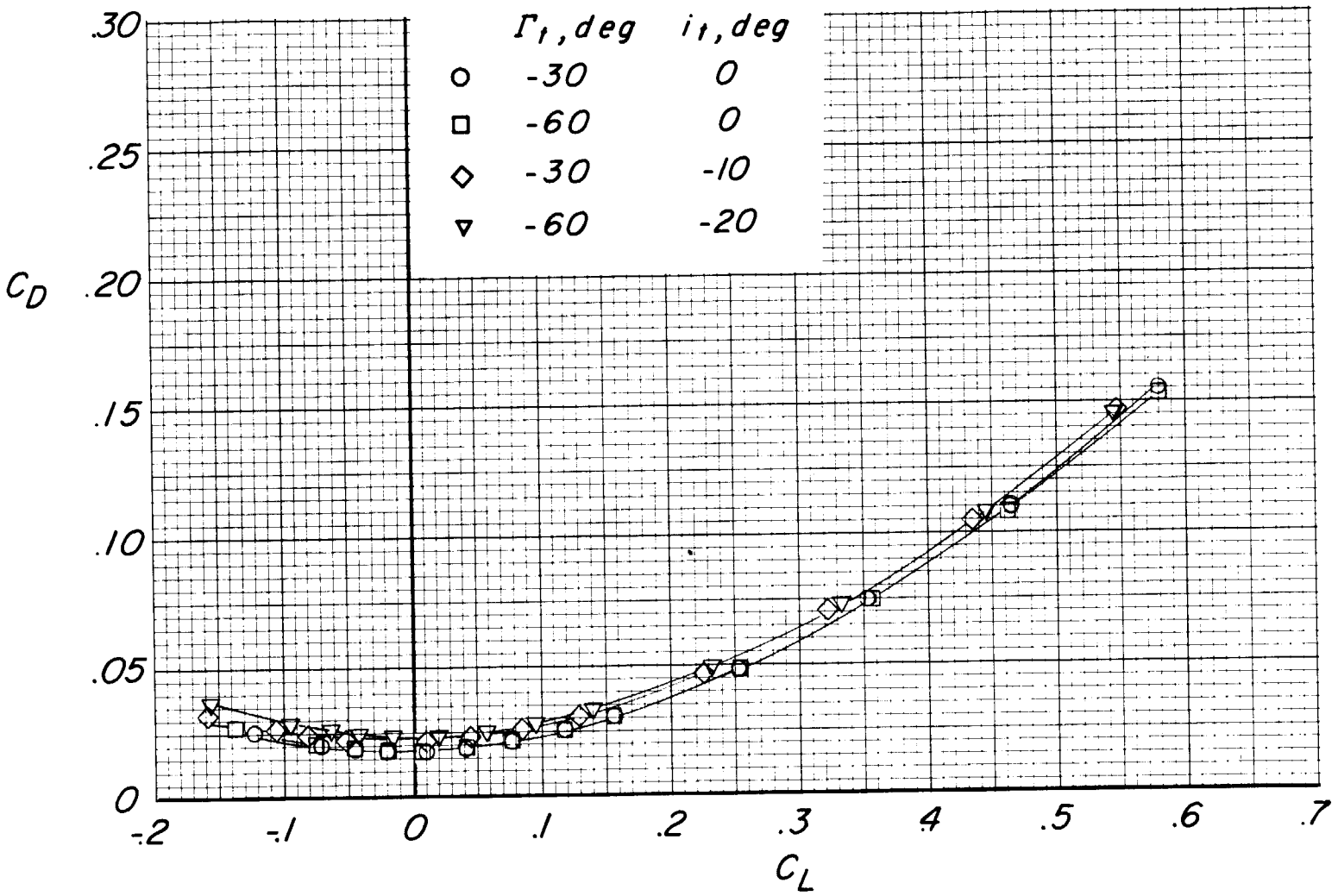

(d) Continued.

Figure 6.- Continued.

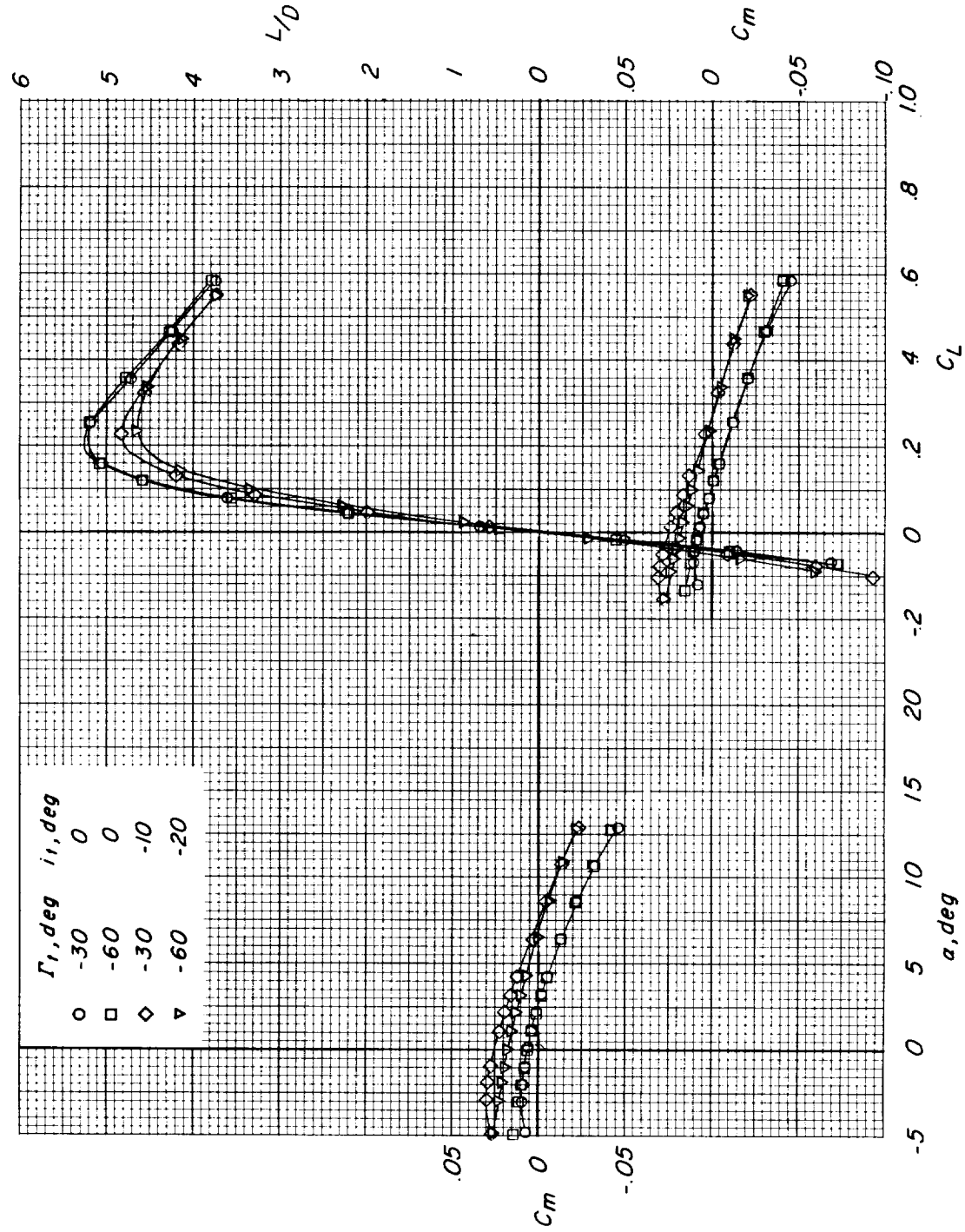

(d) Concluded.

Figure 6.- Continued.

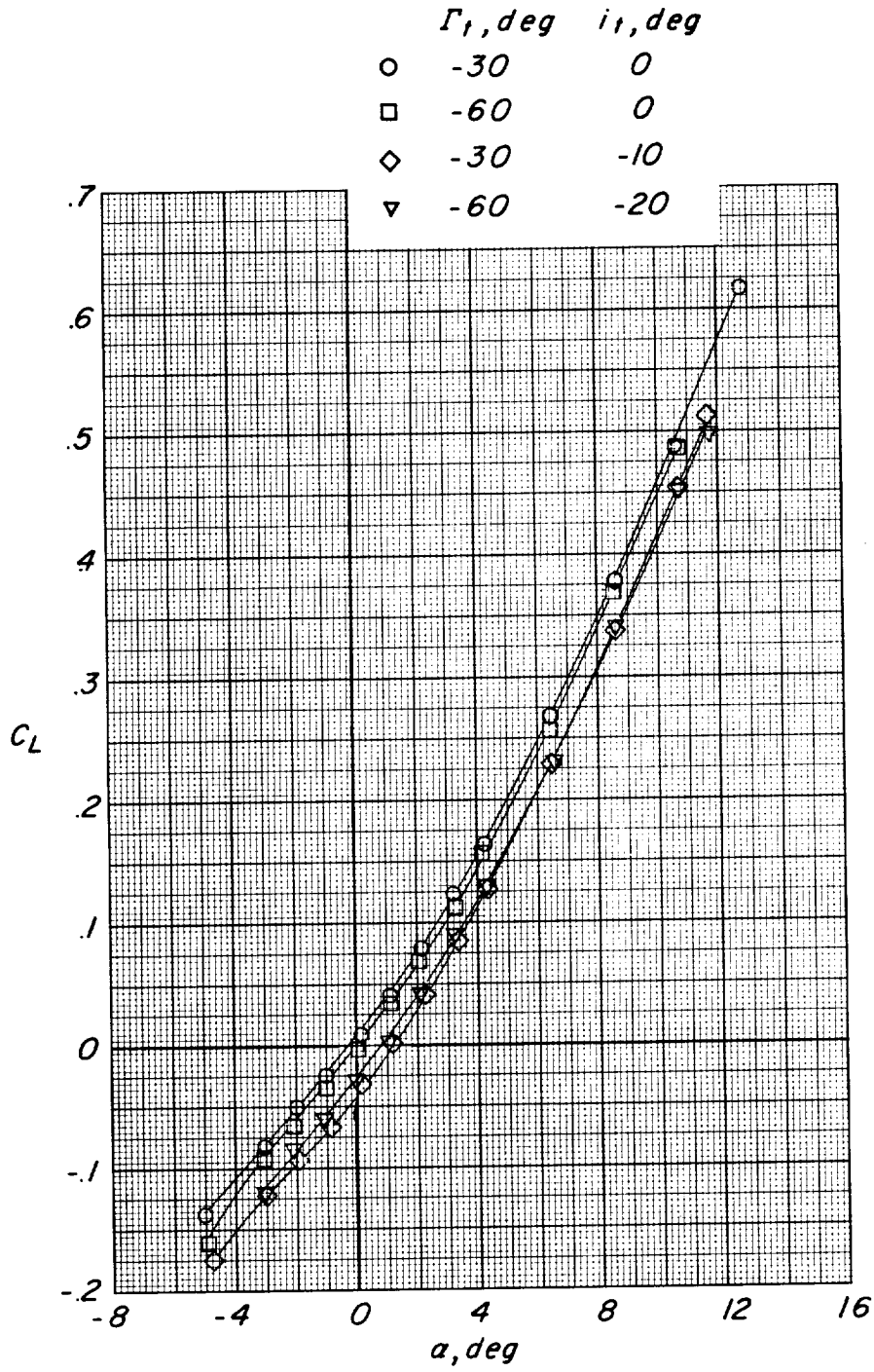

(e) M = 1.00.

Figure 6.- Continued.

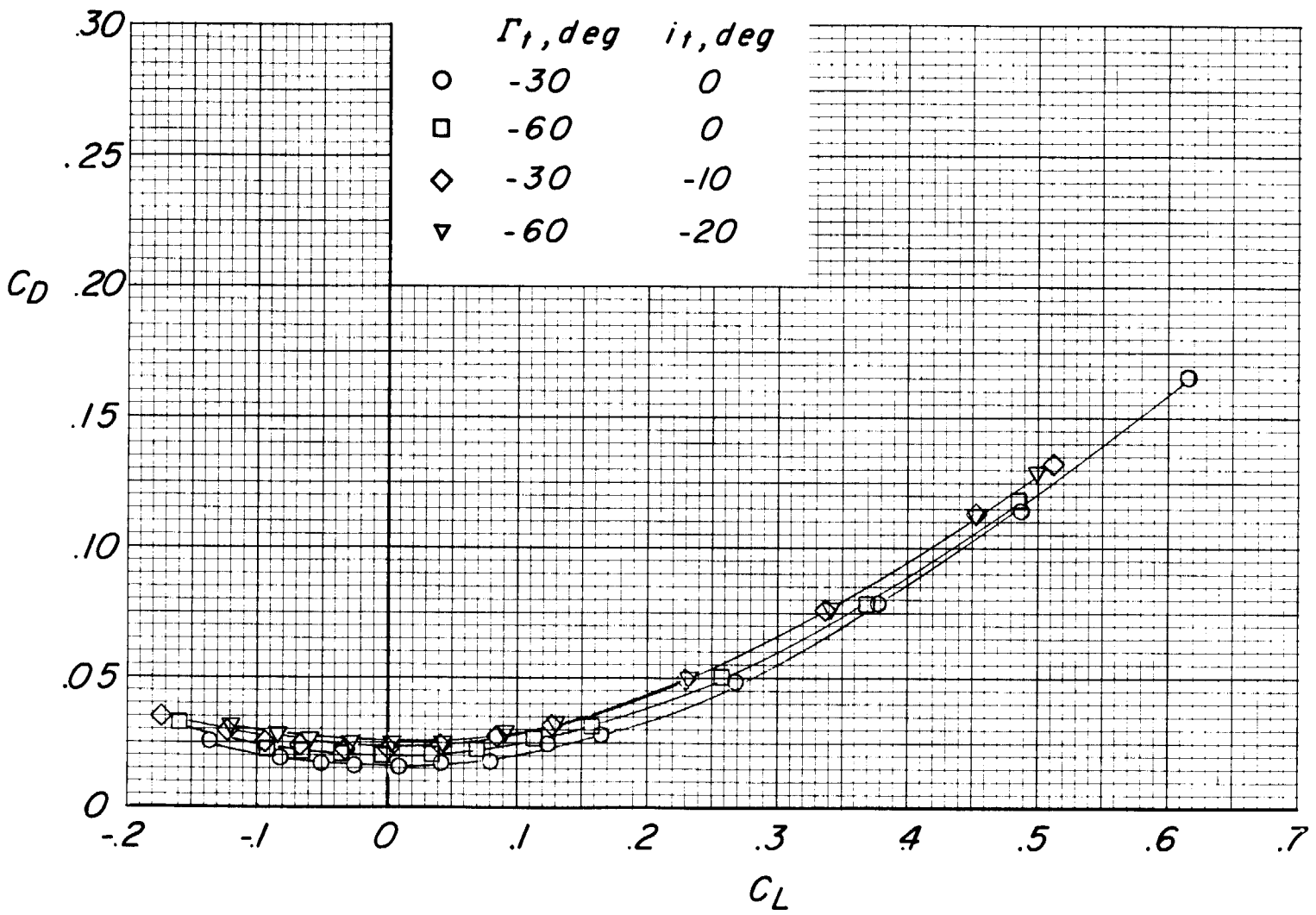

(e) Continued.

Figure 6.- Continued.

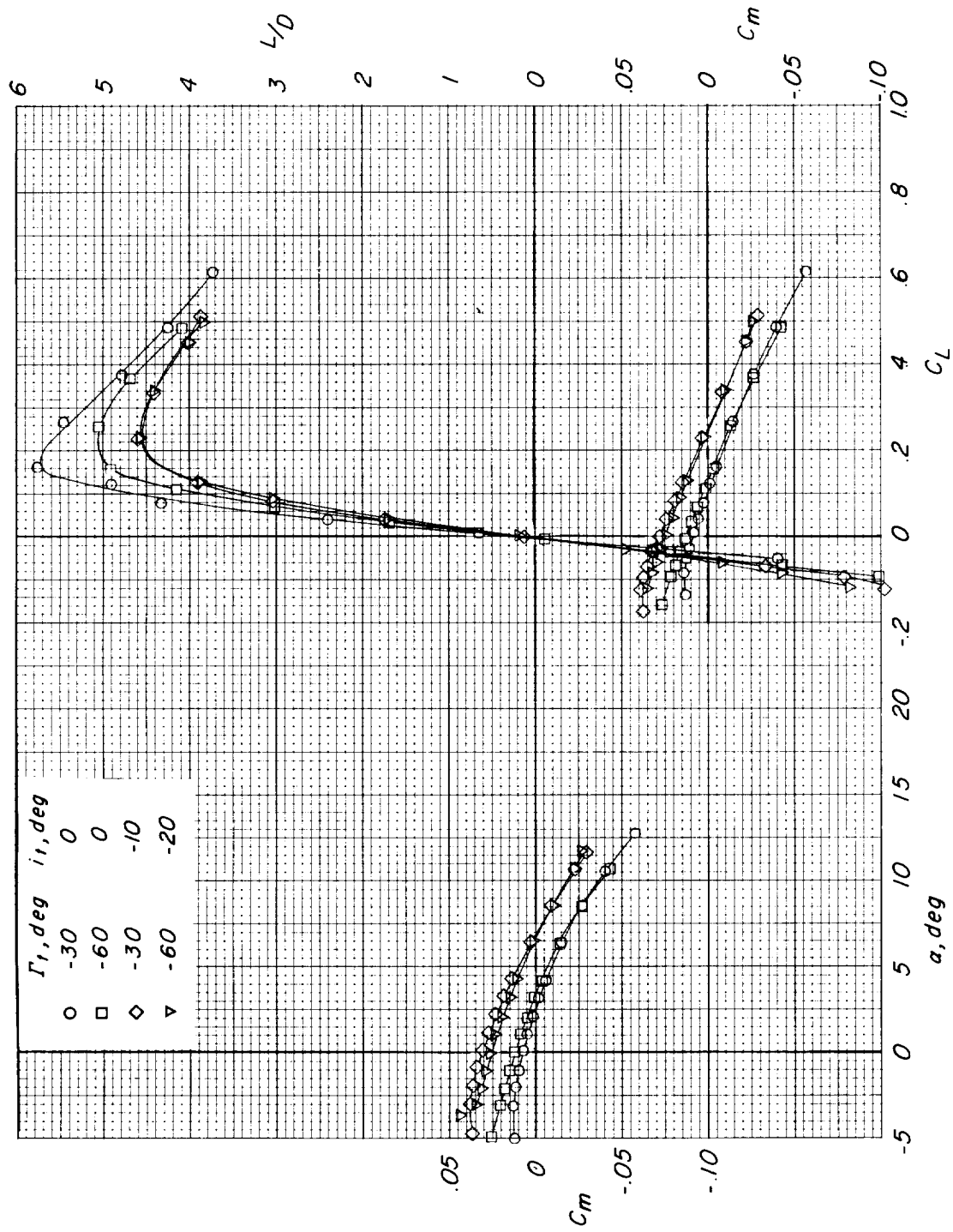

(e) Concluded.

Figure 6.- Continued.

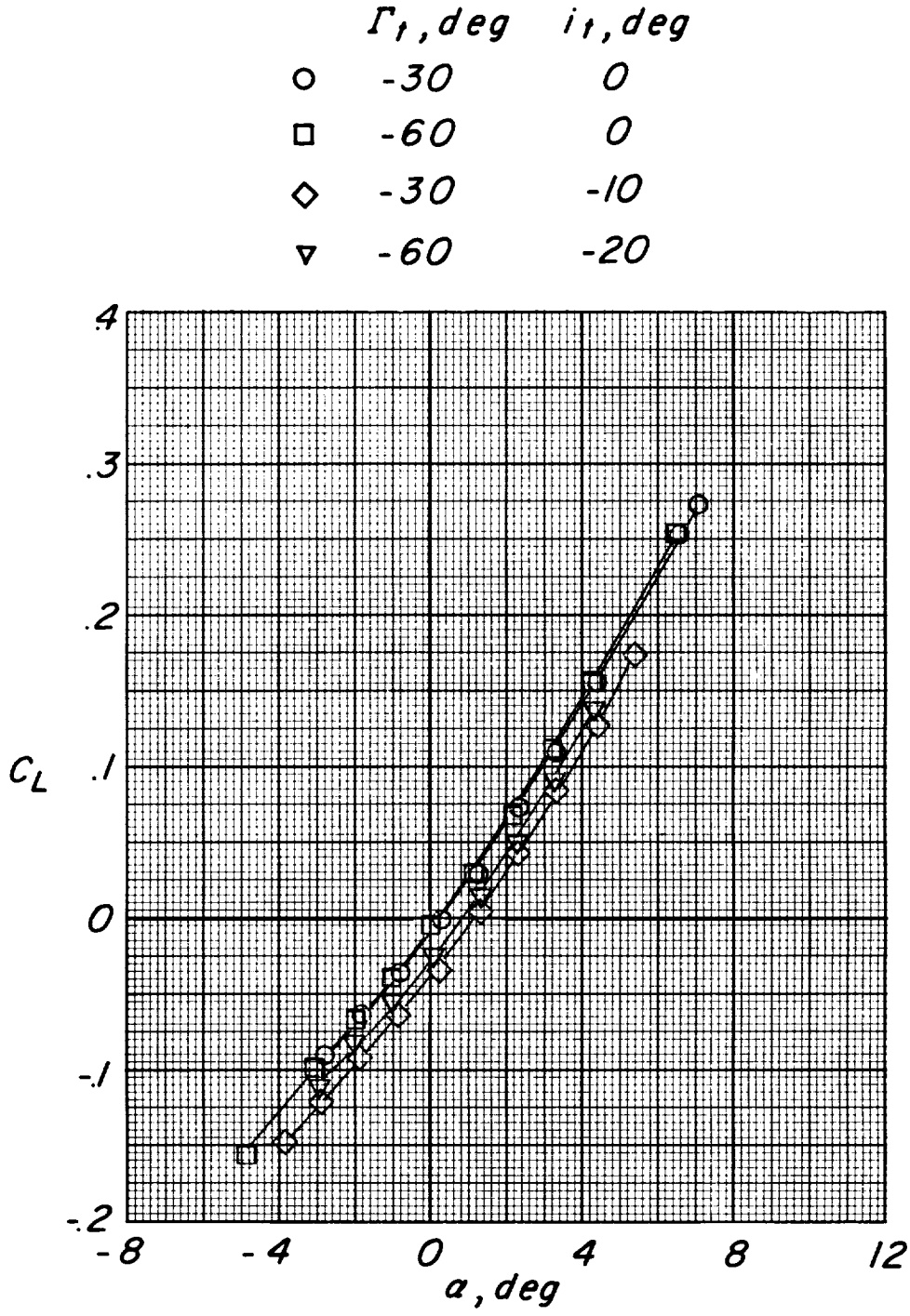

(f) M = 1.13.

Figure 6.- Continued.

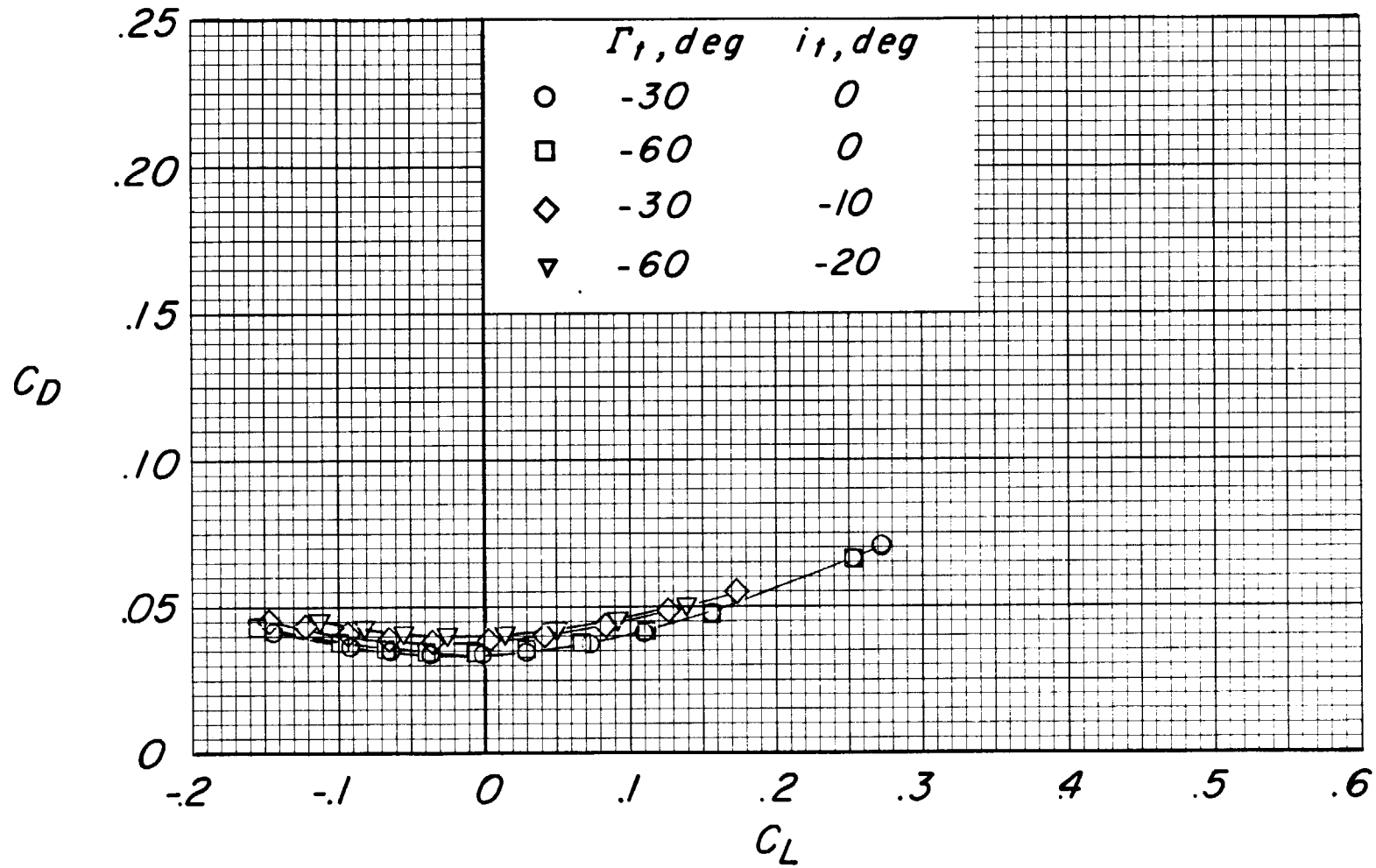

(f) Continued.

Figure 6.- Continued.

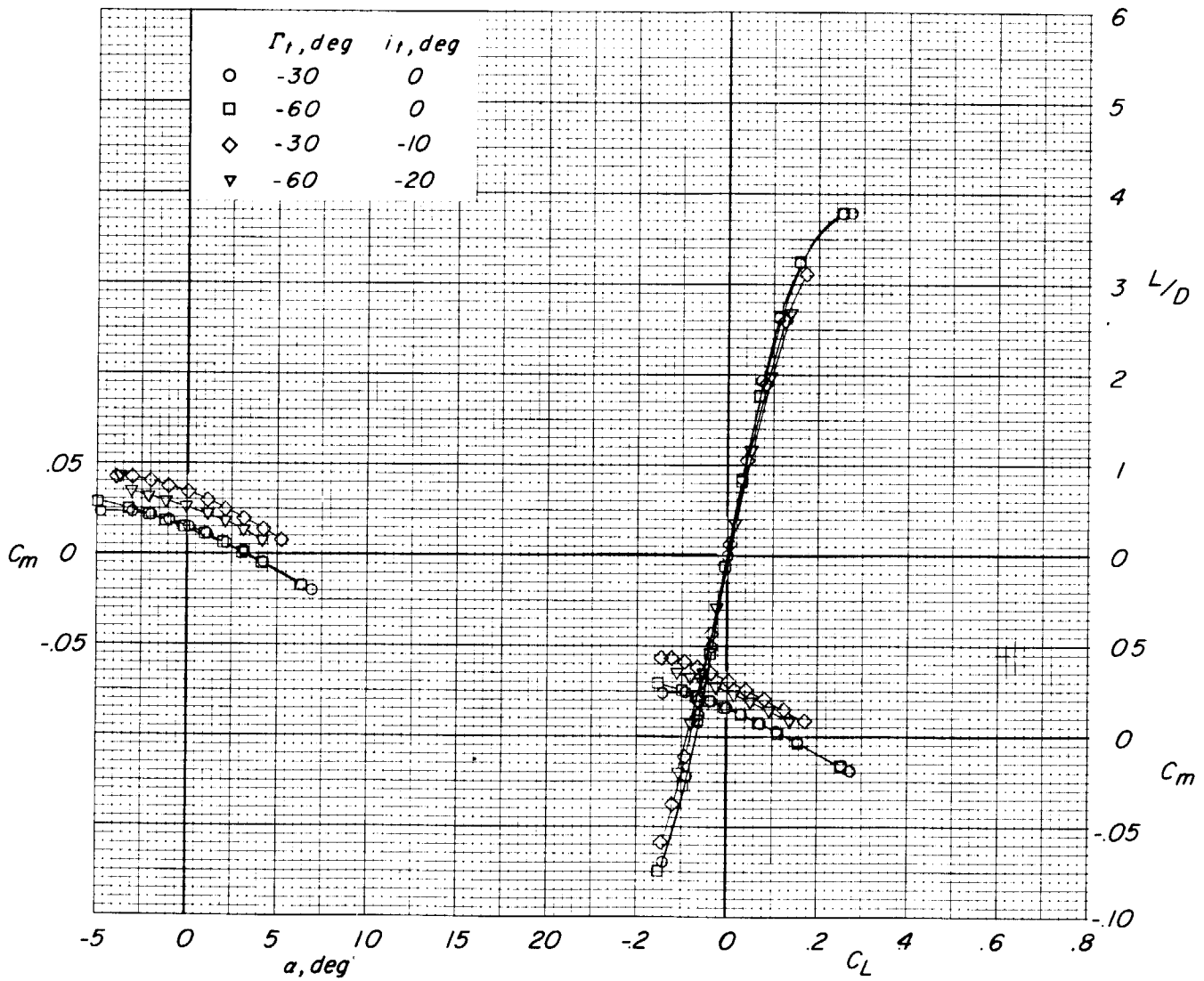

(f) Concluded.

Figure 6.- Concluded.

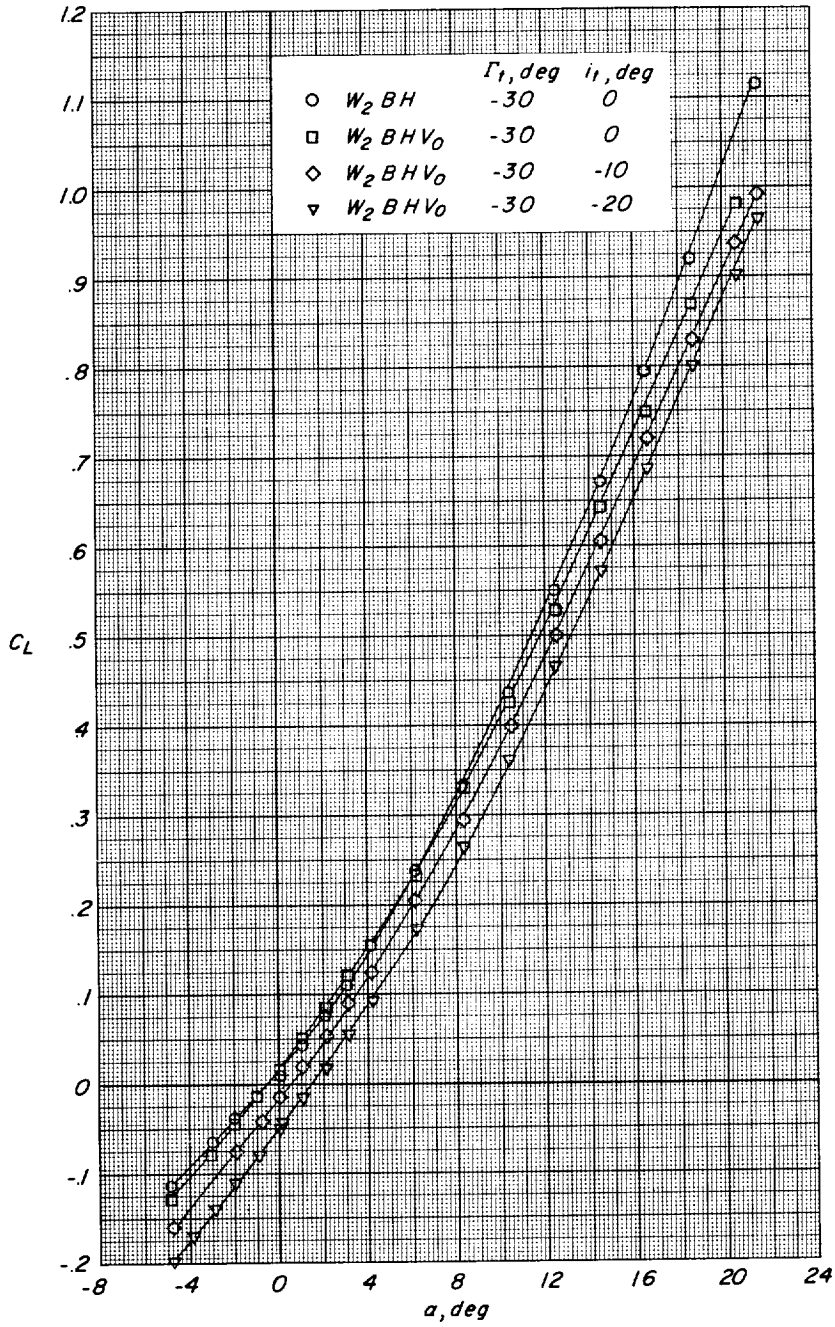

(a) M = 0.40.

Figure 7.- Effects of addition of outboard vertical tails (V_0) on the longitudinal stability and control characteristics of the configuration having the 75° modified arrow wing (W_2) at various Mach numbers. Center vertical tail off.

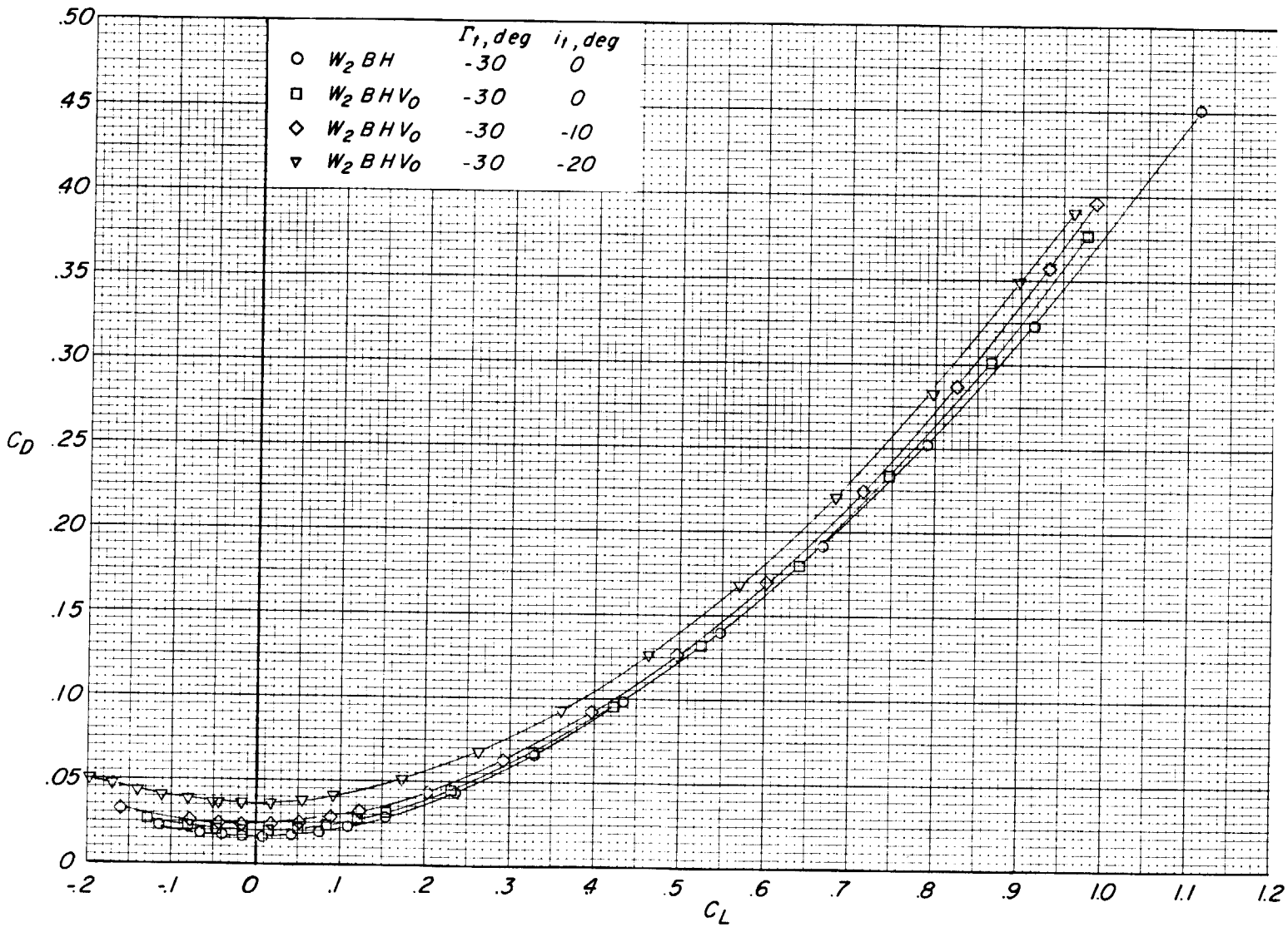

(a) Continued.

Figure 7.- Continued.

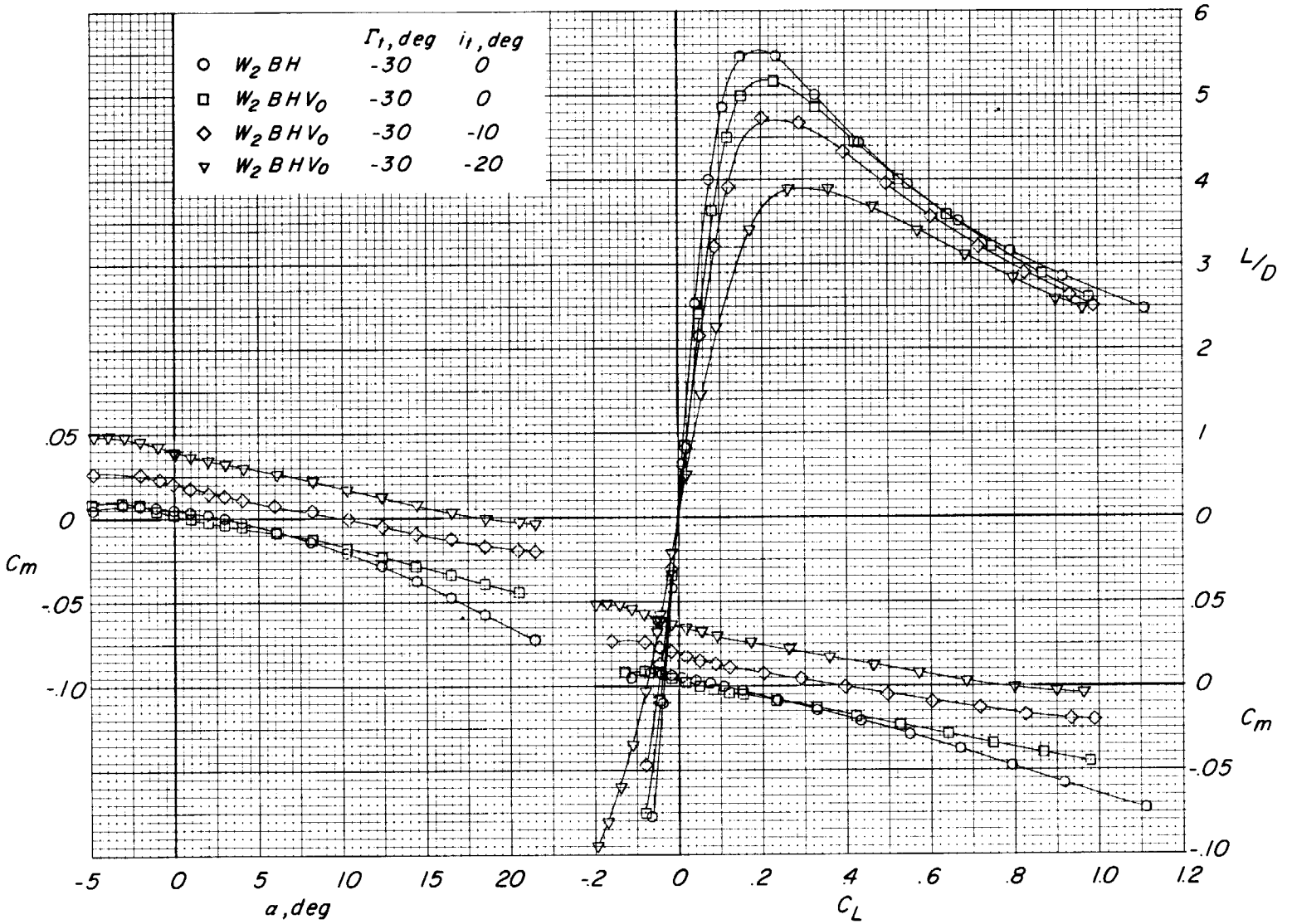

(a) Concluded.

Figure 7.- Continued.

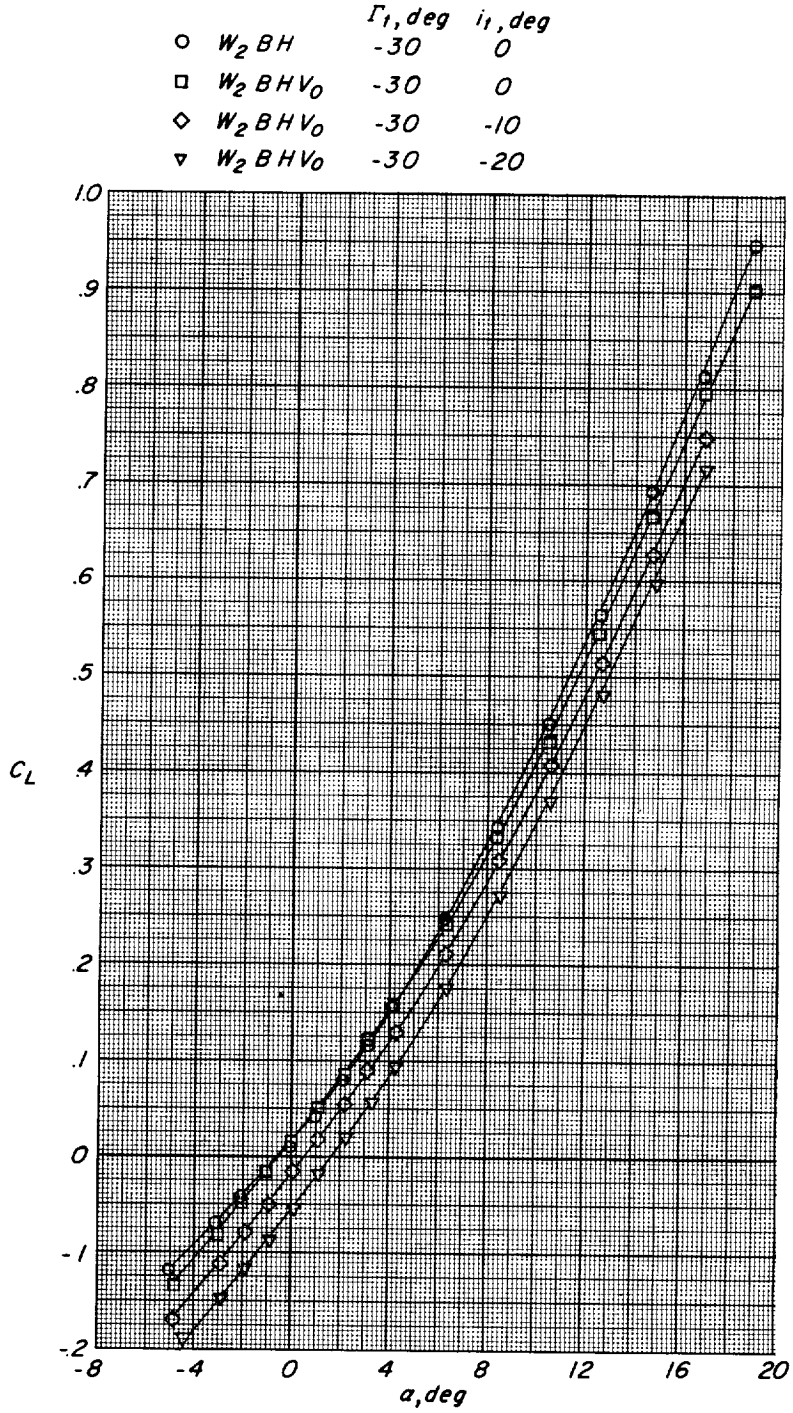

(b) M = 0.60.

Figure 7.- Continued.

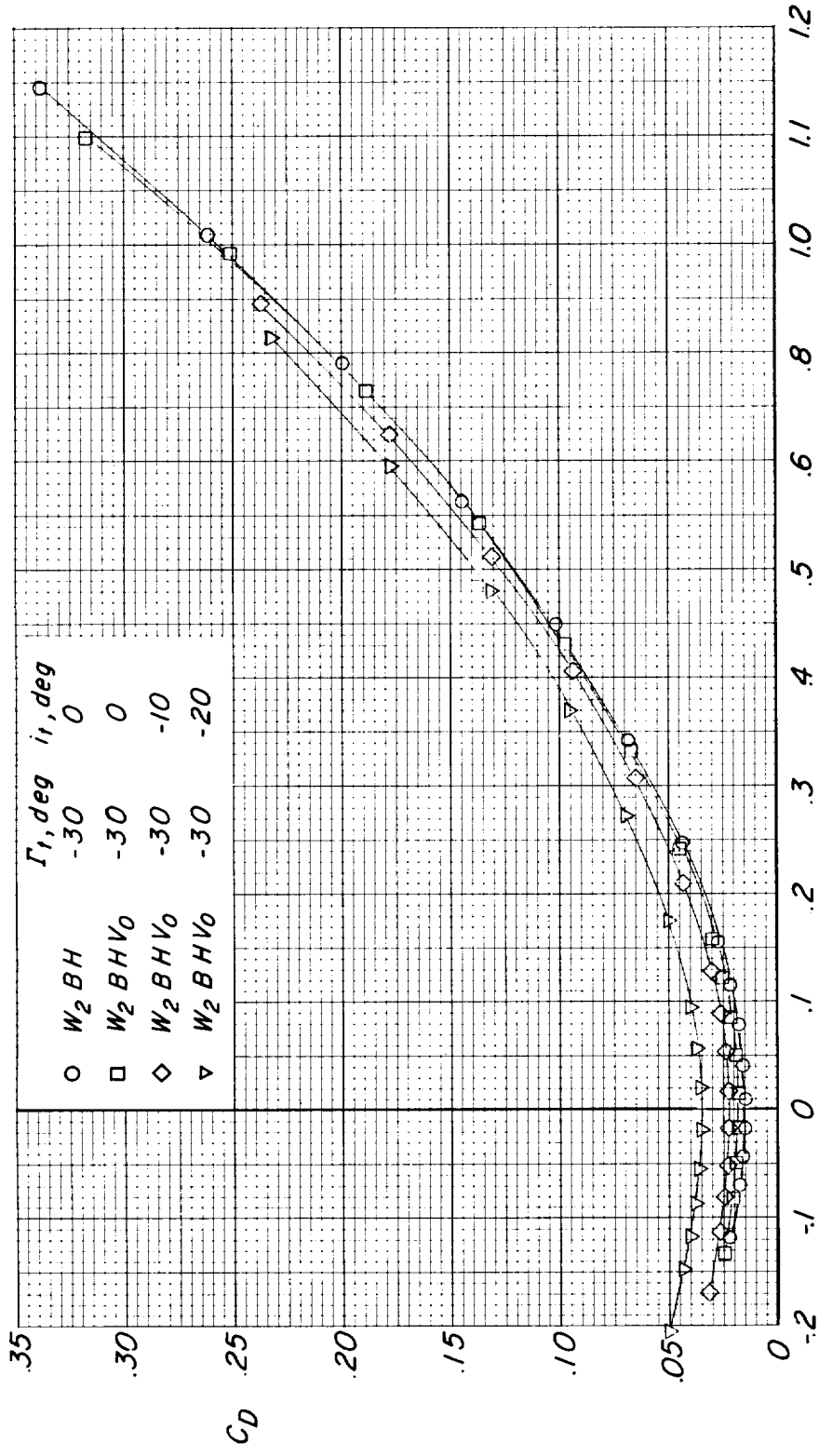

(b) Continued.

Figure 7.- Continued.

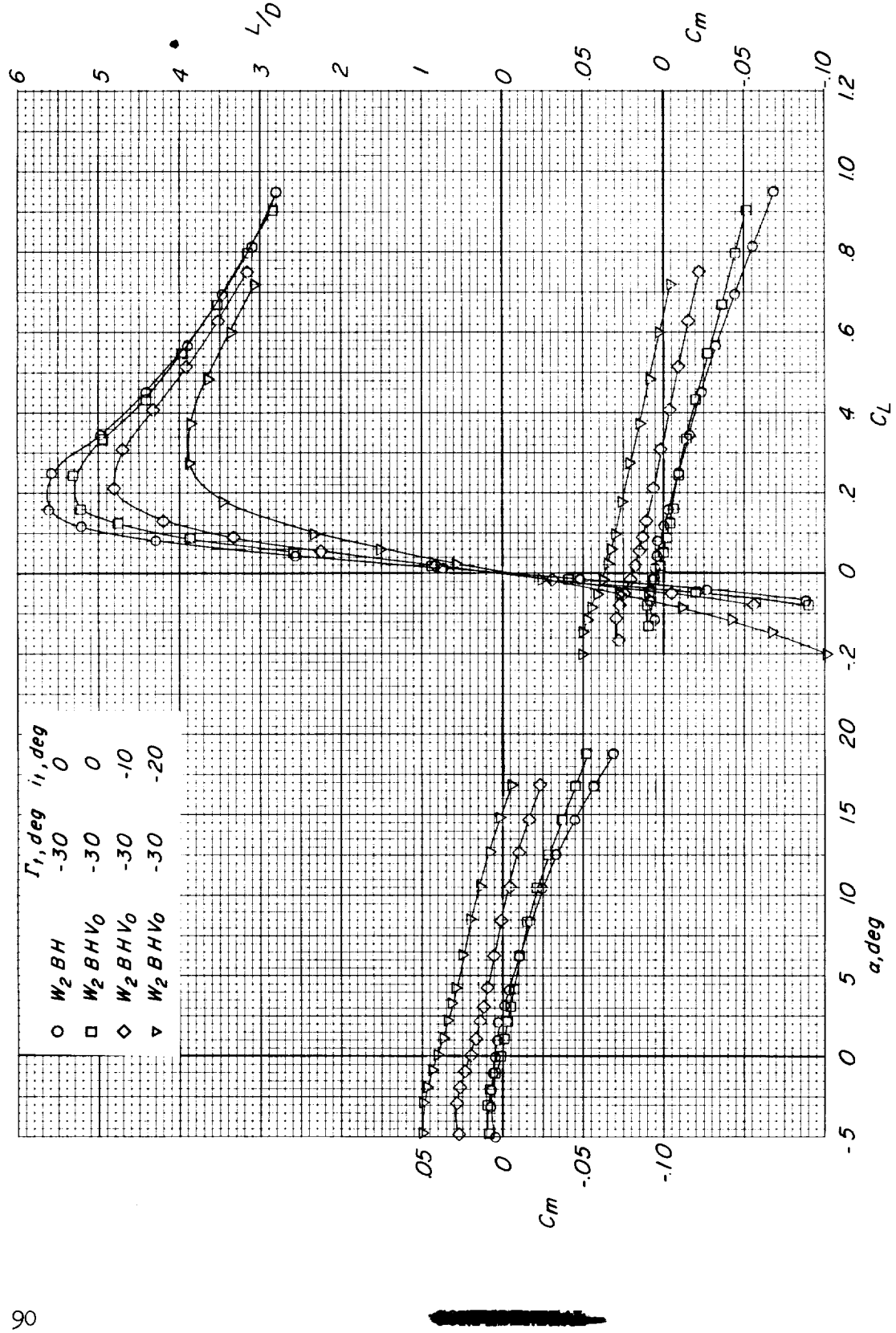

(b) Concluded.

Figure 7.- Continued.

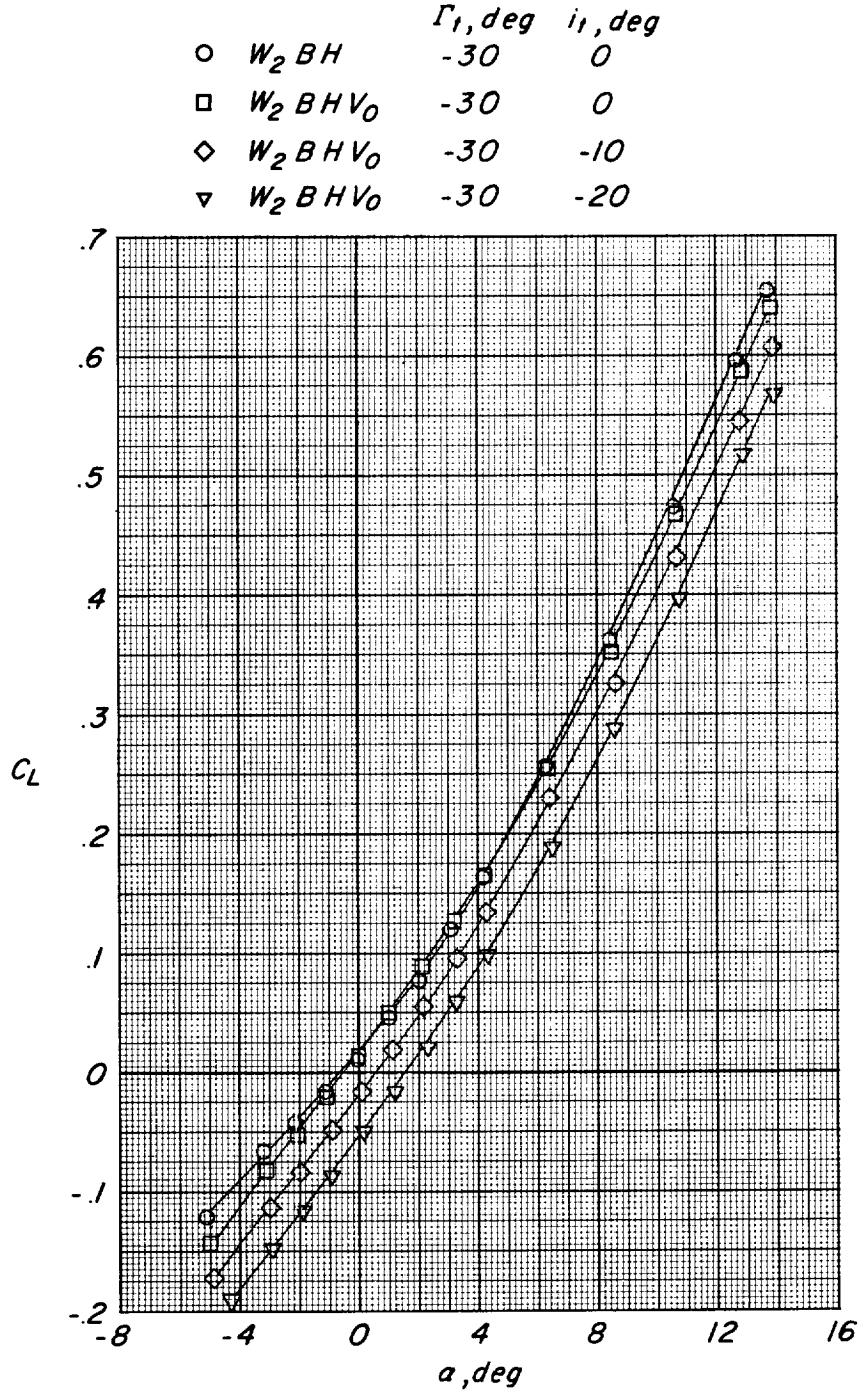

(c) M = 0.80.

Figure 7.- Continued.

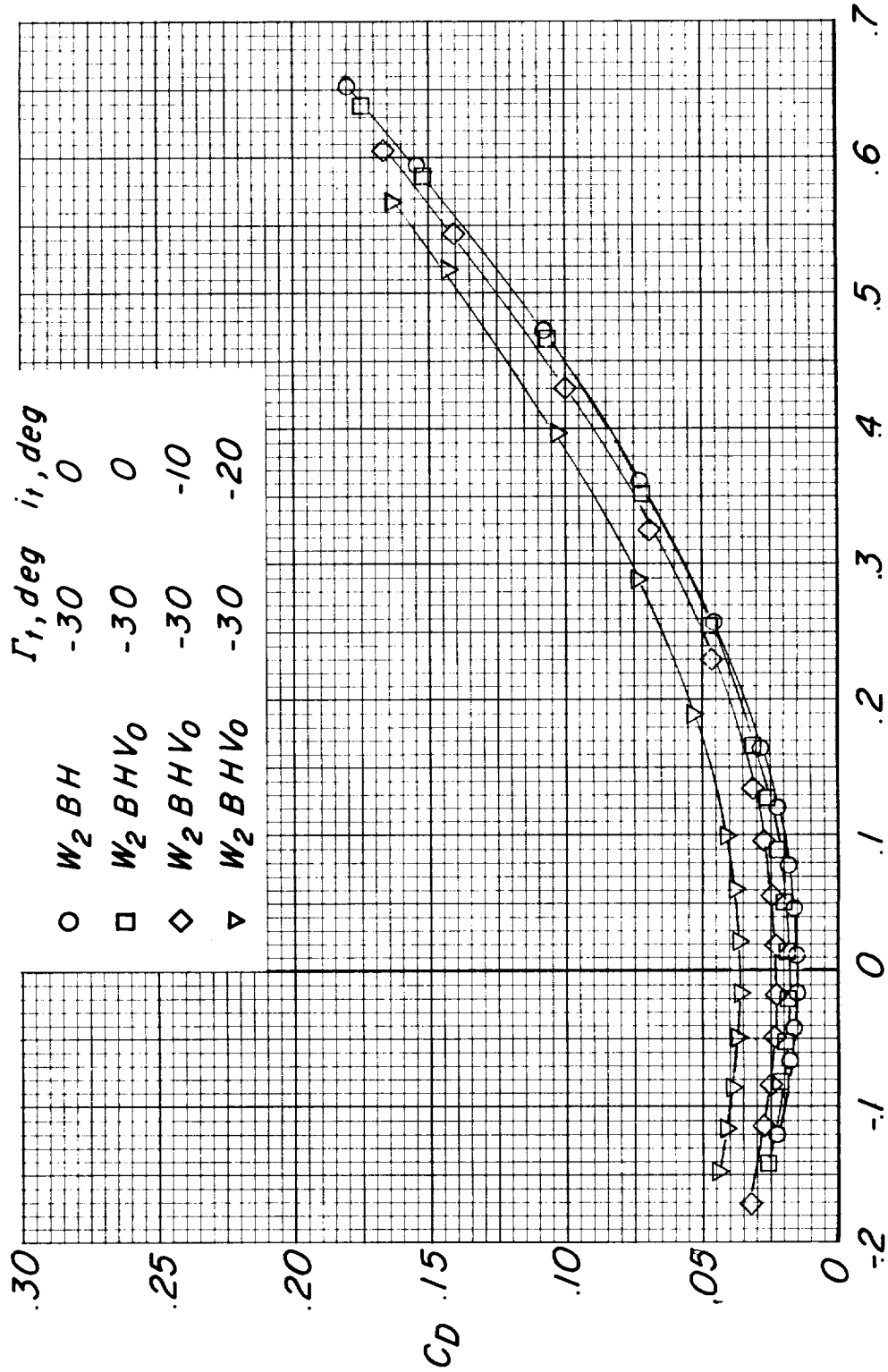

(c) Continued.

Figure 7.- Continued.

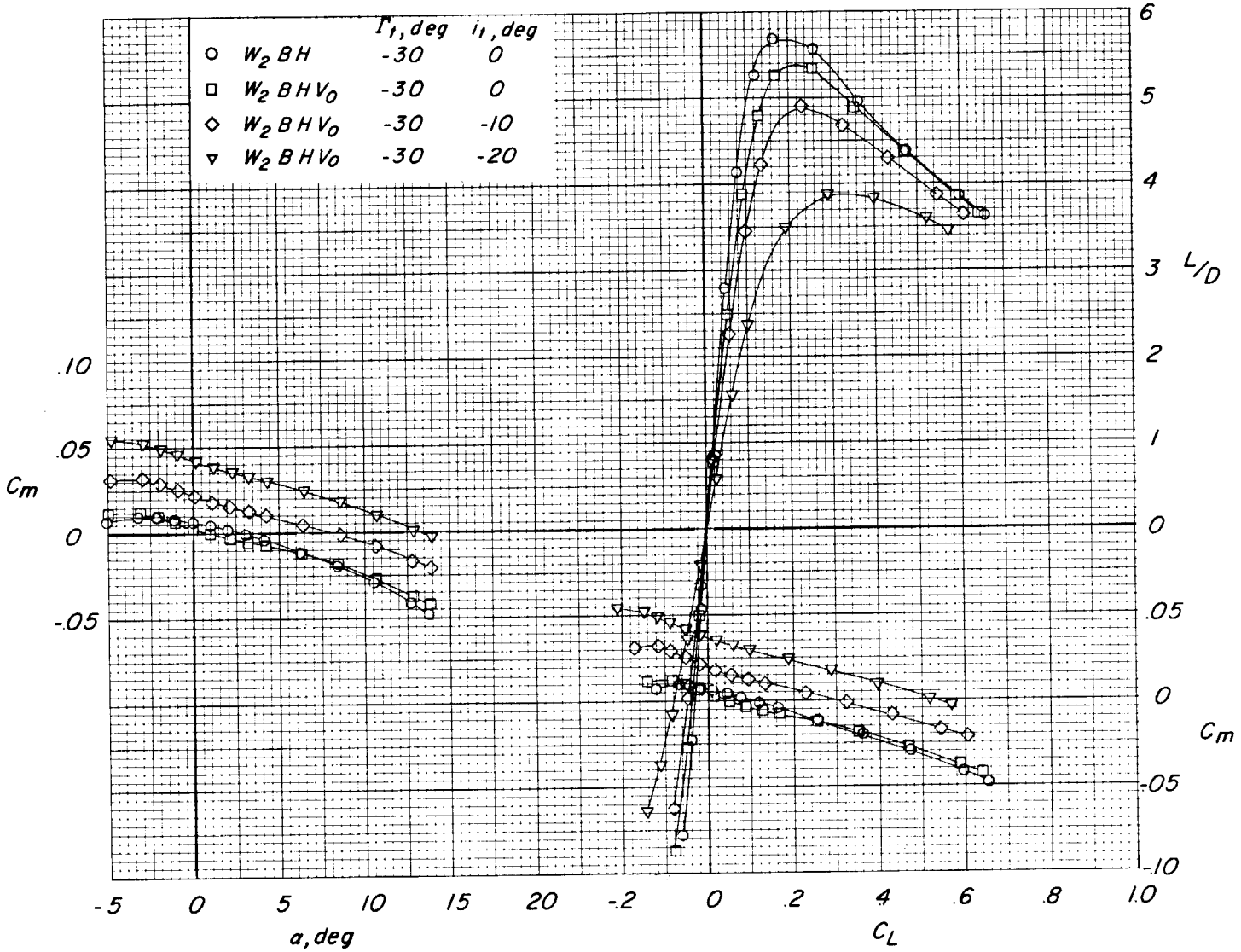

(c) Concluded.

Figure 7.- Concluded.

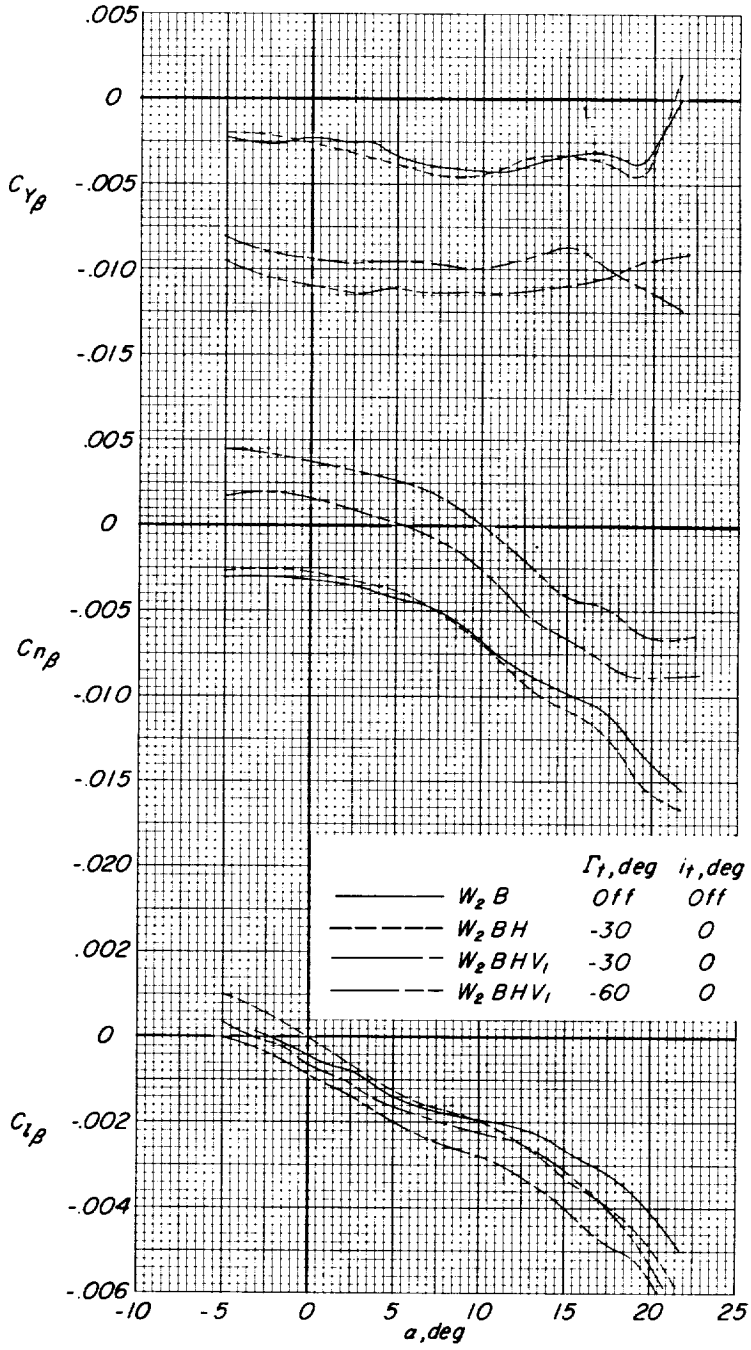

(a) M = 0.40.

Figure 8.- Effect of small center vertical tail (V_1) on the lateral-directional characteristics of the modified 75° arrow wing (W_2) configuration having various model components in combination.

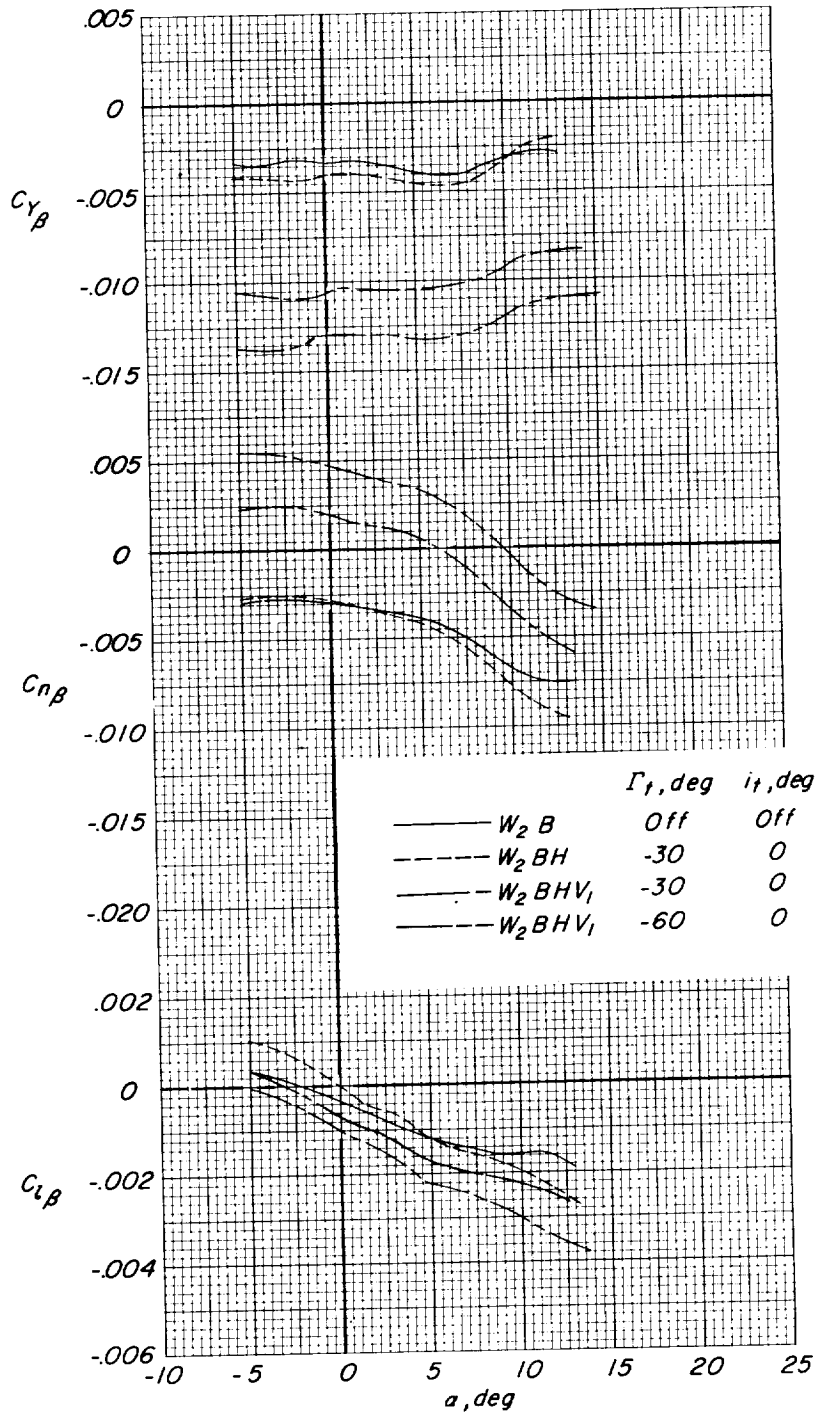

(b) M = 0.90.

Figure 8.- Continued.

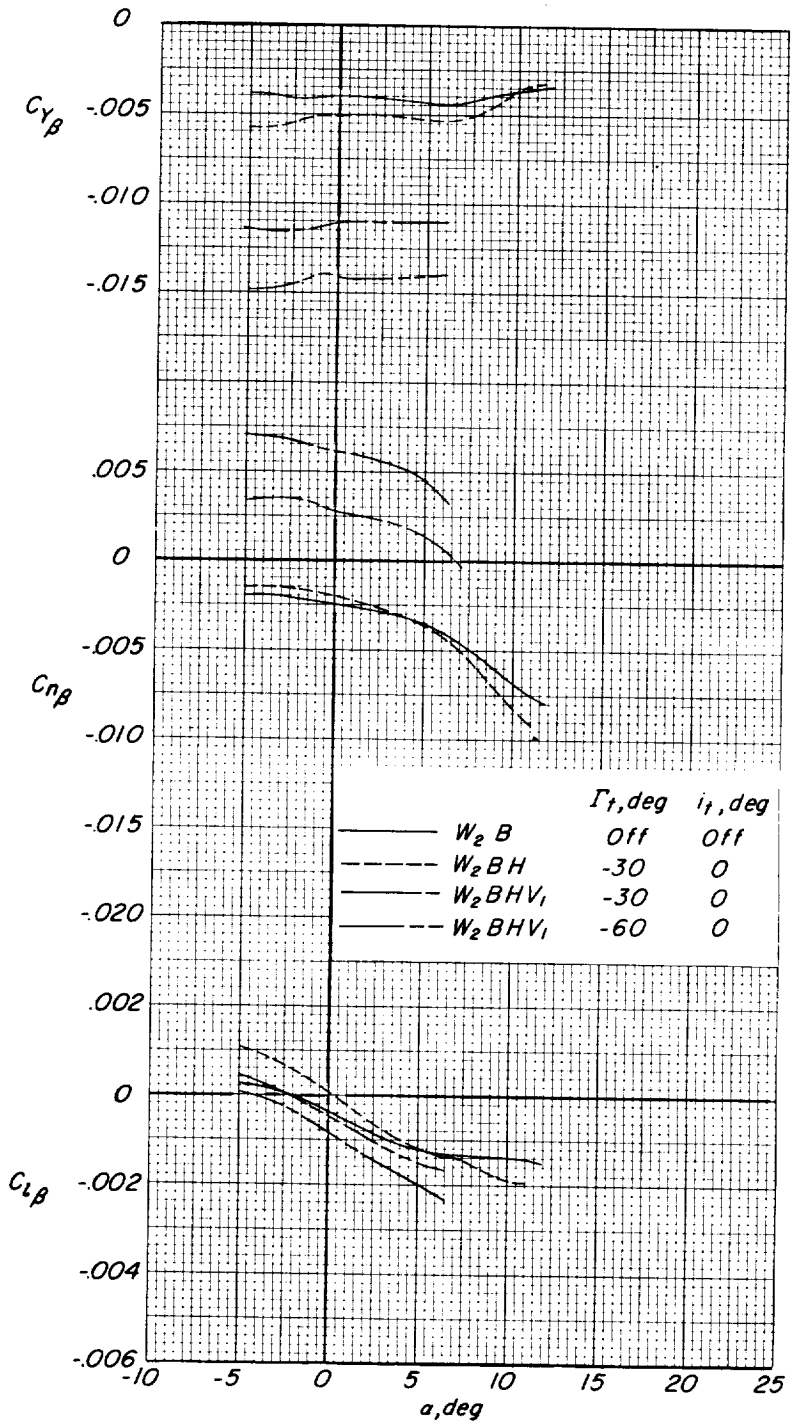

(c) M = 1.13.

Figure 8.- Concluded.

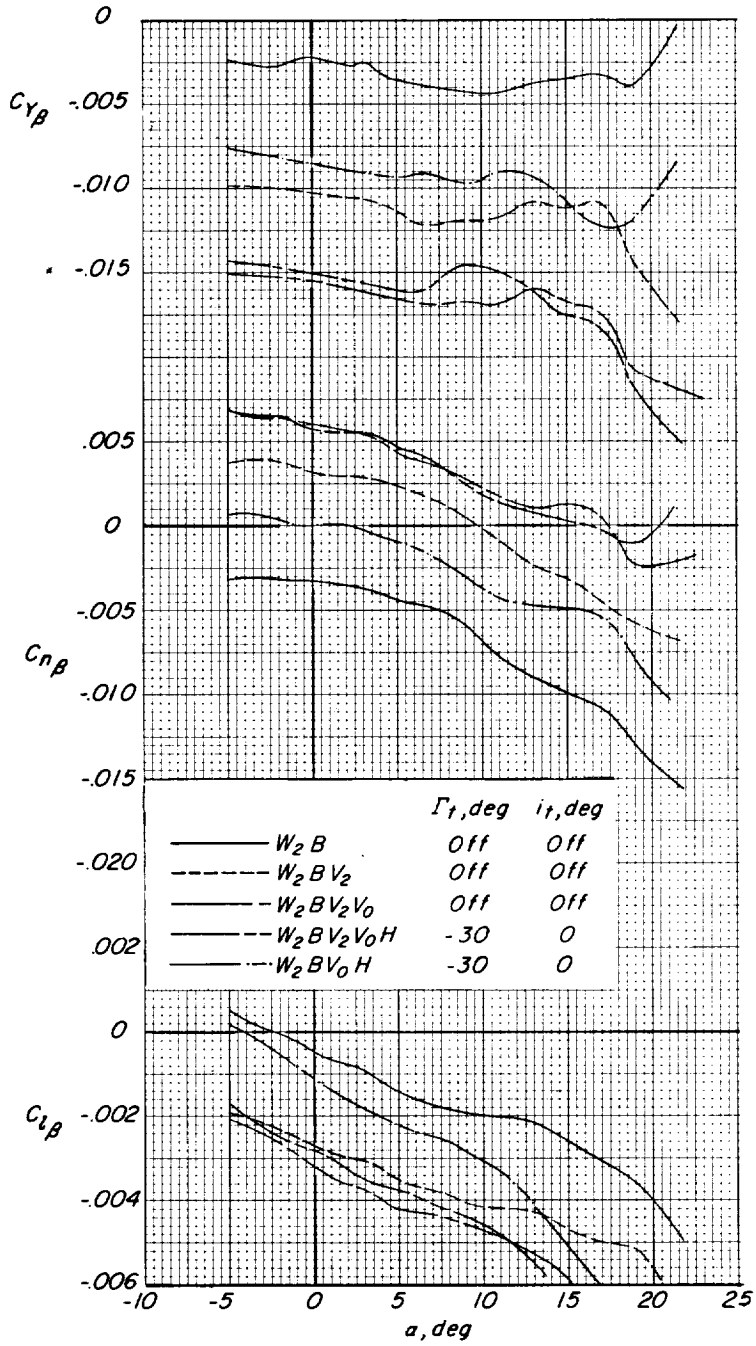

(a) M = 0.40.

Figure 9.- The effects of vertical-tail size and location on the lateral-directional characteristics of the modified 75° arrow wing (W_2) configuration having various model components in combination.

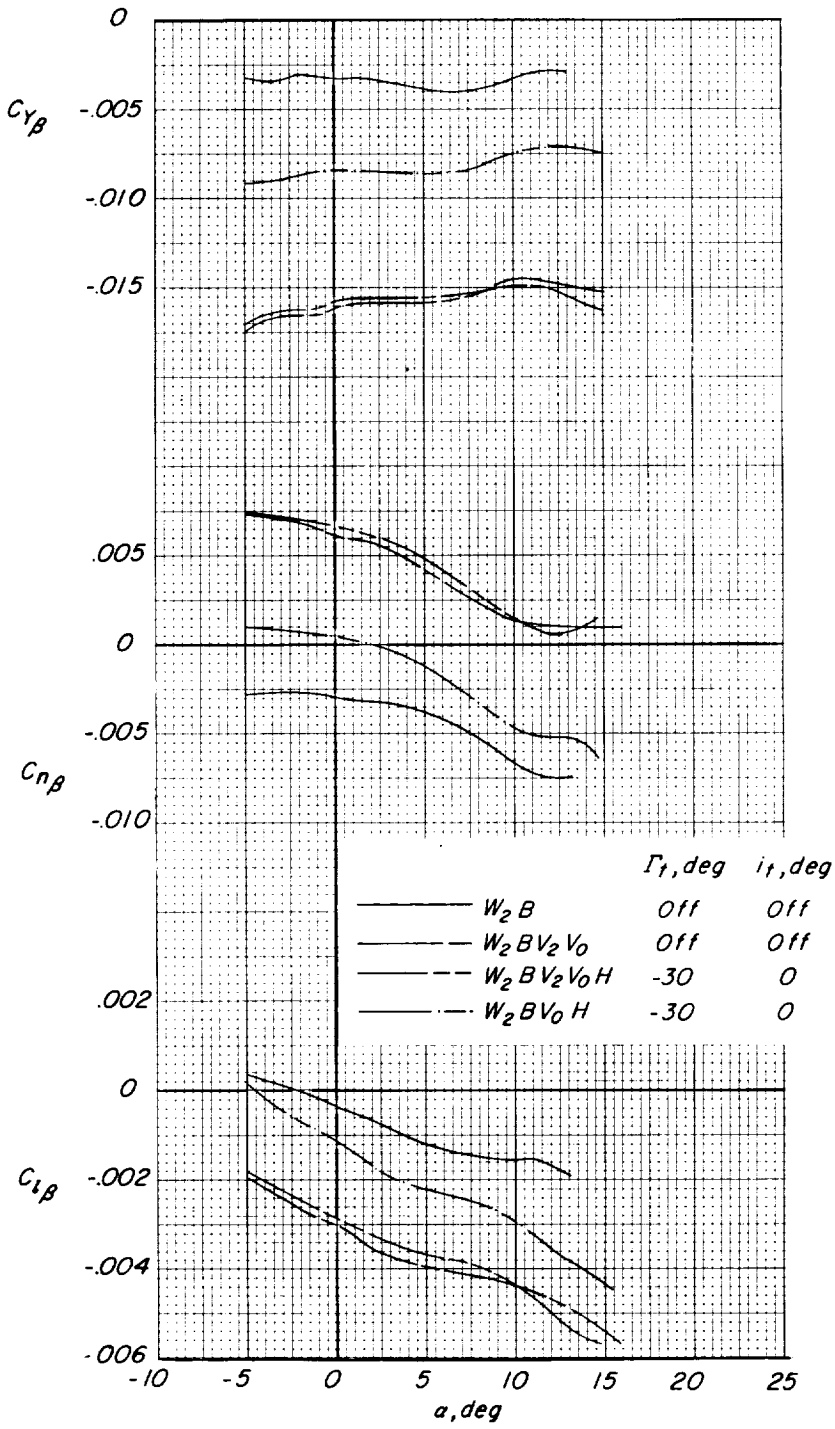

(b) M = 0.80.

Figure 9.- Continued.

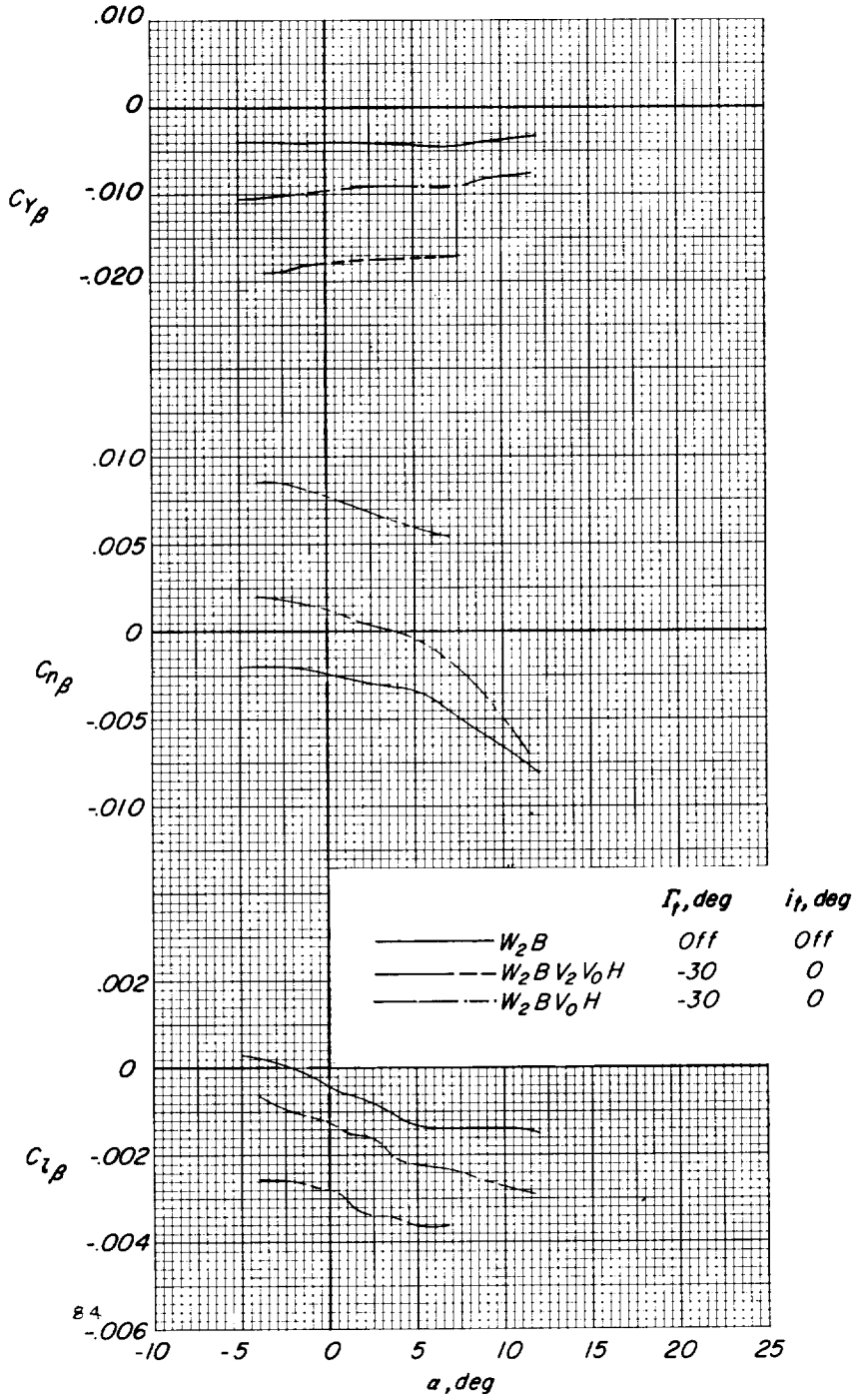

(c) M = 1.13.

Figure 9.- Concluded.

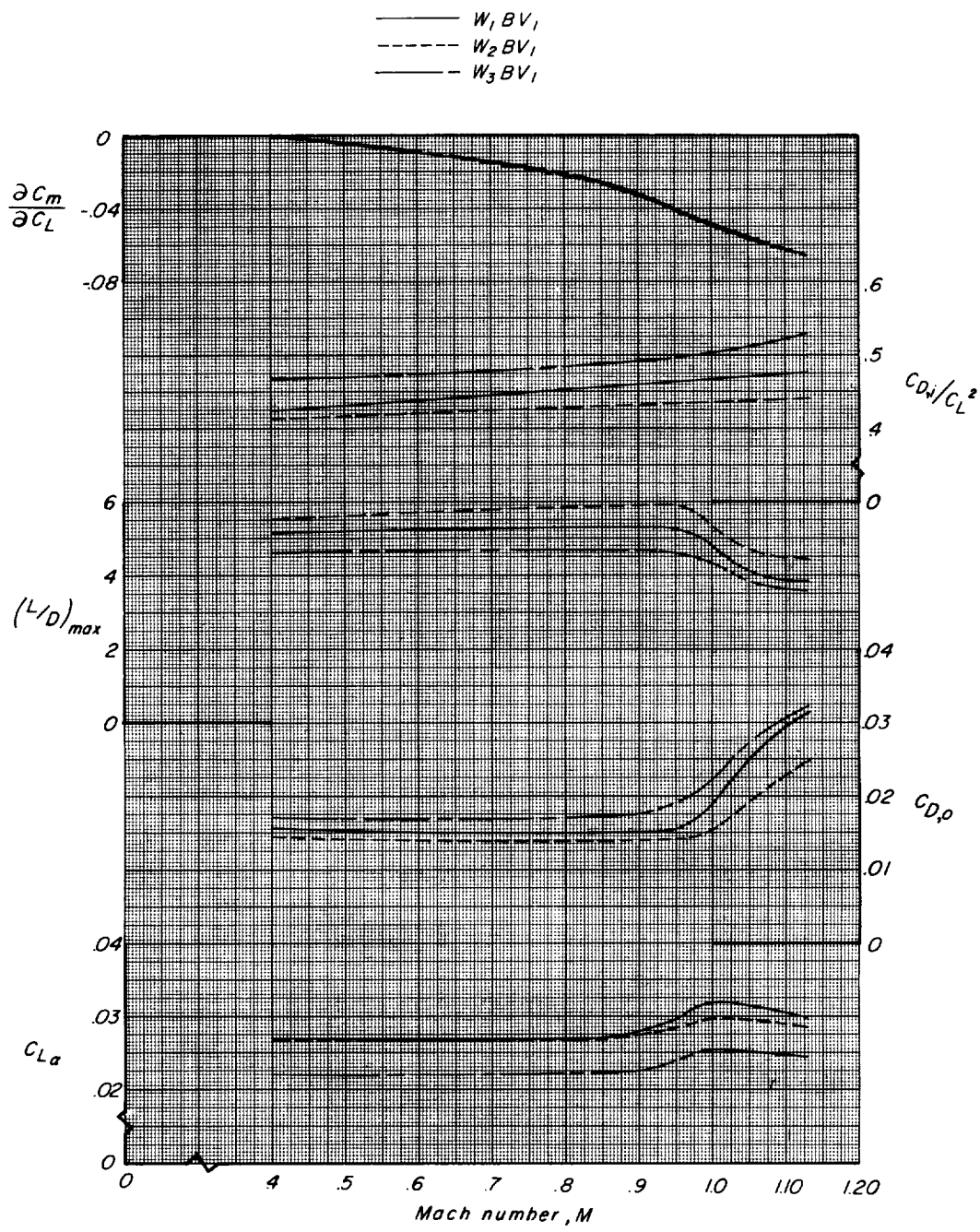

(a) Horizontal stabilizers off.

Figure 10.- Effects of wing planform on the summary longitudinal aerodynamic parameters C_{L_α}, $C_{D,o}$, $(L/D)_{max}$, $C_{D,i}/C_L{}^2$, and $\partial C_m/\partial C_L$ at various Mach numbers.

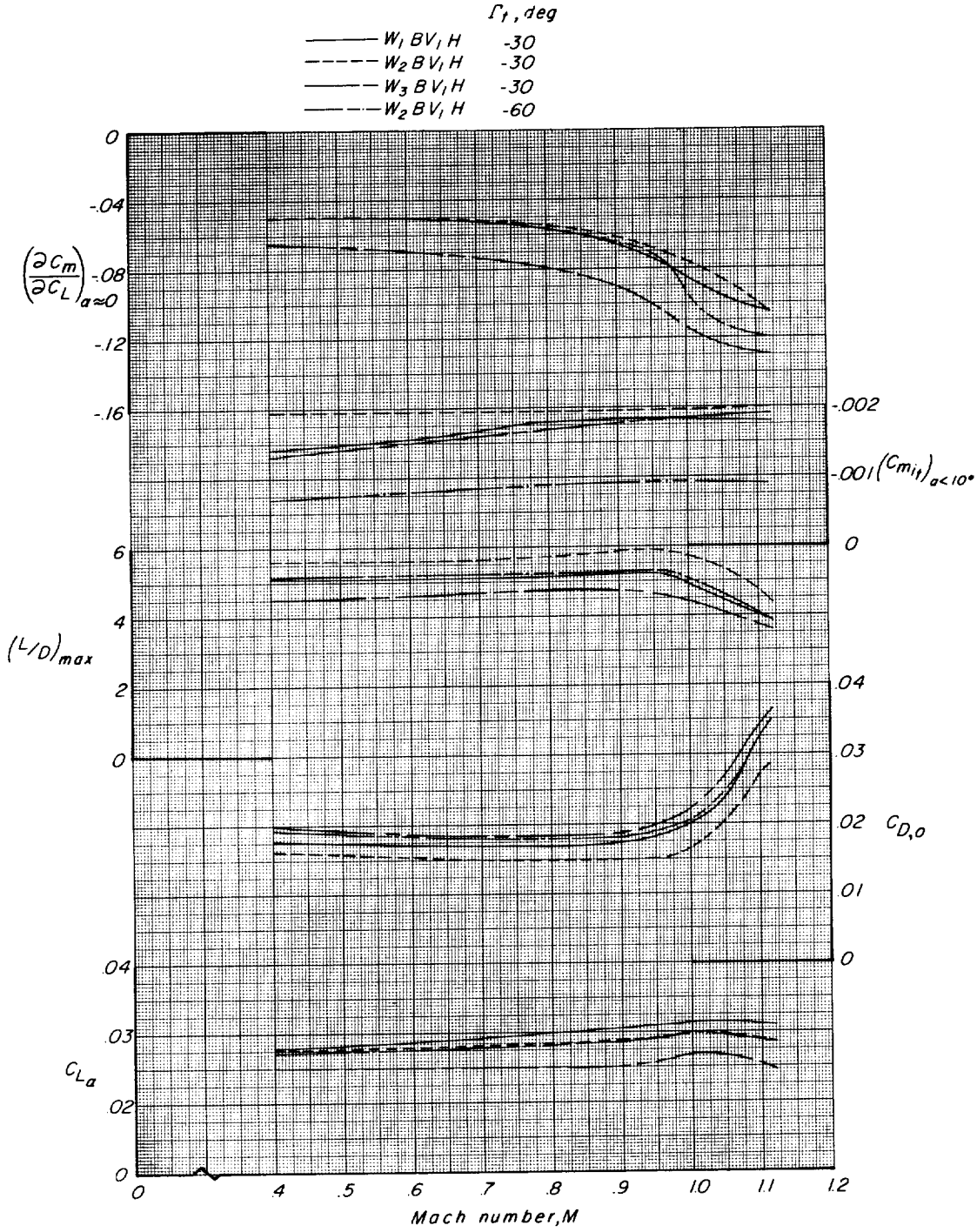

(b) Horizontal stabilizers on.

Figure 10.- Concluded.

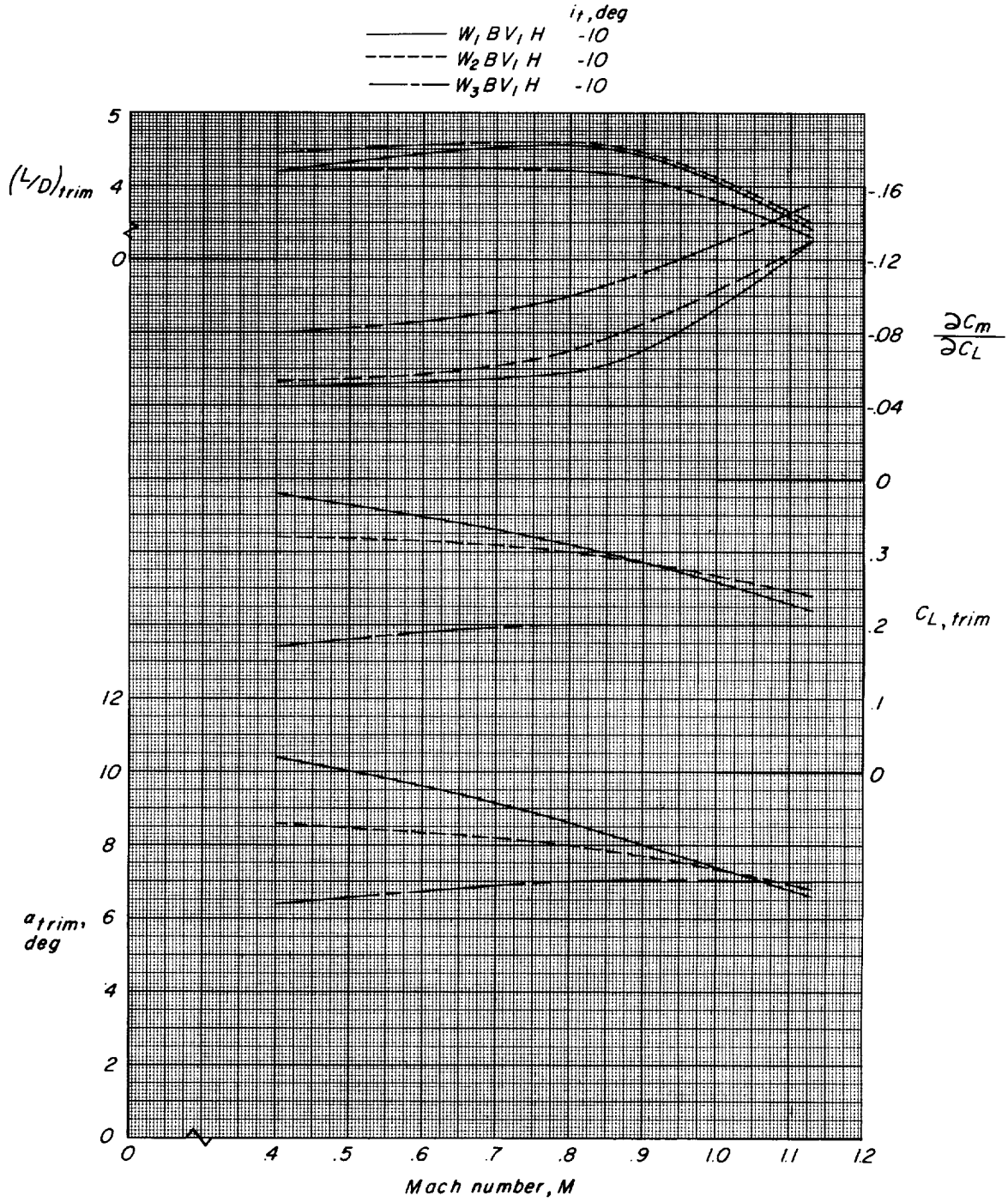

Figure 11.- Summary of the trimmed lift and lift-drag ratio characteristics at various Mach numbers for the three wing planform configurations.

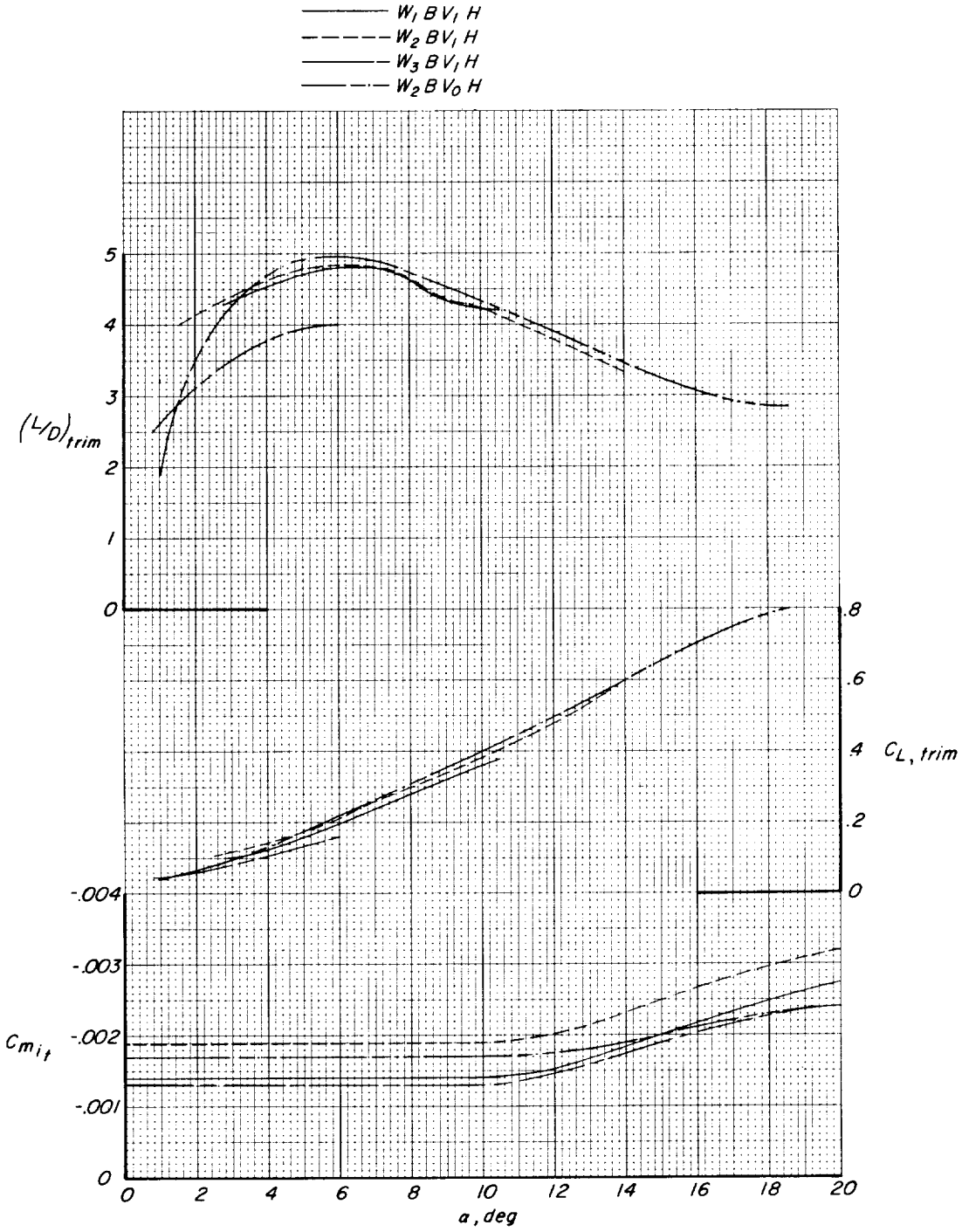

Figure 12.- Summary of the trimmed lift and lift-drag ratio characteristics for the three wing planform configurations throughout the trimmed angle-of-attack range. $M = 0.40$; $\Gamma_t = -30^\circ$; $i_t = 0^\circ$.